

THESIS ON NATURAL AND EXACT SCIENCES B96

**Wave Propagation in
Microstructured Solids:
Solitary and Periodic Waves**

MERLE RANDRÜÜT

TUT
PRESS

TALLINN UNIVERSITY OF TECHNOLOGY
Faculty of Science
Institute of Cybernetics

This dissertation was accepted for the defence of the degree of Doctor of Philosophy in Natural and Exact Sciences on August 27, 2010.

Supervisors: Professor Jüri Engelbrecht, D. Sc., Institute of Cybernetics
at Tallinn University of Technology

Professor Andrus Salupere, Institute of Cybernetics at
Tallinn University of Technology

Opponents: Professor Franco Pastrone, Department of Mathematics,
University of Turin, Turin, Italy

Alexey V. Porubov, D. Sc., Leading Research Fellow,
Institute of Problems in Mechanical Engineering,
Russian Academy of Sciences, Saint-Petersburg, Russia

Defence of the thesis: October 21, 2010

Declaration:

Hereby I declare that this doctoral thesis, my original investigation and achievement, submitted for the doctoral degree at Tallinn University of Technology has not been submitted for any academic degree.

Merle Randrüüt



Copyright: Merle Randrüüt, 2010
ISSN 1406-4723
ISBN 978-9949-23-028-0

LOODUS- JA TÄPPISTEADUSED B96

**Lainelevi mikrostruktuursetes
tahkistes: üksik- ja
perioodilised lained**

MERLE RANDRÜÜT

Contents

Introduction	9
Approbation	13
Acknowledgements	14
1 General ideas of wave motion	15
1.1 Definition of waves	15
1.2 Harmonic waves	17
1.3 1D wave equation	18
1.4 Dispersion	19
1.5 Nonlinearity	22
2 Korteweg–de Vries equation	27
2.1 Solitons	28
2.2 Cnoidal waves	31
2.3 Higher-order KdV equations	35
3 Material model	39
3.1 Microstructured materials	39
3.2 Mindlin’s model	40
3.3 Mindlin–Engelbrecht–Pastrone model	42
3.4 Slaving principle	44
3.5 Evolution equation	46
3.6 Linear case	49
4 Solutions of the extended KdV equation representing solitary waves	56
4.1 Extended KdV equation	56
4.2 Phase curves of solitary waves	57
4.3 Approximate solution of the extended KdV equation	59
4.3.1 Approximate solution of a cubic equation	62
4.4 Analytical solution in the limiting case	64
4.5 Concluding remarks	67
5 Solutions of the extended KdV equation representing periodic waves	69
5.1 Extended KdV equation	69
5.2 Phase portrait	69

5.3	Asymmetric periodic waves	74
5.4	Concluding remarks	75
6	Numerical simulation	76
6.1	Localised initial excitation	77
6.2	Harmonic initial excitation	79
6.3	Comparison of analytical and numerical results	79
6.4	Concluding remarks	90
7	Conclusion	92
	Abstract	97
	Kokkuvõte	98
	References	99
	Appendix A	107
	Publication I: On modelling dispersion in microstructured solids . . .	109
	Publication II: On modelling wave motion in microstructured solids .	121
	Publication III: On one-dimensional solitary waves in microstructured solids	129
	Publication IV: On periodic waves governed by the extended Korteweg–de Vries equation	145
	Appendix B	153
	Curriculum Vitae	155
	Elulookirjeldus	159

List of Figures

1	Harmonic wave	18
2	Dispersion diagram of waves in a thin elastic rod	21
3	Phase and group velocities of waves in a thin elastic rod	22
4	Evolution of a nonlinear wave	25
5	The solution of the periodic boundary value problem for the KdV equation	29
6	Shape of soliton	30
7	Distortion of single hump	31

8	Function $f(q)$ and corresponding phase curve	32
9	Geometrical interpretation of the variable φ	33
10	Periodic and solitary wave solutions of the KdV equation	36
11	Ceramic matrix composites: scanning electron microscopic view on a fracture surface of C/SiC	39
12	Standard continuum	40
13	Cosserat continuum	41
14	Microstructured continuum (Mindlin)	41
15	1D microstructured material	43
16	Dispersion diagram in the special case $c_1 = \bar{c}$	52
17	Dispersion diagram in the case $c_1 > \bar{c}$	53
18	Dispersion diagram in the case $c_1 < \bar{c}$	54
19	Graph of function $g(q')$	57
20	Graph of function $f(q)$	58
21	Phase curves of the extended KdV equation for different values of ε	60
22	Solitary wave governed by the extended KdV equation ($\varepsilon =$ ε_{\max}) in different approximations	61
23	Approximate $O(\varepsilon^3)$ solutions for different values of the micro- nonlinearity parameter	62
24	Phase curve of the extended KdV equation in the limiting case	65
25	Profile of the solitary wave in the limiting case	66
26	Exact and approximate solutions in the limiting case $\varepsilon = 1/16\eta^3$	68
27	Phase portrait of the KdV equation ($\varepsilon = 0$)	70
28	Phase portrait of the extended KdV equation ($\varepsilon = 0.5\varepsilon_{\max}$) . .	70
29	Phase portrait of the extended KdV equation ($\varepsilon = 0.8\varepsilon_{\max}$) . .	71
30	Phase portrait of the extended KdV equation ($\varepsilon = \varepsilon_{\max}$)	71
31	Approximate phase curves of the extended KdV equation with maximal micro-nonlinearity parameter. Upper: periodic wave (with magnified areas). Lower: limiting solitary wave.	73
32	Periodic waves and solitary wave governed by the extended KdV equation	75
33	Time-slice plot for $z = 10^{-2}$, $w = 10^{-2.5}$	77
34	The initial (dashed line) and the deformed (solid line) wave pro- file from Figure 33 ($z = 10^{-2}$, $w = 10^{-2.5}$).	78
35	Asymmetry of the wave profile at the end of integration interval: α_ξ against α for $z = 10^{-2}$, $w = 10^{-2.5}$	78

36	Time-slice plot over two space periods for KdV case, $z = 10^{-0.5}$, $w = 0$	80
37	Time-slice plot over two space periods for $z = 10^{-0.5}$, $w = 10^{-0.9936}$	80
38	Pseudocolour plot over two space periods for KdV case, $z = 10^{-0.5}$, $w = 0$	81
39	Pseudocolour plot over two space periods for $z = 10^{-0.5}$, $w = 10^{-0.9936}$	81
40	Initial harmonic wave (dashed line) and wave profile (solid line) at $\tau = 20.6$ for $z = 10^{-0.5}$, $w = 10^{-0.9936}$	82
41	Asymmetry of solitons: α_ξ against α at $\tau = 20.6$ for $z = 10^{-0.5}$, $w = 10^{-0.9936}$	82
42	Time-slice plot over two space periods for KdV case, $z = 10^{-1.5}$, $w = 0$	83
43	Time-slice plot over two space periods for $z = 10^{-1.5}$, $w = 10^{-2.621}$	83
44	Pseudocolour plot over two space periods for KdV case, $z = 10^{-1.5}$, $w = 0$	84
45	Pseudocolour plot over two space periods for $z = 10^{-1.5}$, $w = 10^{-2.6210}$	84
46	Initial harmonic wave (dashed line) and wave profile (solid line) at $\tau = 14.3$ for $z = 10^{-1.5}$, $w = 10^{-2.621}$	85
47	Asymmetry of solitons: α_ξ against α at $\tau = 14.3$ for $z = 10^{-1.5}$, $w = 10^{-2.621}$	85
48	Time-slice plot over two space periods for KdV case, $z = 10^{-2.5}$, $w = 0$	86
49	Time-slice plot over two space periods for $z = 10^{-2.5}$, $w = 10^{-4.1775}$	86
50	Pseudocolour plot over two space periods for KdV case, $z = 10^{-2.5}$, $w = 0$	87
51	Pseudocolour plot over two space periods for $z = 10^{-2.5}$, $w = 10^{-4.1775}$	87

Introduction

In general, the behaviour of materials depends on properties of the material structure. In contemporary material science and structural mechanics significant attention is devoted to microstructured materials possessing internal scales. For instance, metallic alloys, ceramic composites, polycrystalline solids, functionally graded materials, granular and porous materials, etc., are used for a wide variety of industrial applications since combining the mechanical properties of different constituents can yield optimal properties of solids and establish a new qualitative level in material science.

In principle, every material has some small-scale structure, since material is never distributed continuously. Speaking about microstructured material we do not mean the molecular or atomic scale. Rather these microstructures are assumed in the range of micrometers, so that they still can be considered as continua. The overall material becomes highly nonhomogeneous due to the embedded microstructures with their different behaviour.

Many theories of microstructured materials aim to smooth out this inhomogeneity while retaining its influence on the gross behaviour of the material. This is done by giving the material more internal degrees of freedom describing the behaviour of the embedded microstructures. So the ordinary but highly inhomogeneous material is turned into a homogeneous material which, however, is equipped with more than just a displacement field. Corresponding theories can be traced back to the meanwhile classical papers by Mindlin [1] and Sun et al. [2]. The connection of these theories to Cosserat continua has been established by Herrmann and Achenbach [3].

The problem from the physical side is how to describe the dispersive effects due to microstructure, still using the concept of continuity. There are many studies in this field, starting from the papers of Mindlin [1] and Eringen [4] several decades ago. Now we have a solid theoretical background, see for example [5, 6], but another problem has arisen: the governing equations tend to be rather complicated and the number of material parameters needed to describe the stress field is rather high. Therefore there is an urgent need to find simplified governing equations, but the physical effects should still be described with the needed accuracy.

The problem is not only in the mathematical complexity of governing equations but also in the number of waves. If in the linear theory, for example, longitudinal and shear waves can be easily separated then in the nonlinear theory the coupling can affect both waves considerably. In a general case of a complicated system of equations the main question is to understand to which wave which physical effects are related both qualitatively and quantitatively.

One of the possibilities to overcome such difficulties in contemporary mathe-

mathematical physics is to introduce the notion of evolution equations governing just one single wave. Physically it means the separation, if possible, of a multi-wave process into separate waves. The waves are then governed by the so-called evolution equations each of which describes the distortion of a single wave along a properly chosen characteristic or ray.

The application of fast changing loading conditions, including impact, means generation of deformation waves. The embedding of a microstructure into an otherwise homogeneous matrix material is reflected in an inherent length scale causing dispersion of propagating waves. Nonlinear effects, if taken into account, will counteract dispersion. A suitable balance of nonlinearity and dispersion may permit the propagation of solitary waves. The solitary waves can be considered as the long-wave limit of periodic solutions which, in the Korteweg–de Vries case, have the form of cnoidal waves.

The theory of solitary waves has originated from the study of surface waves in fluids. Meanwhile, solitary wave propagation in solids as well as in optical systems has gained widespread interest. If one takes shock waves and dispersive waves as two extreme examples of wave motion, the solitary waves share some properties of each of the two classes. They are localised like shock waves and smooth like dispersive waves. Solitary waves may keep their shape over long distances and are, therefore, applicable to signal transmission.

Apart from the possible technical applications, solitary waves are an attractive phenomenon from the mathematical point of view. Especially the solitons, i.e., solitary waves preserving their identity after a collision and satisfying an infinite set of conservation laws, have initiated an extended mathematical research.

The underlying physical model equations giving rise to solitary waves must combine two opposing effects, namely dispersivity and nonlinearity. Dispersion requires an inherent length scale, which might represent the scale of a microstructure or simply the cross-sectional scale of a rod. Nonlinearity is always present, at least to a certain degree, since any strictly linear model is just a first approximation of some more general nonlinear theory.

Mindlin [1] has formulated a linear theory of a three-dimensional, elastic continuum sharing some properties of a crystal lattice by including the idea of a unit cell into the theory. The unit cell may also be interpreted as *a molecule of a polymer, a crystallite of a polycrystal or a grain of a granular material* [1]. The mathematical model of the cell is a linear version of Ericksen and Truesdell's deformable directors [7]. If the cell is made rigid, the equations reduce to those of a linear Cosserat continuum [8].

According to Mindlin's model of a microstructured solid [1] any material point of the solid represents itself a microcontinuum subject to some deformation. The overall deformation of the microstructured continuum is then de-

scribed by the macroscopic displacements of its material points, i.e., the centres of the microcontinua, and by the deformation of the microcontinua themselves. The micro-deformations are assumed to be uniform at the microscopic level but may depend on the macroscopic location of the microcontinuum element.

Engelbrecht and Pastrone [9] have specialised Mindlin’s model of a microstructured solid to one dimension and augmented it by including nonlinear terms in both macro- and microlevel. To describe the motion of the one-dimensional microstructured solid, they have complemented the macroscopic displacement by the microstrain, both of which are considered as functions of the space coordinate and time. The governing equations appear as a system of coupled partial differential equations for the two field variables. Using the so-called slaving principle, Engelbrecht and Pastrone [9] have distilled from it a single partial differential equation, which governs mainly the macrodisplacement while retaining, in a first approximation, the influence of the microstructure. On the basis of this equation the propagation of solitary waves was studied by Janno and Engelbrecht [10]. They have shown that the wave profile becomes asymmetric due to the influence of micro-nonlinearity.

This thesis will focus on wave propagation in microstructured solids. The main aim of the investigation is analysing dynamical properties of 1D microstructured solids as described by a Mindlin-type model. The specific objectives are

- to derive an evolution equation corresponding to the Mindlin–Engelbrecht–Pastrone model;
- to look for solutions of the evolution equation representing undistorted waves;
- to establish conditions under which solitary waves are possible solutions of the evolution equation;
- to provide approximate and, if possible, exact solutions for the evolution equation;
- to generalise the results to periodic waves;
- to provide numerical solutions of the evolution equation for localised and harmonic initial conditions.

The thesis is organised as follows. Section 1 involves the general concept of wave motion including definition of waves, relations between the common wave parameters, one-dimensional wave equation with its well-known general solution, and important effects of wave propagation such as dispersion and nonlinearity. Section 2 is devoted to the equation named for Diederik Korteweg and

Gustav de Vries, Korteweg–de Vries (KdV) equation, and its solitary and periodic wave solutions. In Section 3 Mindlin’s model of a microstructured material is described and the corresponding one-dimensional Mindlin–Engelbrecht–Pastrone (MEP) model augmented by nonlinear terms in both macro- and microlevel is introduced. The procedure to obtain the approximate equation for the basic model, called the “slaving principle”, is presented, and the evolution equation to the Mindlin–Engelbrecht–Pastrone model is derived for both the nonlinear (extended KdV equation) and the linear case. In Section 4 the extended KdV equation is solved approximately and in a special case exactly. It is shown that solitary waves as solutions of the extended KdV equation are possible only up to a certain limit of the micro-nonlinearity parameter which causes the asymmetry of the wave profile. Solutions of the extended KdV equation representing periodic waves are discussed in Section 5. It is demonstrated that, due to the nonlinearity in microscale, the cnoidal waves stay periodic but become inclined in the same manner as the solitary waves. Numerical solutions of the evolution equation for localised and harmonic initial conditions are presented in Section 6. Conclusions and further prospects are given at the end of the thesis.

The present thesis is based on the following academic papers:

- Publication I*** Tanel Peets, **Merle Randrüüt**, and Jüri Engelbrecht: On modelling dispersion in microstructured solids. *Wave Motion* **45**(4) (2008) 471–480.
- Publication II** **Merle Randrüüt**, Andrus Salupere, and Jüri Engelbrecht: On modelling wave motion in microstructured solids. *Proceedings of the Estonian Academy of Sciences* **58**(4) (2009) 241–246.
- Publication III** **Merle Randrüüt** and Manfred Braun: On one-dimensional solitary waves in microstructured solids. *Wave Motion* **47**(4) (2010) 217–230.
- Publication IV** Manfred Braun and **Merle Randrüüt**: On periodic waves governed by the extended Korteweg–de Vries equation. *Proceedings of the Estonian Academy of Sciences* **59**(2) (2010) 133–138.

*Tanel Peets and Merle Randrüüt have contributed equally to this work.

To a minor extent some results are also included in the following publications, which are not part of the thesis:

Publication V Andrus Salupere, **Merle Randrüüt**, and Kert Tamm: Emergence of soliton trains in microstructured materials. In: J. Denier, M. Finn, T. Mattner (editors), *XXII International Congress of Theoretical and Applied Mechanics ICTAM 2008*, CD-ROM Proceedings, August 24–29, Adelaide, Australia 2008.

Publication VI **Merle Randrüüt** and Manfred Braun: On solitary waves in one-dimensional microstructured solids. *Proceedings in Applied Mathematics and Mechanics PAMM* **9**(1) (2010) 495–496.

Approbation

The results of the thesis have been presented at the following conferences and seminars:

1. **Merle Randrüüt**. On modelling deformation waves in microstructured materials: evolution equations. *11th EUROMECH–MECAMAT conference*, Mechanics in microstructured solids: cellular materials, fibre reinforced solids and soft tissues, Torino, Italy, March 10–14, 2008 — special award for the best poster presentation of a young researcher.
2. Jüri Engelbrecht, **Merle Randrüüt**, and Andrus Salupere. On modelling wave motion in microstructured solids. *11th EUROMECH–MECAMAT conference*, Mechanics in microstructured solids: cellular materials, fibre reinforced solids and soft tissues, Torino, Italy, March 10–14, 2008 (invited lecture).
3. **Merle Randrüüt**. On deformation waves in microstructured materials: one dimensional case, evolution equations. *Kolloquium Mechanik*. University of Duisburg-Essen, Germany, July 16, 2008.
4. Andrus Salupere, **Merle Randrüüt**, and Kert Tamm. Emergence of soliton trains in microstructured materials. *XII International Congress of Theoretical and Applied Mechanics ICTAM 2008*, Adelaide, Australia, August 24–29, 2008.
5. **Merle Randrüüt**. Deformatsioonilained mikrostruktuuriga materjalides: ühedimensioonilised evolutsioonivõrrandid (Deformation waves in

microstructured materials: evolution equations). *XIII Estonian Days of Mechanics*, September 15–16, 2008.

6. **Merle Randrüüt** and Manfred Braun. On solitary waves in one-dimensional microstructured solids. *80th Annual Meeting of the International Association of Applied Mathematics and Mechanics GAMM 2009*, Gdańsk University of Technology, Gdańsk, Poland, February 9–13, 2009.
7. Manfred Braun and **Merle Randrüüt**. On periodic waves governed by the extended Korteweg–de Vries equation. *International Conference on Complexity of Nonlinear Waves*, Institute of Cybernetics, Tallinn University of Technology, Tallinn, Estonia, October 5–7, 2009.

Acknowledgments

I would like to thank my supervisors Professor Jüri Engelbrecht and Professor Andrus Salupere for their guidance, advice and support during my studies at the Institute of Cybernetics.

Also I express my deep gratitude to Professor Manfred Braun from the University of Duisburg-Essen for valuable scientific discussions, his useful comments and remarks related to my PhD research, and inspiring collaboration. I appreciate highly the three academic papers published as a result of our scientific co-operation.

My special thanks go to my first supervisor from the Faculty of Mechanics at TUT, Associate Professor Jüri Kirs, whose impressive lectures of theoretical mechanics have encouraged me to continue my studies in this interesting area of science.

Financial support from the Estonian Science Foundation (Grant No 7035) and the TUT Development Fund: Tiina Mõis Scholarship (2008) and Eesti Raudtee Scholarship (2008) is greatly appreciated.

Many thanks to all my colleagues and friends for their advice and enthusiastic company.

I devote this thesis to my mother. Without her continuous support and love my PhD studies would not have been possible.

1 General ideas of wave motion

1.1 Definition of waves

The existence of waves as a recognisable form of disturbance is one of the most familiar features of the physical world providing a link between diverse areas of physics, and establishing one of the broadest scientific subjects. The manifestations of this phenomenon are well known to everyone in such forms as the transmission of sound in the air, the transmission of radio waves, the spreading of ripples on a pond of water, the seismic waves in earthquakes, or even the waves of traffic as a propagation of different densities of motor vehicles. These and a number of other examples could be accentuated to illustrate the propagation of waves through gaseous, liquid, and solid media and free space.

The term “wave” is often understood intuitively as the transport of disturbances in space, not associated with motion of the medium occupying this space as a whole. Thus, by a wave, no material is transported. According to Hall [11], in a wave, the energy of a vibration is moving away from the source in the form of a disturbance within the surrounding medium. However, this notion is not satisfactory for a standing wave (for instance, a wave on a string), where energy is moving in both directions equally, or for electromagnetic/light waves in a vacuum, where the concept of medium does not apply. Nevertheless, most wave motions are essentially oscillations propagating in space. To describe them the time t and at least one space coordinate x are required as independent variables. Since the equations governing wave propagation involve at least two independent variables, the equations generally involve partial derivatives.

Some definitions of waves available in online dictionaries:

- propagation of disturbances from place to place in a regular and organised way (Britannica Online Encyclopedia);
- disturbance propagated in a medium in such a manner that at any point in the medium the quantity serving as the measure of disturbance is a function of the time, while at any instant the displacement at a point is a function of the location of the point (Webster’s Online Dictionary);
- disturbance or variation that transfers energy progressively from point to point in a medium and that may take the form of an elastic deformation or of a variation of pressure, electric or magnetic intensity, electric potential, or temperature (Merriam–Webster Online Dictionary).

Notwithstanding a number of attempts to formulate the concept of a wave, there appears to be no single precise definition of what exactly constitutes a

wave. A famous American applied mathematician G. B. Whitham [12] admits that various restrictive definitions can be given, but to cover the whole range of wave phenomena it seems preferable to be guided by the intuitive view that a wave is any recognisable signal that is transferred from one part of the medium to another with a recognisable velocity of propagation. He writes:

The signal may be any feature of the disturbance, such as a maximum or an abrupt change in some quantity, provided that it can be clearly recognised and its location at any time can be determined. The signal may distort, change its magnitude, and change its velocity provided it is still recognisable. This may seem a little vague, but it turns out to be perfectly adequate and any attempt to be more precise appears to be too restrictive; different features are important in different types of wave.

Whitham has proposed to distinguish two main classes of waves from which the first one is formulated mathematically in terms of hyperbolic partial differential equations, and such waves will be referred to as *hyperbolic*. The second class cannot be characterised as easily, but since it starts from the simplest cases of dispersive waves in linear problems, the whole class can be referred to as *dispersive*. It should be emphasised that these classes are not exclusive — there is assumed to be some overlap in that certain wave motions exhibit both types of behaviour, and there are certain exceptions that fit neither.

Another definition of waves, proposed in continuum mechanics by Truesdell and Noll [13], says:

A wave is a state moving into another state with a finite velocity.

Apparently it is not easy to characterise wave motion, and the definitions above are not satisfactory in every respect. Waves occur in quite different forms. The water waves plunging periodically towards the shore are rather different from a flood wave caused by the braking of a dam or the shock wave carried along by a hypersonic aircraft or the blast wave of a detonation. The definition offered by Truesdell and Noll covers only the latter type of waves, where a disturbance enters a quiet area ahead of the front. It excludes the usual, periodic waves and would also include other kinds of propagating fronts, like moving phase transition surfaces in a material or a weather front in the atmosphere, which are not necessarily understood as “wave”. The definition in Webster’s online dictionary is rather poor, since it holds for any kind of function of space and time whether it represents a wave or not. Diffusive processes like heat conduction, for instance, are not understood as waves.

Waves can be characterised only in a rather vague manner to include all possible aspects and appearances. In this sense, Whitham’s definition seems to

be most satisfactory. It emphasises that a “recognisable” signal is transferred, leaving open what kind of signal it is and how we can recognise it. It can represent a wave crest of a periodic wave or the moving location of a sharp shock front. Still there are processes which may or may not be called waves. As an example, standing waves do not propagate and are, strictly speaking, oscillations. But since they might occur as a limit of propagating waves whose phase velocity tends to zero, it is reasonable not to exclude them.

1.2 Harmonic waves

Mathematically, the most basic wave is the harmonic wave (or sine wave or sinusoid), see Figure 1, with a field variable u described by the equation

$$u(x, t) = a \cos(kx - \omega t + \phi), \quad (1.1)$$

where the amplitude of the wave a , the maximum distance from the highest point of the disturbance in the medium (the crest) to the equilibrium point during one wave cycle, the wave number (spatial frequency) k , and the angular frequency ω are assumed to be constant; x and t are the space and time coordinates, respectively, and ϕ is a phase offset.

Here the field variable u can express nearly everything, for instance, it can be interpreted as a pressure, the height of the water surface above the mean level, an electric field, a displacement, etc.

Relations between the common wave parameters are

- wave number

$$k = \frac{2\pi}{\lambda}, \quad (1.2)$$

where λ is the wavelength of the wave, the distance between two sequential crests or troughs;

- frequency

$$f = \frac{1}{T}, \quad (1.3)$$

where T is the time for one complete cycle of an oscillation of a wave, the wave period;

- angular frequency, often called simply frequency,

$$\omega = 2\pi f = \frac{2\pi}{T}; \quad (1.4)$$

- wavelength λ of a sinusoidal waveform travelling at constant speed c

$$\lambda = \frac{c}{f}. \quad (1.5)$$

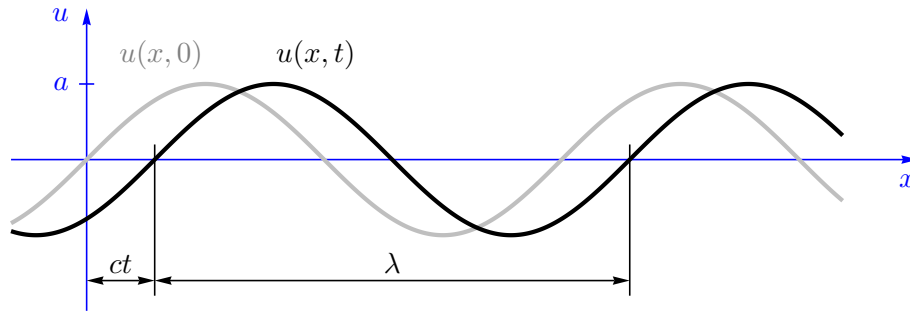


Figure 1: Harmonic wave

By adding two harmonic waves, identical in amplitude, but propagating in opposite directions, a standing wave solution can be constructed [14]. For instance,

$$u = a \cos(kx - \omega t) + a \cos(kx + \omega t) = 2a \cos kx \cos \omega t. \quad (1.6)$$

In such a standing wave, the solution has an envelope that is fixed in space, here $\cos kx$, which is modulated by a time dependent motion, here $\cos \omega t$.

1.3 1D wave equation

The one-dimensional wave equation

$$\frac{\partial^2 u}{\partial t^2} = c^2 \frac{\partial^2 u}{\partial x^2} \quad (1.7)$$

is an important second-order linear partial differential equation of waves, such as sound waves, light waves and water waves, describing the evolution of a wave over time in a medium where the wave propagates at the same speed independent of wavelength (no dispersion), and independent of amplitude (linear media) [15].

The general solution for the wave equation in one dimension was given by d'Alembert and is known as d'Alembert's solution

$$u(x, t) = f(x - ct) + g(x + ct), \quad (1.8)$$

where f and g are arbitrary functions that will be specifically determined by the initial conditions or forcing function of a given problem, representing propagating disturbances [16]. The function $f(x - ct)$ attains a constant value if its argument $x - ct$ is constant. However, increasing time requires increasing values of x to maintain the argument of the function constant, so the solution $u = f(x - ct)$ corresponds to a wave propagating in the positive x direction.

Similarly, the solution $u = g(x + ct)$ represents a disturbance propagating in the negative x direction.

One should emphasise regarding the solution (1.8) that whatever the shapes of the disturbances $f(x - ct)$, $g(x + ct)$ initially are, these shapes are maintained during the propagation. Thus, the waves propagate without distortion. According to Graff [16] appreciation of the undistorted nature of the wave propagation is important for two reasons: (i) it represents a fundamental characteristic of the one-dimensional wave equation, and (ii) it will serve as a comparison against many physical systems where the opposite is true and where pulse distortion occurs during propagation.

The wave equation arises in fields such as acoustics, electromagnetics, and fluid dynamics. Amongst other things, the wave equation governs the propagation of small amplitude waves on a stretched string. Historically, the problem of a vibrating string such as that of a musical instrument was studied by Jean le Rond d'Alembert, Leonhard Euler, Daniel Bernoulli, and Joseph-Louis Lagrange.

1.4 Dispersion

There are two velocities that are associated with linear waves, the *phase velocity* and the *group velocity*. Many physical systems that exhibit wave motion can be modelled using linear equations which are different from the usual wave equation. These may also have harmonic wave solutions of the form

$$u(x, t) = a \cos [k(x - ct)], \quad (1.9)$$

which is of the general form $f(x - ct)$ and thus clearly represents a travelling wave. The argument $k(x - ct)$ is called the phase of the wave; points of constant phase are propagated with the phase velocity c . At any position the field variable $u(x, t)$ is time-harmonic with time period T . Generally, for mathematical convenience instead of (1.1), the expression

$$u = a \exp \{i(kx - \omega t)\}, \quad (1.10)$$

is used, where $i = \sqrt{-1}$. For the physical interpretation of the solution, the real or imaginary part of the equation is to be taken [17].

Here the angular frequency is a known function of the wave number k , so that

$$\omega = \omega(k). \quad (1.11)$$

For the one-dimensional wave equation $\omega = ck$, and the wave crests move at a constant speed c , independent of the wave number k or of the angular

frequency ω . However, in most systems ω is not proportional to k , and the wave crests move with velocity

$$c_p(k) = \frac{\omega(k)}{k}, \quad (1.12)$$

which is known as the phase velocity, and is usually a function of the wave number. In other words, the wave crests move at different velocities for different wave numbers, and hence also wavelengths [14].

In solutions that are a combination of harmonic waves of different wavelengths, this eventually leads to a separation or *dispersion* of various components. Such a system is said to be dispersive and (1.11) is the dispersion relation. Dispersion is an important phenomenon since it governs the change of shape of a pulse as it propagates through a dispersive medium [17]. If the phase velocity does not depend on the wave number (or wavelength) the system is called nondispersive.

The group velocity is defined as

$$c_g = \frac{\partial \omega}{\partial k}, \quad (1.13)$$

having a fundamental significance in the theory of linear, dispersive waves. If ω is directly proportional to k , then the group velocity is exactly equal to the phase velocity. Otherwise, the envelope of the wave will become distorted as it propagates. This “group velocity dispersion” is an important effect in the propagation of signals through optical fibers and in the design of high-power, short-pulse lasers.

However, as long as one considers a single harmonic wave the group velocity cannot be realised. One needs a modulated wave, either amplitude or frequency modulated, to see the meaning of group velocity. If there is dispersion, i.e., the phase speed depends on the wave number, then the modulated signal will not propagate with the phase speed but at a different velocity, the group velocity, which might be bigger or smaller than the phase velocity. For nondispersive waves both velocities are the same.

Packets of waves of nearly the same length propagate with the group velocity, individual components moving through the packet with their phase velocity. In general, it can be shown that energy of a wave disturbance is propagated at the group velocity, not the phase velocity [18].

There is a long list of examples of dispersive wave motions like wave propagation along an elastic beam treated by Fung and Tong [19], and Bower [20], or transverse waves along an elastically supported taut string [21], for instance. Longitudinal waves in a thin elastic rod as an illustrative example of dispersive wave motion is presented below.

Example

Longitudinal waves in a thin elastic rod, including effects of lateral inertia, are described by [21, 22]

$$u_{tt} - c_b^2 u_{xx} - i^2 \nu^2 u_{xxtt} = 0, \quad (1.14)$$

where u is the longitudinal displacement, ν is Poisson's ratio, i and c_b are defined as

$$i = \sqrt{\frac{I}{A}} \quad \text{and} \quad c_b = \sqrt{\frac{E}{\rho}}, \quad (1.15)$$

denoting the geometric radius of inertia and the so-called bar velocity, respectively. Here the quantities I and A are the geometric moment of inertia and the cross-sectional area, and E and ρ denote Young's modulus and the mass density, respectively. Equation (1.14) is known as the linear Boussinesq equation for shallow-water waves. The same equation was derived by Love [22, page 428], and therefore it is also known as Love's equation for waves in rods.

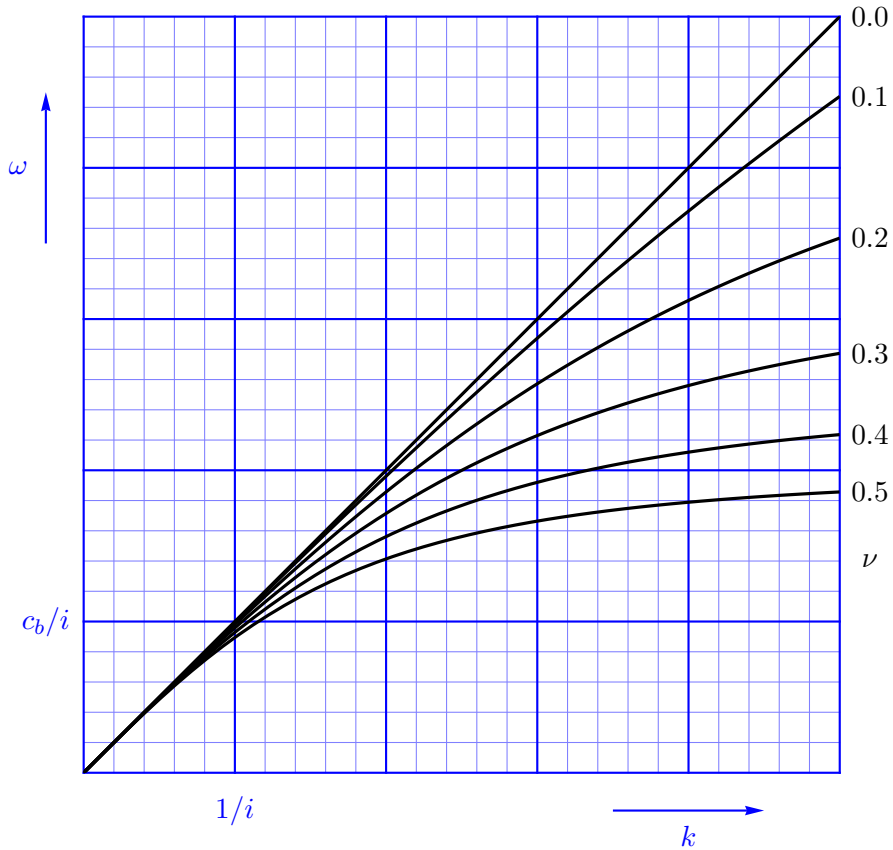


Figure 2: Dispersion diagram of waves in a thin elastic rod

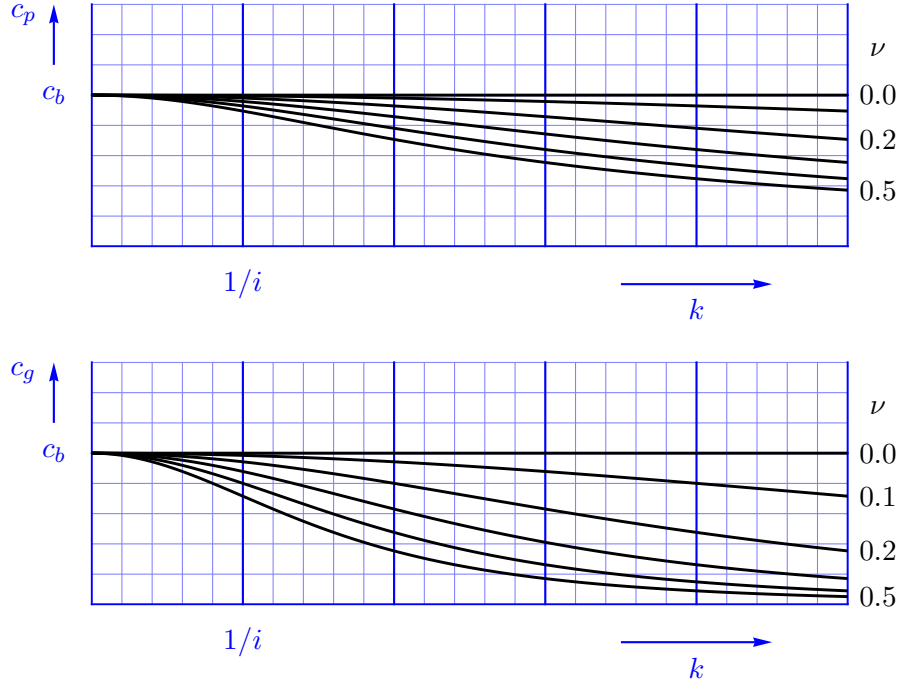


Figure 3: Phase and group velocities of waves in a thin elastic rod

It can be shown that the equation (1.14) admits solutions in form of harmonic waves

$$u = a \cos(kx - \omega t) \quad (1.16)$$

yielding the dispersion relation

$$\omega = \frac{c_b k}{(i^2 \nu^2 k^2 + 1)^{1/2}} \quad (1.17)$$

and the corresponding phase and group velocities

$$c_p = \frac{c_b}{(i^2 \nu^2 k^2 + 1)^{1/2}} \quad \text{and} \quad c_g = \frac{c_b}{(i^2 \nu^2 k^2 + 1)^{3/2}}. \quad (1.18)$$

Figure 2 shows the graph of the dispersion relation (1.17) for different values of Poisson's ratio ν . The dependence of the phase and group velocities on the wave number k for different values of ν is shown in Figure 3.

1.5 Nonlinearity

A major role in wave propagation is played by nonlinearity. Several effects like shock formation and solitary waves can be understood only if nonlinearity

is taken into account. Sources of nonlinearity can be found everywhere in nature, since nonlinear behaviour is the normal case. It is, on the contrary, an exception if strictly linear equations are encountered. In most cases linearity appears just as an approximation, which allows to find explicit solutions, while the real world is too complicated.

According to the Encyclopedia of Nonlinear Science [23] a system is said to be linear if the system's response to an applied force is directly proportional to the magnitude of that force, otherwise the system is nonlinear.

Actually, linearity and nonlinearity should be attributed in the first place to the mathematical formulation. A function φ is linear if it has the properties

$$\varphi(x_1 + x_2) = \varphi(x_1) + \varphi(x_2) \quad \text{and} \quad \varphi(\lambda x) = \lambda\varphi(x), \quad (1.19)$$

whatever these quantities are. Of course, addition and multiplication with a scalar must be available in order to formulate these properties.

The above definition in the Encyclopedia of Nonlinear Science emphasises only the second property, the *homogeneity* of the mapping. In order to satisfy also the *additivity* property the system's response to the combined application of two forces must be the sum of the responses to each of the forces applied alone. Also it should be noted that whether a *system* is linear or nonlinear may depend on the selection of the input and output variables. In the definition the input is assumed to be some force. But what is the output? It may happen that taking one output variable, some displacement, for instance, shows a linear behaviour while another, a pressure, say, reacts in a nonlinear manner. So linearity and nonlinearity is mainly a property of a system with specified input and output variables.

Engelbrecht [24, 25, 26] has studied different types of nonlinearities influencing wave motion like material (physical) nonlinearities, geometrical nonlinearities, kinematical nonlinearities, structural nonlinearities, etc. In continuum mechanics one distinguishes between geometrical and physical nonlinearity. Physical or material nonlinearity comes from the constitutive equations describing the behaviour of material under deformation, while geometrical nonlinearity is due to a nonlinear relation between strain and displacement gradient.

There is some ambiguity in the classification of nonlinearity as physical or geometric, since it depends on what kind of strain measure is used. According to the general, nonlinear theory of elasticity, the strain tensor must be a function of the right Cauchy-Green tensor \mathbf{C} [27], and, for small deformations, it should reduce to the classical linear strain tensor. An overview of different nonlinear strain tensors is given in [28, page 118–119]. Most frequently used is the Green-Lagrange strain tensor $\frac{1}{2}(\mathbf{C} - \mathbf{I})$, since it is the only one that is a linear function of the right Cauchy-Green tensor \mathbf{C} .

The present analysis is restricted to the one-dimensional case. Here the simplest choice of a strain measure is the displacement derivative u_x itself, while the Green-Lagrange strain would be $u_x + \frac{1}{2}u_x^2$. The derivative u_x coincides with the classical definition of linear strain. Moreover, it can be interpreted as the one-dimensional version of Biot's strain tensor $\mathbf{C}^{1/2} - \mathbf{I}$, which is also an admissible nonlinear strain measure.

The main goal of this thesis is to study the combined effect of dispersion and nonlinearity on the propagation of waves. In order to see the influence of nonlinearity alone an example of nonlinear waves without dispersion is presented.

Example

Considering the one-dimensional motion of a *linear* elastic solid, the dynamics of the displacement $u(x, t)$ is governed by the equation

$$\rho u_{tt} = (\lambda + 2\mu)u_{xx}, \quad (1.20)$$

where ρ denotes the mass density and the elastic properties are specified by the Lamé's constants λ and μ . Thus the motion is governed by the simple wave equation

$$u_{tt} = c_0^2 u_{xx}, \quad (1.21)$$

and the wave speed

$$c_0 = \sqrt{\frac{\lambda + 2\mu}{\rho}} \quad (1.22)$$

is the speed of longitudinal waves propagating in the unbounded elastic solid.

If nonlinearity is taken into account the wave equation (1.21) is modified and assumes the form, see Engelbrecht [29],

$$u_{tt} = c_0^2 (1 + m u_x) u_{xx}, \quad (1.23)$$

with some nonlinearity parameter m . There is no need to specify whether the nonlinearity is physical or geometric. This depends on the choice of the strain measure. If "strain" is understood in the sense of Biot as u_x , then the whole nonlinearity comes through the stress-strain law. If, however, the Green-Lagrange strain $u_x + (1/2)u_x^2$ is preferred, the nonlinearity is partially geometric and partially physical in nature. Regardless of its classification as physically or geometrically nonlinear, the governing equation (1.23) is a nonlinear partial differential equation governing the longitudinal displacement $u(x, t)$ in an elastic solid.

Concentrating on a wave propagating to the right, i.e., in the direction of the space coordinate x , it is reasonable to introduce a moving coordinate

$\xi = x - c_0 t$. The solution of the nonlinear wave equation (1.23) can be assumed in the form

$$u = \varepsilon U(\xi, \tau) = \varepsilon U\left(x - c_0 t, \frac{1}{2}\varepsilon t\right), \quad (1.24)$$

where the factor $1/2$ has been introduced for convenience to make subsequent equations simpler. The factor $\varepsilon \ll 1$ in front of U provides for small displacements while the same factor in the second argument is responsible for a slow evolution of the wave profile. Inserting the ansatz (1.24) into the governing nonlinear equation (1.23) and keeping only terms of the order ε yields

$$-c_0 U_{\xi\tau} = c_0^2 m U_{\xi} U_{\xi\xi}. \quad (1.25)$$

To simplify this equation one can introduce the new variable

$$\alpha = U_{\xi} = \frac{1}{\varepsilon} u_x, \quad (1.26)$$

which represents a magnified strain. It has to satisfy the nonlinear equation

$$\alpha_{\tau} + m c_0 \alpha \alpha_{\xi} = 0. \quad (1.27)$$

This is a first example of a so-called evolution equation. It governs the slow evolution of a wave profile during its propagation. One of the main goals of this thesis is to derive an evolution equation for some more complicated nonlinear wave equation.

Suppose that, at the initial time instant $\tau = 0$, the wave profile has a given shape

$$\alpha(\xi, 0) = \varphi(\xi). \quad (1.28)$$

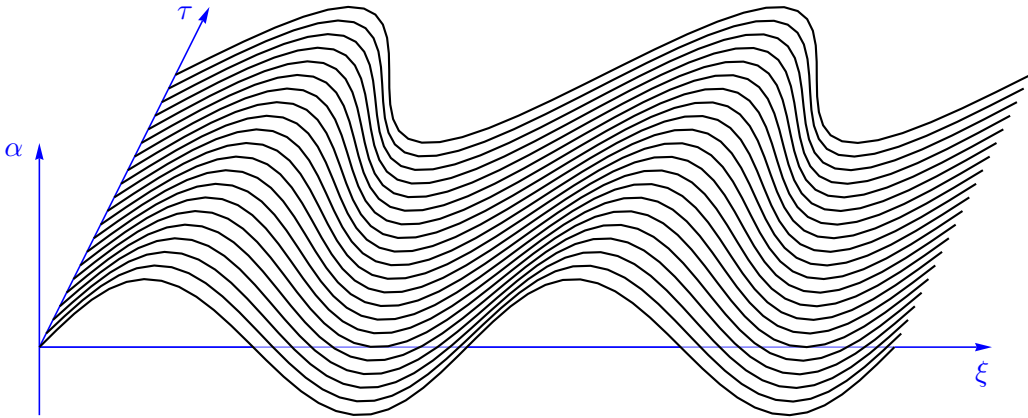


Figure 4: Evolution of a nonlinear wave

Then, at time τ , the function $\alpha(\xi, \tau)$ satisfies the *implicit* equation

$$\alpha = \varphi(\xi - mc_0\tau\alpha). \quad (1.29)$$

Although the solution of the evolution equation is available only in an implicit form, it can be graphically displayed. To take a concrete example let us assume the initial wave shape to be

$$\varphi(\xi) = a \sin k\xi, \quad (1.30)$$

where k is wave number. According to (1.29) the solution $\alpha(\xi, \tau)$ of the evolution equation is provided by the implicit equation

$$\alpha = a \sin k(\xi - mc_0\tau\alpha). \quad (1.31)$$

This solution is plotted in Figure 4.

As can be seen from the graph the leading flank of the sine wave becomes steeper while the trailing flank becomes more gentle as the slow time τ increases. Actually the smooth solution (1.31) is valid only for

$$\tau \leq \frac{1}{mc_0ak}. \quad (1.32)$$

Afterwards a shock will form at the leading flank of the wave. This is outside the scope of our analysis. It is, however, a typical effect of nonlinear wave propagation that a discontinuous solution can develop, although the initial data were smooth.

2 Korteweg–de Vries equation

The equation named for Diederik Korteweg and Gustav de Vries, the Korteweg–de Vries equation (KdV equation), given here in canonical form [23]

$$u_t + 6uu_x + u_{xxx} = 0, \tag{2.1}$$

is widely recognised as a paradigm for the description of weakly nonlinear waves in many branches of physics and engineering. Here $u(x, t)$ is a field variable, t is the time, and x is the space coordinate in the relevant direction. The equation describes how waves evolve under the competing but comparable effects of nonlinearity and dispersion. As outlined in Subsections 1.5 and 1.4, nonlinearity may lead to steepening of the wave profile while dispersion as a contrary effect tries to flatten it out. A suitable balance between nonlinear and dispersive effects may permit the propagation of solitary waves [18]. However, besides the solitary waves the KdV equation admits a whole family of periodic solutions, the so-called cnoidal waves [30], of which the solitary wave is just the limit if the period tends to infinity. It should be stressed that both solitons and cnoidal waves propagate without distortion, while in general, solutions of the KdV equation represent waves changing their shape during propagation.

The KdV equation is particularly remarkable as the prototypical example of an exactly solvable model, a nonlinear partial differential equation whose solutions can be exactly and precisely specified. But the solutions in turn include prototypical examples of solitons. KdV equation can be solved by means of the inverse scattering transform. The mathematical theory behind the KdV equation is rich and interesting, and, in the broad sense, is a topic of active mathematical research.

The KdV equation has several connections to physical problems. In addition to being the governing equation of the string in the Fermi–Pasta–Ulam problem [31] in the continuum limit, it approximately describes the evolution of long, one-dimensional waves in many physical settings, including

- shallow-water waves with weakly nonlinear restoring forces;
- long internal waves in a density-stratified ocean;
- ion-acoustic waves in a plasma;
- acoustic waves on a crystal lattice;
- and more.

Although the KdV equation owes its name to the famous paper of Diederik Korteweg and Gustav de Vries [32], published in 1895, the history of the KdV

equation started with experiments by John Scott Russell in 1834 who observed a solitary wave in the Union Canal in Scotland and reproduced the phenomenon in a wave tank naming it the “great wave of translation”. He demonstrated four facts about solitary waves [23]:

- solitary waves have a hyperbolic secant shape;
- a sufficiently large initial mass of water produces two or more independent solitary waves;
- solitary waves cross each other “without change of any kind”;
- a wave of height h and travelling in a channel of depth d has a velocity given by the expression $\sqrt{g(d+h)}$ (where g is the acceleration of gravity), implying that a large amplitude solitary wave travels faster than one of low amplitude.

These observations were followed by theoretical investigations by Lord Rayleigh and Joseph Boussinesq around 1870. After the ground-breaking work of Korteweg and de Vries related to small-amplitude long water waves, interest in solitary waves and the KdV equation declined until the dramatic discovery of the *soliton* by Norman Zabusky and Martin Kruskal [33] in 1965.

2.1 Solitons

The KdV equation (2.1) is characterised by its family of solitary wave solutions

$$u = a \operatorname{sech}^2 [\eta (x - ct)], \quad (2.2)$$

where $a = 2\eta^2$ and $c = 4\eta^2$. Equation (2.2) describes a family of steady isolated wave pulses. Thus the amplitude a and the propagation speed c are uniquely determined by the width parameter η , which in [23] is called wave number, although it is different from its original meaning.

According to the Encyclopedia of Nonlinear Science [23], a soliton is a localised nonlinear wave that maintains its shape and speed as it travels, even through interaction with other waves. The term *soliton* was coined by Zabusky and Kruskal [33] to reflect both the solitary-wave-like character and the particle-like interaction properties. The surprising discovery has had an enormous impact on the field of nonlinear mathematics and science.

The phenomenon of preservation of identity through interaction was known already before, from describing solutions of linear nondispersive wave equations. A simple example is a linear wave equation (1.7) for which the general solution is given by d’Alembert’s formula (1.8) expressing a right and a left going waves at a speed c . Two such wave profiles interact when they meet

head-on but they both come out of the interaction with the same shape and speed.

However, until the discovery of solitons, it was not believed that such property could hold for nonlinear equations. Common understanding in mathematics and physics in the 1950s suggested that nonlinear wave solutions either break, dissipate, or thermalise, that is, distribute initial energy between different solutions over time, and therefore, lose their identities with time. Thus, in 1965, numerical studies of the Korteweg–de Vries equation published by Zabusky and Kruskal changed the above described common beliefs about nonlinear waves forever [23]. Ten years before that, in 1955, Fermi, Pasta and Ulam [31] were working on a numerical model of phonons in an anharmonic lattice, a model which turned out to be closely related to discretisation of the KdV equation. Taking this up in 1965, Zabusky and Kruskal considered the initial value problem for the equation [34]

$$u_t + uu_x + \delta^2 u_{xxx} = 0 \quad (2.3)$$

with periodic boundary conditions. The equation (2.3) was solved with

$$u(x, 0) = \cos \pi x, \quad 0 \leq x \leq 2, \quad (2.4)$$

and u , u_x , u_{xxx} periodic on $[0, 2]$ for all t ; $\delta = 0.022$ was chosen. A well-known set of their results is expressed in Figure 5. It can be seen that after a short time period the wave steepens and is about producing a shock, but at the same time the dispersive term δu_{xxx} becomes significant and balances

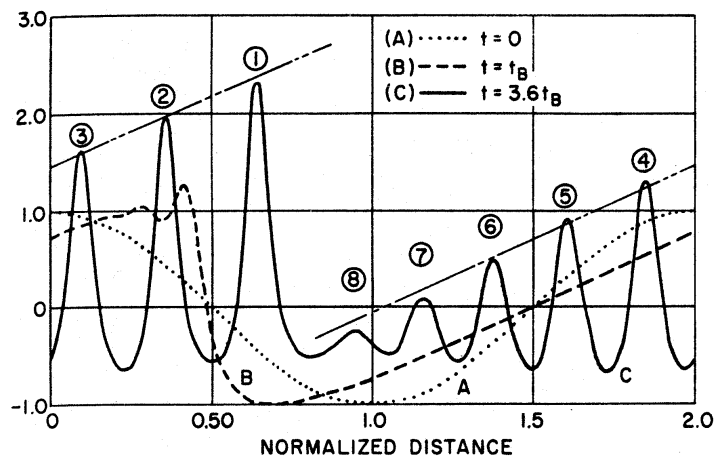


Figure 5: The solution of the periodic boundary value problem for the KdV equation [18, 34]. Curve A corresponds to the time moment $t = 0$, curve B corresponds to the time moment $t = 1/\pi$ and curve C corresponds to the time moment $t = 3.6/\pi$.

the nonlinear effect. After some time the solution develops a train of eight well-defined waves, each of them like a sech^2 function, faster (taller) waves catching up and overtaking the slower (smaller) ones. It was discovered that these nonlinear waves can interact strongly and continue travelling as if there had been no interaction at all, preserving the shape and the speed of them.

The shape of the soliton (2.2) is shown in Figure 6. The higher the amplitude of the wave, the narrower it is and the faster it will move, the propagation speed here is determined by $4\eta^2$. More generally the Korteweg–de Vries equation,

$$u_t + 6uu_x + \delta^2 u_{xxx} = 0, \quad (2.5)$$

has a solitary wave solution of the form

$$u = 2\delta^2 \eta^2 \text{sech}^2 \eta(x - 4\delta^2 \eta^2 t), \quad (2.6)$$

which vanishes for $\delta \rightarrow 0$ and η fixed.

For $\delta = 0$ the Korteweg–de Vries equation (2.5) is reduced to the simple first-order equation

$$u_t + 6uu_x = 0. \quad (2.7)$$

The solution $u = u(x, t)$ satisfying an arbitrary initial condition $u(x, 0) = f(x)$ has to be computed from the implicit equation

$$u = f(x - 6ut). \quad (2.8)$$

Alternatively, the profile $u = u(x, t)$ at a fixed time instant t can be represented in the parametric form

$$x = \lambda + 6tf(\lambda), \quad u = f(\lambda). \quad (2.9)$$

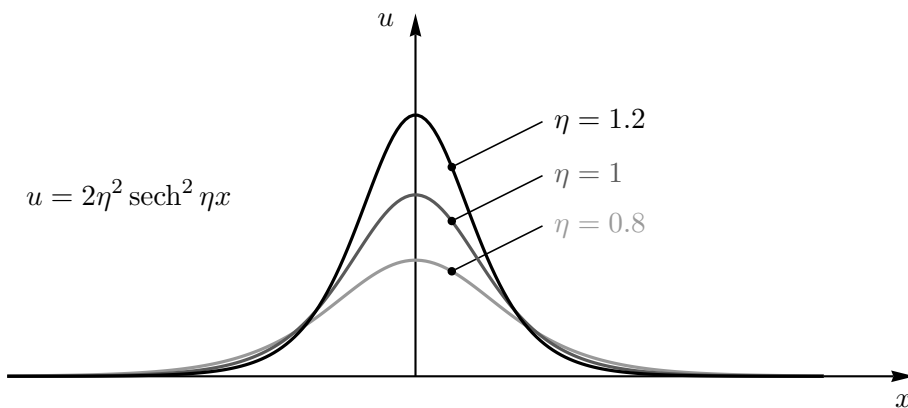


Figure 6: Shape of soliton

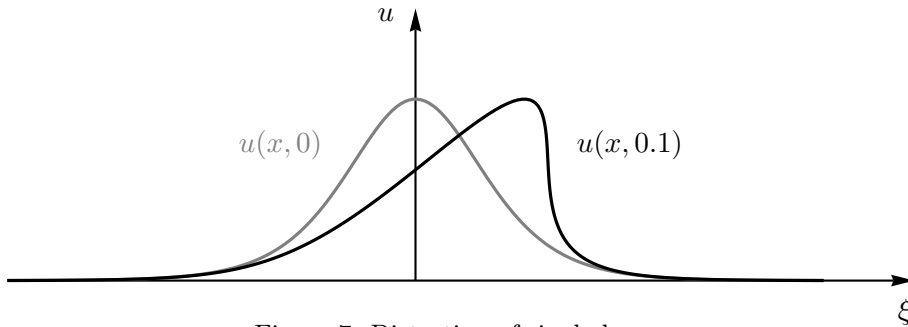


Figure 7: Distortion of single hump

The distortion of the wave profile according to equation (2.7) is shown in Figure 7. Here the initial profile is chosen as a single symmetric hump of the form $f(x) = 2 \operatorname{sech}^2 x$. During propagation the profile is inclined to the right until it will overturn.

Equation (2.7) is the evolution equation of small-amplitude waves in nonlinear elastic materials, see Braun [37].

2.2 Cnoidal waves

A *cnoidal wave* is a nonlinear and exact periodic wave solution of the Korteweg–de Vries equation. These solutions are in terms of the Jacobi elliptic function cn , therefore they are coined cnoidal waves [32].

The Korteweg–de Vries equation, in its standardised form

$$u_t + 3(u^2)_x + u_{xxx} = 0, \quad (2.10)$$

admits solutions of the form

$$u(x, t) = q(\theta), \quad \theta = x - ct \quad (2.11)$$

which describe waves propagating without distortion at a velocity c . The KdV equation (2.10) integrated twice yields a first-order differential equation of the form

$$\frac{dq}{d\theta} = \pm \sqrt{f(q)}, \quad (2.12)$$

where f is a third-order polynomial of the form

$$f(q) = 2B + 2Aq + cq^2 - 2q^3 \quad (2.13)$$

with integration constants A and B . The further analysis depends on the behaviour of this function, i.e., on the values of its coefficients. Neither the integration constants A and B , nor the velocity c are known in advance.

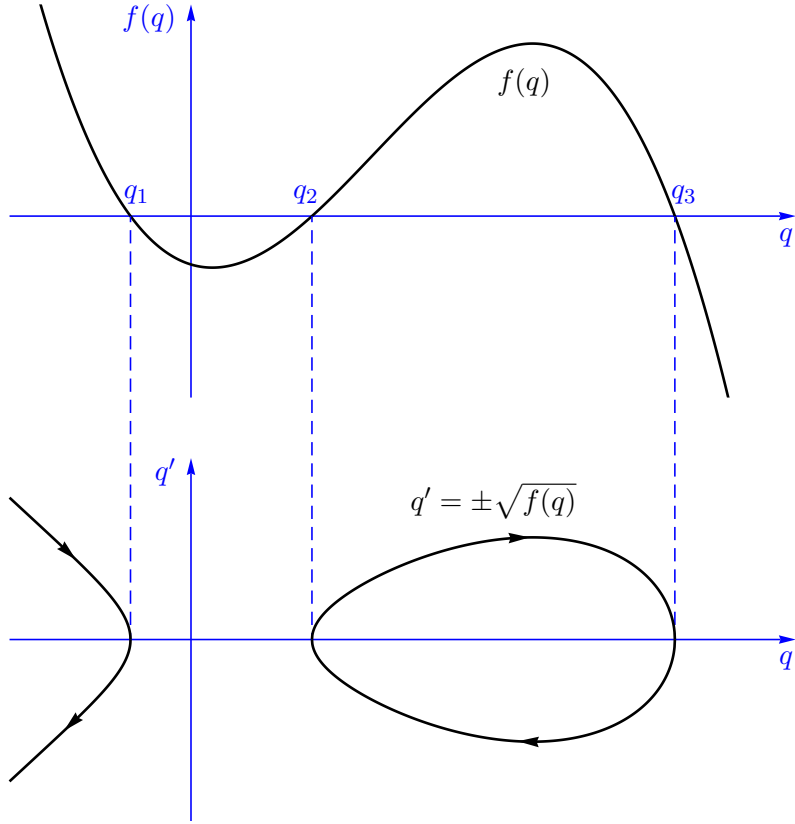


Figure 8: Function $f(q)$ and corresponding phase curve

The analysis will be restricted to the case where the function $f(q)$ has three real zeros $q_1 \leq q_2 < q_3$. Then the function can also be written in the form

$$\begin{aligned} f(q) &= 2(q - q_1)(q - q_2)(q_3 - q) = \\ &= 2 [q_1 q_2 q_3 - (q_1 q_2 + q_1 q_3 + q_2 q_3)q + (q_1 + q_2 + q_3)q^2 - q^3]. \end{aligned} \quad (2.14)$$

Instead of the unknown coefficients A , B , c the roots q_1 , q_2 , q_3 are introduced as parameters. Comparing (2.14) with (2.13) yields the propagation velocity

$$c = 2(q_1 + q_2 + q_3). \quad (2.15)$$

The corresponding expressions for A and B are irrelevant.

A typical curve progression of the function $f(q)$, together with the corresponding phase curve $q'(q)$ according to (2.12), is shown in Figure 8. Since the function $f(q)$ is negative for large values of q , real solutions are possible only for $q \leq q_3$ where q_3 is the largest zero of the polynomial $f(q)$. For $q \rightarrow -\infty$,

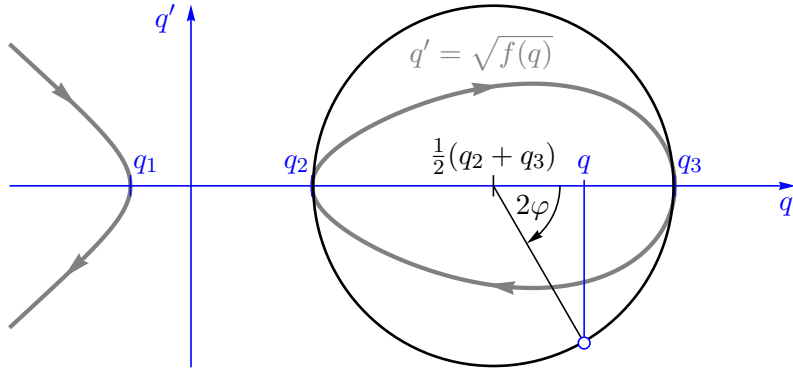


Figure 9: Geometrical interpretation of the variable φ

the polynomial is positive but tends to infinity. Therefore the corresponding branch for $q < q_1$ is not of interest. Bounded solutions are possible only for $q_2 \leq q \leq q_3$. The closed phase curve between q_2 and q_3 is traversed in clockwise sense as always in a phase plane, since positive values of q' means growing values of q .

The differential equation (2.12) can be integrated by separation of variables. Without loss of generality one may assume that q attains its maximum value q_3 at $\theta = 0$. Using this as initial condition for the definite integration, the values of q will decrease as θ increases. Therefore the negative sign in (2.12) is chosen. Thus the integration yields

$$\theta = \int_{q_3}^q \frac{-dq}{\sqrt{f(q)}}, \quad (2.16)$$

where $f(q)$ is the third-order polynomial (2.14). Integrals of this kind can always be expressed in terms of elliptic integrals [35, Chapter 17].

In order to evaluate the integral explicitly the dependent variable q is transformed by[†]

$$q = q_2 + (q_3 - q_2) \cos^2 \varphi = \frac{1}{2}(q_2 + q_3) + \frac{1}{2}(q_3 - q_2) \cos 2\varphi. \quad (2.17)$$

Geometrically, 2φ represents the angle measured along a kind of Mohr's circle which is fit in the gap between the zeros q_2 and q_3 , see Figure 9. Using the abbreviation

$$\frac{q_3 - q_2}{q_3 - q_1} = k^2 \quad (2.18)$$

[†]Gröbner and Hofreiter [36, page 78] recommend a different substitution which, of course, must lead to the same result. It seems, however, that the one given here is simpler.

the factors of which the polynomial $f(q)$ is composed are obtained as

$$\begin{aligned} q - q_1 &= q_2 - q_1 + (q_3 - q_2) \cos^2 \varphi = (q_3 - q_1)(1 - k^2 \sin^2 \varphi), \\ q - q_2 &= (q_3 - q_2) \cos^2 \varphi, \\ q_3 - q &= (q_3 - q_2) \sin^2 \varphi. \end{aligned} \quad (2.19)$$

The differential dq is transformed as

$$dq = -2(q_3 - q_2) \sin \varphi \cos \varphi d\varphi. \quad (2.20)$$

Thus the integral (2.16) is converted to

$$\theta = \int_{q_3}^q \frac{-dq}{\sqrt{f(q)}} = \sqrt{\frac{2}{q_3 - q_1}} \int_0^\varphi \frac{d\varphi}{\sqrt{1 - k^2 \sin^2 \varphi}}. \quad (2.21)$$

The incomplete elliptic integral of the first kind is defined as [35, Chapter 17]

$$F(\varphi; k) = \int_0^\varphi \frac{d\varphi}{\sqrt{1 - k^2 \sin^2 \varphi}}, \quad (2.22)$$

where k , $0 \leq k \leq 1$, denotes the modulus of the integral. Using the abbreviation

$$\eta = \sqrt{\frac{q_3 - q_1}{2}} \quad (2.23)$$

the integral (2.21) can be written as

$$\eta\theta = F(\varphi; k), \quad (2.24)$$

where the modulus k of the elliptic integral is defined by (2.18).

In the next step equation (2.24) has to be solved for φ . The inverse function of the incomplete elliptic integral of the first kind is the function ‘‘amplitudo’’ defined by

$$y = \text{am}(x; k) \Leftrightarrow x = F(y; k). \quad (2.25)$$

Thus the auxiliary angle φ in (2.24) can be expressed by

$$\varphi = \text{am}(\eta\theta; k). \quad (2.26)$$

In order to find back to the original variable q the transformation (2.17) has to be reversed. The transformation formula contains the cosine of the angle φ which in turn is the amplitudo function of $\eta\theta$. The composition of these two functions, i.e., the cosine of the amplitudo or, in Latin, *cosinus amplitudinis*,

$$\text{cn } x = \cos \text{am } x, \quad (2.27)$$

is one of the Jacobian elliptic functions, see [35, Chapter 16]. Thus inserting the solution (2.26) into the transformation formula (2.17) yields the solution

$$q = q_2 + 2\eta^2 k^2 \operatorname{cn}^2(\eta\theta; k), \quad (2.28)$$

where the modulus k and the width parameter η are defined by (2.18) and (2.23), respectively.

The elliptic function cn is periodic, its full period being $4K(k)$, where

$$K(k) = F\left(\frac{\pi}{2}; k\right) = \int_0^{\frac{\pi}{2}} \frac{d\varphi}{\sqrt{1 - k^2 \sin^2 \varphi}} \quad (2.29)$$

denotes the complete elliptic integral of the first kind. For $k \rightarrow 1$ this integral tends to infinity. Thus (2.28) represents a periodic wave if $k < 1$ and the period tends to infinity for $k \rightarrow 1$. In the limit case $k = 1$ the cosinus amplitudinis function becomes [35, Formula 16.6.2]

$$\operatorname{cn}(x; 1) = \operatorname{sech} x \quad (2.30)$$

which is not periodic anymore. So the solitary wave

$$q = q_2 + 2\eta^2 \operatorname{sech}^2 \eta\theta \quad (2.31)$$

is just a limiting case of the more general cnoidal wave (2.28).

Figure 10 shows cnoidal waves with different moduli k .

2.3 Higher-order KdV equations

The solitary waves propagate keeping their shape and transferring their energy over long distances due to the result of a balance between nonlinearity and dispersion. However, the features of the solitary wave depend on the type of nonlinear and dispersive terms in the governing equation. In addition to the KdV equation itself, significant attention by many authors has been paid to the KdV equations with additional higher-order dispersive or nonlinear terms in order to describe the physical effects with the needed accuracy. Some examples are presented below.

Hunter and Scheurle [38] have studied the existence of perturbed solitary wave solutions to a model equation for water waves, proving the existence of travelling wave solutions to a fifth-order partial differential equation,

$$u_t + uu_x + du_{3x} + u_{5x} = 0, \quad (2.32)$$

which is a formal asymptotic approximation for water waves with surface tension.

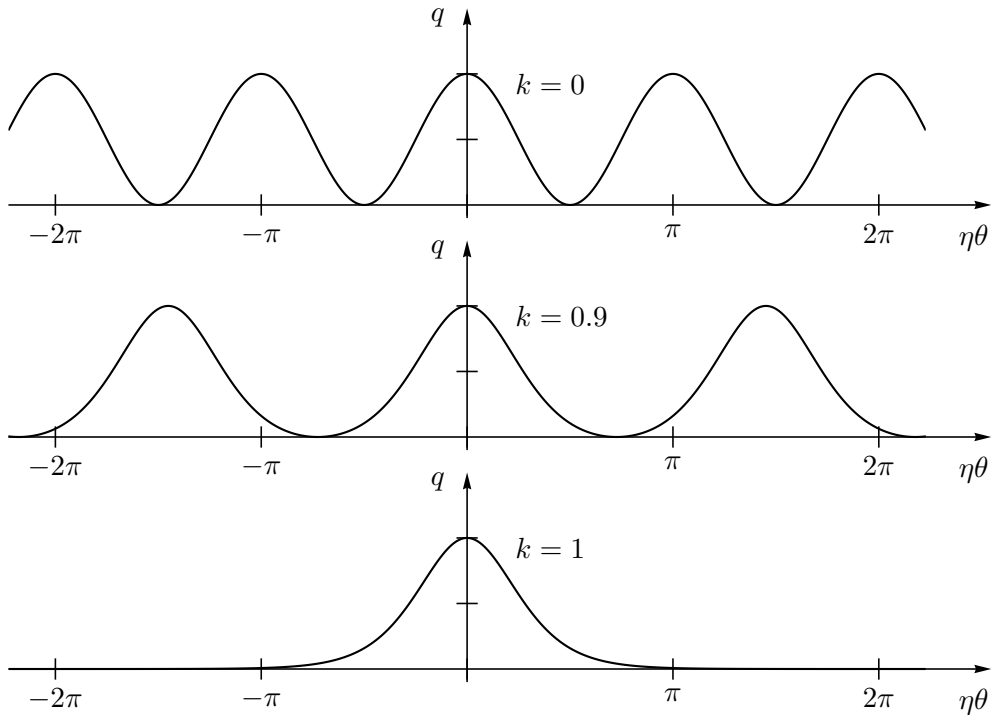


Figure 10: Periodic and solitary wave solutions of the KdV equation

Karpman and Vanden-Broeck [39] have shown numerically that the higher-order dispersion term, i.e., the fifth-order derivative in the equation

$$u_t + \alpha u^p u_x + \beta u_{3x} + \gamma u_{5x} = 0, \quad (2.33)$$

plays a crucial part in soliton stability. It has been demonstrated that in the absence of higher-order dispersion, solitons with sufficiently high nonlinearities in the equations are unstable with respect to collapse-type instabilities, which agrees with the general theory of collapse. The instabilities have not been detected in the presence of fifth-order dispersion, which shows that the latter plays a stabilizing role.

Kakutani and Ono [40] have treated hydromagnetic waves with small but finite amplitude in a cold collision-free plasma. In the lowest order of perturbation, it can be shown that the system of equations for the magneto-acoustic wave propagating along a “critical” direction is reduced to a simple dispersive equation similar to the Korteweg–de Vries equation except that the third-order derivative (the dispersion term) is replaced by the fifth-order one,

$$u_t + uu_x + u_{5x} = 0. \quad (2.34)$$

O. Ilison and Salupere [41, 42] and Salupere et al. [43] have studied the equation

$$u_t + [P(u)]_x + du_{3x} + bu_{5x} = 0, \quad (2.35)$$

describing the wave propagation in shape memory alloys where the higher-order dispersion is caused by the crystal structure. Here d and b denote the third- and the fifth-order dispersion parameters, respectively, and

$$P(u) = \left(-\frac{u^2}{2} + \frac{u^4}{4} \right) \quad (2.36)$$

is the fourth-order elastic potential.

By Holloway, E. Pelinovsky and Talipova [44] the equation, also known as Gardner equation,

$$u_t + \alpha uu_x + \beta u^2 u_x + \delta u_{xxx} = 0 \quad (2.37)$$

has been used as a model of strongly nonlinear internal ocean waves. The coefficient β of the cubic nonlinear term may have a different sign depending on the fluid stratification. It is a popular model for the description of internal solitary waves in shallow seas (see, for instance, the review article by Grimshaw [45] and the article by Grimshaw et al. [46]).

Porubov et al. [47] have studied the influence of higher-order nonlinear terms on the shape of solitary waves for mechanical systems governed by a generalisation of the fifth-order Korteweg–de Vries equation

$$u_t + 2buu_x + 3cu^2u_x + ruu_{3x} + su_xu_{xx} + du_{3x} + fu_{5x} = 0, \quad (2.38)$$

which appears, in particular, in the shallow water theory, see [48] and references therein. The equation (2.38) may be used for a modelling of weak nonlocality in solids [49] and it may account for a continuum limit of discrete models with far neighbour interactions [50].

Kawamoto [51] has considered the Korteweg–de Vries equation with higher-order nonlinearity

$$u_t + (\alpha u^3 + \beta u^2 + \gamma u) u_x + \delta u_{3x} = 0 \quad (2.39)$$

as a model for the wave propagation in a one-dimensional nonlinear lattice or nonlinear LC network. Here α , β , γ and δ denote arbitrary constants.

Tan, Yang and D. Pelinovsky [52] have studied the evolution of perturbed embedded solitons in the case of the general Hamiltonian fifth-order Korteweg–de Vries equation

$$u_t + u_{3x} + u_{5x} + [N(u)]_x = 0, \quad (2.40)$$

where the nonlinear term $N(u)$ is of the form

$$N(u) = \alpha_0 u^2 + \alpha_1 uu_{xx} + \alpha_2 u_x^2 + \alpha_3 u^3. \quad (2.41)$$

It has been shown in [52] that, when an embedded soliton of the fifth-order KdV equation is perturbed, it sheds some continuous-wave radiation in front of the soliton.

Kudryashov and Sinelshchikov [53] have considered nonlinear waves in bubbly liquids with consideration for viscosity and heat transfer. They have presented the equation

$$u_t + \alpha uu_x + u_{xxx} = (uu_{xx})_x + \beta u_x u_{xx} \quad (2.42)$$

describing the evolution of waves in a liquid with gas bubbles.

Giovine and Oliveri [54] have derived the equation

$$u_t + uu_x + \alpha_1 u_{xxx} + \beta (u_t + uu_x + \alpha_2 u_{xxx})_{xx} = 0 \quad (2.43)$$

as a model for one-dimensional wave propagation in dilatant granular materials. The equation (2.43) consists of two Korteweg–de Vries operators, the first of them describing the motion in macrostructure, and the second one (in parenthesis) the motion in microstructure. Here u is the bulk density, x is the space coordinate, t is the time coordinate, α_1 and α_2 are the macro- and microlevel dispersion parameters, respectively, and β is a parameter involving the ratio of the grain size to the wavelength.

All these equations are modifications and extensions of the classical KdV equation describing certain deviations from the classical KdV-like behaviour due to higher-order dispersion and modified nonlinearities. In this work the evolution equation

$$u_t + 3(u^2)_x + u_{xxx} + 3\varepsilon (u_x^2)_{xx} = 0 \quad (2.44)$$

is derived. It describes the slow variations of longitudinal solitary waves propagating in microstructured solids. The small parameter ε at the last term is responsible for the influence of micro-nonlinearity. The detailed derivation and analysis of the equation (2.44) will be presented later in this thesis.

In general, of course, in models of wave motion also damping should be taken into account (see, for instance, Grimshaw et al. [57] and Demiray [58]), but dissipative effects are out of the focus of this thesis.

3 Material model

3.1 Microstructured materials

Materials with some microstructure, like sand, soil, concrete, or even alloys, have always been used and their behaviour has been described by special theories. A more general point of view came up with the advent of a new generation of microstructured materials like modern metallic alloys, ceramic composites, polycrystalline solids, functionally graded materials, granular, porous materials, etc. They are used for a wide variety of industrial applications since combining the mechanical properties of different constituents, as in composites, yields optimal properties of solids. An illustration of a microstructured material is presented in Figure 11.

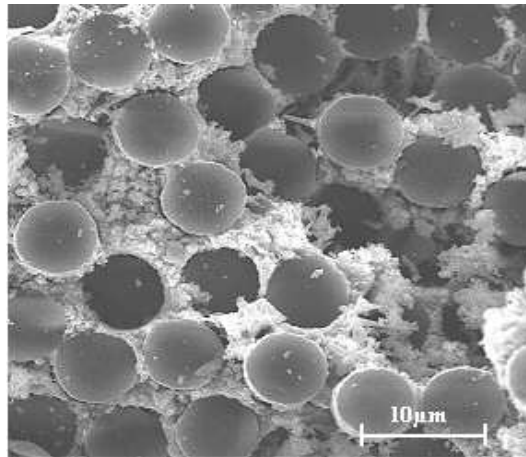


Figure 11: Ceramic matrix composites: scanning electron microscopic view on a fracture surface of C/SiC. Source: <http://www.fz-juelich.de>

In principle, every material has some small-scale structure, since material is never distributed continuously. Microstructure in our sense is not related to the molecular or atomic scale. Rather these microstructures are assumed in the range of micrometers, so that they still can be considered as continua. The overall material becomes highly nonhomogeneous due to the embedded microstructures with their different behaviour.

Many theories of microstructured materials aim to smooth out this inhomogeneity while retaining its influence on the gross behaviour of the material. This is done by giving the material more internal degrees of freedom describing the behaviour of the embedded microstructures. So the ordinary but highly inhomogeneous material is turned into a homogeneous material which, however, is equipped with more than just a displacement field. Corresponding theories

can be traced back to the meanwhile classical papers by Mindlin [1] and Sun et al. [2]. The connection to Cosserat continua has been established by Herrmann and Achenbach [3].

The application of severe loading conditions, including impact, means generation of deformation waves. The embedding of a microstructure in an elastic material is reflected in an inherent length scale causing dispersion of propagating waves. Nonlinear effects, if taken into account, will counteract dispersion. It is well known that a suitable balance of nonlinearity and dispersion may permit the propagation of solitary waves.

3.2 Mindlin's model

In the usual continuum material points are points in a mathematical sense which undergo some displacement \mathbf{u} when the material is deformed, see Figure 12.

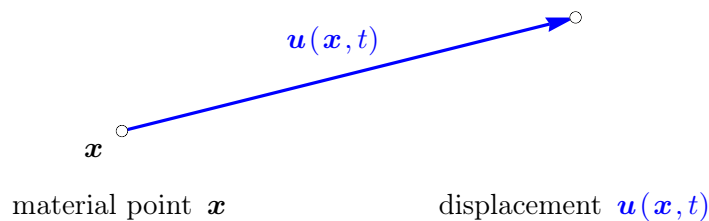


Figure 12: Standard continuum

The material points can be augmented by some ambient material. If this is assumed to be rigid it still can undergo a microrotation, in addition to the translation described by the displacement vector. This concept leads to the Cosserat continuum, see Figure 13.

More generally the ambient material itself can undergo a homogeneous microdeformation which may depend on the material point \mathbf{x} . The deformation of the microstructured material is described by the displacement vector \mathbf{u} of the central point and the homogeneous microdeformation $\mathbf{\Phi}$ of the ambient material. This is the basic idea of a microstructured continuum in the sense of Mindlin, see Figure 14.

According to Mindlin's model of a microstructured solid [1] any material point of the solid represents itself a microcontinuum subject to some deformation. The overall deformation of the microstructured continuum is then described by the macroscopic displacements of its material points, i.e., the centres of the microcontinua, and by the deformation of the microcontinua themselves.

such that the microdeformation

$$\frac{\partial \mathbf{u}'}{\partial \mathbf{x}'} = \mathbf{\Phi}(\mathbf{x}, t) \quad (3.2)$$

is constant throughout the microelement but may depend on the initial position \mathbf{x} of its center.

Mindlin's original formulation of the theory uses coordinates and components [1], see also [59], but its essence is as described above. It represents a linear theory of a three-dimensional, elastic continuum sharing some properties of a crystal lattice by including the idea of a unit cell into the theory. According to Mindlin, the unit cell may be interpreted as a molecule of a polymer, a crystallite of a polycrystal or a grain of a granular material. The mathematical model of the cell is a linear version of Ericksen and Truesdell's deformable directors [7]. If the cell is made rigid, the equations reduce to those of a linear Cosserat continuum [8].

The equations yield wave-dispersion relations with acoustic and optical branches of the same character as those found at long wavelengths in crystal lattice theories and observed in neutron scattering experiments. The method of derivation of the equations is analogous to one used in deducing two-dimensional equations of high-frequency vibrations of plates from the three-dimensional equations of classical linear elasticity. The equations have been shown to reduce at low frequencies and very long wavelengths in isotropic materials to those of an elastic continuum with potential energy density dependent on strain and strain gradient and kinetic energy density dependent on velocity and velocity gradient.

A linear form of Toupin's [60] generalisation of couple-stress theory is obtained by eliminating the difference between the deformation of the unit cell and the surrounding medium, and linear couple-stress theory itself is obtained by eliminating the symmetric part of the strain gradient. Both of these special cases are also limited to low frequencies and very long wavelengths.

3.3 Mindlin–Engelbrecht–Pastrone model

The one-dimensional version of Mindlin's model, as formulated by Engelbrecht and Pastrone [9, 59, 61], is described by two scalar functions, the macro-displacement $u(x, t)$ and the micro-strain $\varphi(x, t)$, both depending on the material coordinate x and the time t . Their relevance is sketched in Figure 15. In the sequel, subscripts x and t will indicate partial derivatives with respect to the material coordinate x and the time t , respectively. In order to clarify the principal essence and the role of parameters of the model, we repeat here the basic steps of modelling.

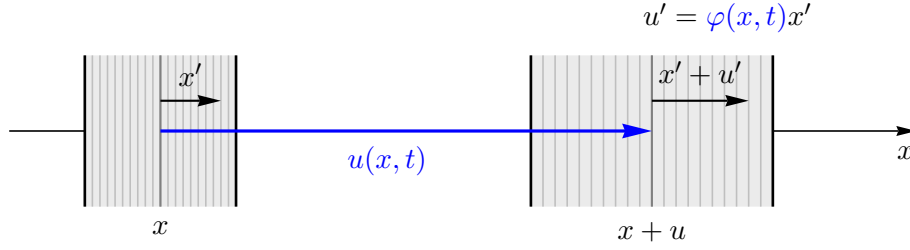


Figure 15: 1D microstructured material

The kinetic energy density is composed of its macroscopic and microscopic contributions,

$$K = \frac{1}{2}\rho u_t^2 + \frac{1}{2}I\varphi_t^2, \quad (3.3)$$

where ρ and I denote the macroscopic density and the microinertia, respectively. All densities, like ρ , I or the kinetic-energy density K itself, are understood per unit length rather than per unit volume, due to the one-dimensional model. The strain energy or potential energy density, again per unit length, is assumed to depend on the macro-strain u_x , the micro-strain φ and its gradient φ_x ,

$$W = W(u_x, \varphi, \varphi_x). \quad (3.4)$$

By invoking the Euler-Lagrange equations for the Lagrangian density $L = K - W$ one obtains the equations of motion

$$\rho u_{tt} = \sigma_x, \quad I\varphi_{tt} = \eta_x - \tau \quad (3.5)$$

representing the balances of macro- and micromomentum. The stress quantities entering these balances are the derivatives of the strain energy (3.4) with respect to its arguments, namely the macrostress, the microstress, and a quantity called the interactive force,

$$\sigma = \frac{\partial W}{\partial u_x}, \quad \eta = \frac{\partial W}{\partial \varphi_x}, \quad \tau = \frac{\partial W}{\partial \varphi}, \quad (3.6)$$

respectively. It should be noted that, in the one-dimensional setting, the stresses σ and τ have the dimension of force while η has the dimension of a moment.

Up to now the strain energy function has not yet been specified. Following [9, 10, 62] we consider the strain energy function

$$W = \frac{1}{2}(\alpha u_x^2 + 2A u_x \varphi + B \varphi^2 + C \varphi_x^2) + \frac{1}{6}(N u_x^3 + M \varphi_x^3) \quad (3.7)$$

involving cubic terms, where α , A , B , C and N , M are material constants. The stresses (3.6) are then

$$\sigma = \alpha u_x + A\varphi + \frac{1}{2}N u_x^2, \quad \tau = A u_x + B\varphi, \quad \eta = C\varphi + \frac{1}{2}M \varphi_x^2, \quad (3.8)$$

and the balance equations (3.5) assume the form

$$\begin{aligned}\rho u_{tt} &= \alpha u_{xx} + A\varphi_x + \frac{1}{2}N(u_x^2)_x, \\ I\varphi_{tt} &= C\varphi_{xx} - Au_x - B\varphi + \frac{1}{2}M(\varphi_x^2)_x.\end{aligned}\tag{3.9}$$

The first of these equations governs the macro-displacement $u(x, t)$, which is regarded as the main kinematic variable. The equation, however, is coupled to the second equation which governs the micro-deformation $\varphi(x, t)$.

3.4 Slaving principle

To study the propagation of waves in the microstructured solid it would be comfortable to have a single partial differential equation for the macroscopic displacement which, however, retains the influence of the microstructure. In principle, the system of equations (3.9) could be contracted to a single equation without neglecting any terms. It would contain time derivatives of fourth order.

The objective of this thesis and related papers is, however, to study waves corresponding to the acoustical branch and how they are influenced by the presence of the microstructure. To this end, a single partial differential equation is extracted from the system (3.9) which describes a motion in which the macro-displacement prevails while retaining the influence of the microstructure. The procedure to obtain the approximate equation, called the “slaving principle”, is explained in detail in papers by Pastrone and Engelbrecht [9, 61].

Solving the second equation (3.9)₂ for the micro-strain one obtains

$$\varphi = -\frac{A}{B}u_x - \frac{1}{B}(I\varphi_{tt} - C\varphi_{xx}) + \frac{M}{2B}(\varphi_x^2)_x.\tag{3.10}$$

From the original material constants one inherent length and several characteristic velocities can be extracted. The inherent length represents the size of the microstructure. In order to consider this to be small one first has to choose a reference length scale ℓ . The inherent length is then introduced by

$$(\delta\ell)^2 = \frac{IA^2}{\rho B^2},\tag{3.11}$$

where the small number $\delta \ll 1$ specifies the size of the microstructure to be small compared to the reference length ℓ . Further the characteristic velocities \bar{c} , c_1 , c_N and c_M are introduced by

$$\bar{c}^2 = \frac{1}{\rho} \left(\alpha - \frac{A^2}{B} \right), \quad c_1^2 = \frac{C}{I}, \quad c_N^2 = \frac{N}{\rho}, \quad c_M^2 = \frac{MA}{IB\ell}.\tag{3.12}$$

Thus one can write equation (3.10) in the form

$$\varphi = -\frac{A}{B}u_x - \frac{\delta^2 \ell^2 \rho B}{A^2} \left[\varphi_{tt} - c_1^2 \varphi_{xx} - \frac{c_M^2 \ell B}{2A} (\varphi_x^2)_x \right]. \quad (3.13)$$

The variable φ can be expanded in powers of δ^2 as

$$\varphi = \varphi_0 + \delta^2 \varphi_2 + \delta^4 \varphi_4 + \dots \quad (3.14)$$

This expansion is now inserted into equation (3.13). Collecting powers of the same order leads to the equations

$$O(1): \quad \varphi_0 = -\frac{A}{B}u_x, \quad (3.15)$$

$$O(\delta^2): \quad \varphi_2 = -\frac{\ell^2 \rho B}{A^2} \left(\varphi_{0tt} - c_1^2 \varphi_{0xx} - \frac{c_M^2 \ell B}{A} \varphi_{0x} \varphi_{0xx} \right), \quad (3.16)$$

⋮

Substituting (3.15) into (3.16) we obtain

$$\varphi_2 = \frac{\ell^2 \rho}{A} (u_{xtt} - c_1^2 u_{xxx} + c_M^2 \ell u_{xx} u_{xxx}). \quad (3.17)$$

Thus the expansion (3.14) yields

$$\varphi = -\frac{A}{B}u_x + \frac{\delta^2 \ell^2 \rho}{A} (u_{xtt} - c_1^2 u_{xxx} + c_M^2 \ell u_{xx} u_{xxx}). \quad (3.18)$$

Inserting this into the first equation (3.9)₁ the governing equation assumes the form

$$u_{tt} = \bar{c}^2 u_{xx} + \frac{1}{2} c_N^2 (u_x^2)_x + (\delta \ell)^2 \left(u_{tt} - c_1^2 u_{xx} + \frac{1}{2} \ell c_M^2 u_{xx}^2 \right)_{xx}. \quad (3.19)$$

In a final step the dimensionless variables

$$X = \frac{x}{\ell}, \quad T = \frac{\bar{c}t}{\ell}, \quad \epsilon U = \frac{u}{\ell} \quad (3.20)$$

are introduced. The normalization of the displacement includes another small number $\epsilon \ll 1$, which emphasises that the displacement u is small compared to the reference length ℓ . The nondimensional form of the governing equation (3.24) is now obtained as

$$U_{TT} = U_{XX} + \frac{1}{2} \epsilon \gamma_N^2 (U_X^2)_X + \delta^2 \left(U_{TT} - \gamma_1^2 U_{XX} + \frac{1}{2} \epsilon \gamma_M^2 U_{XX}^2 \right)_{XX}, \quad (3.21)$$

where the velocity ratios

$$\gamma_1 = \frac{c_1}{\bar{c}}, \quad \gamma_N = \frac{c_N}{\bar{c}}, \quad \gamma_M = \frac{c_M}{\bar{c}} \quad (3.22)$$

have been introduced. The macro-nonlinearity is controlled by the small number ϵ , which measures the size of the amplitude, the dispersion is governed by the small number δ^2 emerging from the size of the microstructure, and the micro-nonlinearity is influenced by both numbers.

It should be noted that the normalization of time (3.20)₂ is based on the velocity \bar{c} which seems to be the most natural inherent velocity. Therefore the normalised equation (3.21) differs from the one presented in [9], where the normalization is based on the velocity $c_0 = \sqrt{\alpha/\rho}$.

The approximation can be derived also in a heuristic way [55] (Publication III) which leads to the same result as the rigorous treatment described above. The first step is the same as above, leading to (3.10). This is still a partial differential equation for the micro-strain $\varphi(x, t)$, whose partial derivatives appear on the right-hand side.

In a first, rather crude approximation these derivatives are omitted such that the micro-strain is expressed explicitly as $\varphi \approx -(A/B)u_x$ in terms of the macro-strain u_x . This expression is reinserted into the right-hand side of (3.10) to provide the better approximation

$$\varphi = -\frac{A}{B}u_x + \frac{A}{B^2}(Iu_{tt} - Cu_{xx})_x + \frac{A^2M}{2B^3}(u_{xx}^2)_x, \quad (3.23)$$

by which the micro-strain is expressed explicitly in terms of the macro-strain u_x and its derivatives. This expression can be inserted into the first equation (3.9)₁ which becomes a nonlinear fourth-order differential equation for the displacement $u(x, t)$,

$$\begin{aligned} \rho u_{tt} = & \left(\alpha - \frac{A^2}{B} \right) u_{xx} + \frac{A^2}{B^2} (Iu_{tt} - Cu_{xx})_{xx} + \\ & + \frac{1}{2} \left[N (u_x^2)_x + M \frac{A^3}{B^3} (u_{xx}^2)_{xx} \right]. \end{aligned} \quad (3.24)$$

This equation can still be condensed by introducing normalised variables and corresponding parameters presented before, yielding finally the nondimensional governing equation (3.21).

3.5 Evolution equation

If nonlinear and dispersive terms were absent in the governing equation (3.21) a simple wave equation would remain, whose general solution would allow left

and right going waves of arbitrary shape traveling undisturbed. Due to the normalization their speed would be unity. To include the cumulative effects of the additional nonlinear and dispersive terms in the governing equation we allow the wave profile to change slowly in time.

Here we follow the *reductive perturbation method* described in [26, 63, 64]. It is possible to express the equation (3.21) in the matrix form

$$\begin{aligned} \frac{\partial \mathbf{V}}{\partial T} - \tilde{A} \frac{\partial \mathbf{V}}{\partial X} - \delta^2 \frac{\partial^2}{\partial X^2} \left(\frac{\partial \mathbf{V}}{\partial T} - \tilde{B} \frac{\partial \mathbf{V}}{\partial X} \right) \\ - \epsilon \gamma_N^2 \frac{\partial U}{\partial X} \tilde{C} \frac{\partial \mathbf{V}}{\partial X} - \delta^2 \epsilon \gamma_M^2 \frac{\partial}{\partial X} \left(\frac{\partial^2 U}{\partial X^2} \tilde{C} \frac{\partial^2 \mathbf{V}}{\partial X^2} \right) = 0, \end{aligned} \quad (3.25)$$

where \mathbf{V} is a state vector

$$\mathbf{V} = \begin{bmatrix} U_T \\ U_X \end{bmatrix},$$

and \tilde{A} , \tilde{B} , and \tilde{C} are the following matrices

$$\tilde{A} = \begin{bmatrix} 0 & 1 \\ 1 & 0 \end{bmatrix}, \quad \tilde{B} = \begin{bmatrix} 0 & \gamma_1^2 \\ 1 & 0 \end{bmatrix}, \quad \tilde{C} = \begin{bmatrix} 0 & 1 \\ 0 & 0 \end{bmatrix}.$$

Selecting a right going wave the solution is assumed in the form

$$U = f(\xi, \tau), \quad \xi = X - T, \quad \tau = \frac{1}{2} \epsilon T, \quad (3.26)$$

as suggested in [65, page 6], with a small parameter ϵ . It is possible to develop both the vector \mathbf{V} and U into the power series in the small parameter ϵ

$$\begin{aligned} \mathbf{V} &= \mathbf{V}_0 + \epsilon \mathbf{V}_1 + \epsilon^2 \mathbf{V}_2 + \dots, \\ U &= U_0 + \epsilon U_1 + \epsilon^2 U_2 + \dots. \end{aligned}$$

Substituting the series expansions into the equation (3.25) the following sequence of equations of various powers in the small parameter ϵ is obtained, assuming that δ^2 and ϵ are small quantities of the same order:

$$O(1): \quad \frac{\partial \mathbf{V}_0}{\partial \xi} + \tilde{A} \frac{\partial \mathbf{V}_0}{\partial \xi} = 0, \quad (3.27)$$

$$\begin{aligned} O(\epsilon): \quad \frac{1}{2} \frac{\partial \mathbf{V}_0}{\partial \tau} - \frac{\partial \mathbf{V}_1}{\partial \xi} - \tilde{A} \frac{\partial \mathbf{V}_1}{\partial \xi} + \frac{\partial^3 \mathbf{V}_0}{\partial \xi^3} + \tilde{B} \frac{\partial^3 \mathbf{V}_0}{\partial \xi^3} \\ - \gamma_N^2 \tilde{C} \frac{\partial U_0}{\partial \xi} \frac{\partial \mathbf{V}_0}{\partial \xi} - \epsilon \gamma_M^2 \tilde{C} \left(\frac{\partial^3 U_0}{\partial \xi^3} \frac{\partial^2 \mathbf{V}_0}{\partial \xi^2} + \frac{\partial^2 U_0}{\partial \xi^2} \frac{\partial^3 \mathbf{V}_0}{\partial \xi^3} \right) = 0, \end{aligned} \quad (3.28)$$

⋮

We determine the left and right eigenvectors \mathbf{l}^T and \mathbf{r} , respectively, from the equation

$$\mathbf{l}^T(I + \tilde{A}) = (I + \tilde{A})\mathbf{r} = 0, \quad (3.29)$$

where I is a unit matrix, with the normalizing condition

$$\mathbf{l}^T \cdot \mathbf{r} = 1. \quad (3.30)$$

The solution of the equation (3.27) is

$$\mathbf{V}_0 = \alpha \mathbf{r}, \quad (3.31)$$

where α is an unknown amplitude factor. The left and right eigenvectors are chosen according to the normalizing condition in the form

$$\mathbf{l}^T = \begin{bmatrix} -\frac{1}{2} \\ \frac{1}{2} \end{bmatrix}, \quad \mathbf{r} = \begin{bmatrix} -1 \\ 1 \end{bmatrix}.$$

The next steps of the procedure, namely premultiplying the equation (3.28) by the left eigenvector \mathbf{l}^T , inserting the solution $\mathbf{V}_0 = \alpha \mathbf{r}$ into (3.28) and substituting $\partial U_0 / \partial \xi = \alpha$ yield the evolution equation

$$\alpha_\tau + \frac{1}{2} \gamma_N^2 (\alpha^2)_\xi + (1 - \gamma_1^2) \alpha_{\xi\xi\xi} + \frac{1}{2} \epsilon \gamma_M^2 (\alpha_\xi^2)_{\xi\xi} = 0. \quad (3.32)$$

A simpler but less rigorous derivation of the evolution equation (3.32) is given by Randrüüt and Braun [55]. Namely, inserting the ansatz (3.26) directly into the governing equation (3.21) and discarding higher-order terms we get the equation

$$-f_{\xi\tau} = \frac{1}{2} \gamma_N^2 (f_\xi^2)_\xi + \frac{\delta^2}{\epsilon} \left(f_{\xi\xi} - \gamma_1^2 f_{\xi\xi} + \frac{1}{2} \epsilon \gamma_M^2 f_{\xi\xi}^2 \right)_{\xi\xi}. \quad (3.33)$$

One can realise that the influences of dispersion and nonlinearity, measured by the two small parameters δ and ϵ , are balanced only if the quotient δ^2/ϵ is of the order of unity. Without loss of generality we may assume that ϵ is equal to δ^2 .

Denoting $f_\xi = \alpha$, the evolution equation assumes exactly the form (3.32) given before. Keeping track of the transformations of variables (3.20) one finds

$$u_x = \epsilon \alpha, \quad (3.34)$$

i.e., the new dependent variable α represents a magnified strain. The velocity ratios γ_1 , γ_N and γ_M defined by (3.22) appear as parameters in the evolution equation (3.32) and are responsible for dispersion, macro-nonlinearity and micro-nonlinearity, respectively. If the latter is omitted the evolution equation

reduces to the Korteweg–de Vries (KdV) equation studied in Section 2. The additional term representing micro-nonlinearity includes higher derivatives, like the dispersive term $\alpha_{\xi\xi\xi}$, but in addition it is nonlinear.

By suitable transformations of the variables the coefficients of the equation can be standardised. For the KdV equation, Newell [65] suggests the form

$$q_t + 6qq_x + q_{xxx} = 0 \quad (3.35)$$

which, in our case, has to be supplemented by an additional term representing the micro-nonlinearity. This standardised form is achieved by the transformation

$$\alpha = \frac{6}{\gamma_N^2} (1 - \gamma_1^2)^{1/3} q, \quad \xi = (1 - \gamma_1^2)^{1/3} x, \quad \tau = t, \quad (3.36)$$

where, for convenience, the original space and time variables, x and t , have been reused.

By this transformation, the evolution equation (3.32) becomes

$$q_t + 3(q^2)_x + q_{xxx} + 3\varepsilon(q_x)_{xx} = 0, \quad (3.37)$$

in which only one parameter

$$\varepsilon = \frac{\epsilon\gamma_M^2}{(1 - \gamma_1^2)\gamma_N^2} \quad (3.38)$$

remains. It is responsible for the influence of the micro-nonlinearity measured by γ_M as compared to the combined effects of dispersion and macro-nonlinearity.

3.6 Linear case

In the linear case, i.e., $M = N = 0$ the governing system of two second-order equations assumes the form [59, 61, 66]

$$\begin{aligned} \rho u_{tt} &= \alpha u_{xx} + A\varphi_x, \\ I\varphi_{tt} &= C\varphi_{xx} - Au_x - B\varphi, \end{aligned} \quad (3.39)$$

which can also be represented in the form of one fourth-order equation

$$u_{tt} = (c_0^2 - c_A^2) u_{xx} - p^2 (u_{tt} - c_0^2 u_{xx})_{tt} + p^2 c_1^2 (u_{tt} - c_0^2 u_{xx})_{xx}, \quad (3.40)$$

where material parameters

$$c_0^2 = \frac{a}{\rho}, \quad c_1^2 = \frac{C}{I}, \quad c_A^2 = \frac{A^2}{\rho B}, \quad p^2 = \frac{I}{B} \quad (3.41)$$

are introduced. The parameters c_0, c_1, c_A are velocities while p is a time constant. This is the basic *linear* equation governing 1D longitudinal waves in microstructured solids.

Specializing the nonlinear equations derived in Subsections 3.4 and 3.5 to the linear case, equation (3.24) becomes

$$\rho u_{tt} = \left(\alpha - \frac{A^2}{B} \right) u_{xx} + \frac{A^2}{B^2} (I u_{tt} - C u_{xx})_{xx}, \quad (3.42)$$

which can also be written as

$$u_{tt} = (c_0^2 - c_A^2) u_{xx} + p^2 c_A^2 (u_{tt} - c_1^2 u_{xx})_{xx}. \quad (3.43)$$

This approximate linear equation coincides with [66, Eq. (16)]. The corresponding nondimensional versions of this equation have different coefficients because the dimensionless time coordinates are based on different velocities.

The evolution equation (3.32), when reduced to the linear case, assumes the form

$$\alpha_\tau + (1 - \gamma_1^2) \alpha_{\xi\xi\xi} = 0, \quad (3.44)$$

which corresponds to [66, Eq. (24)]. The variables α, ξ, τ , however, are defined differently in [66] (Publication I). Therefore, the two different versions of the linear evolution equation cannot be compared directly.

It has been shown that the approximate linear equation (3.43) and the full linear equation (3.40) yield the evolution equations in the same form, see [66, Eqs. (24) and (27)]. Consequently, using the idea of evolution equations there is no difference whether one begins the derivation from the full equation (3.40) with the addition term u_{tttt} or from the approximate equation (3.43) with terms u_{xxtt} and u_{xxxx} . However, note that the coefficients of the u_{xxtt} and u_{xxxx} terms in the equations (3.40) and (3.43) are different.

The character of dispersion in the case of microstructured materials is analysed in [59] on the basis of the approximate equation (3.43). It has been shown that both of the effects — inertia of the microstructure, described by the term u_{xxtt} , and elasticity of the microstructure, described by the term u_{xxxx} , have influence on dispersive relations and corresponding dispersion curves. If only inertia of the microstructure is taken into account then the dispersion curve is convex, if only elasticity of the microstructure is taken into account then the dispersion curve is concave. With both terms (double dispersion) the curve tends from one asymptote to another.

In the case of the evolution equation (3.44) these two effects are described by a single term $\alpha_{\xi\xi\xi}$ but the sign of this term (the sign of its coefficient) depends on the ratio of the double dispersion effects. It is possible to conclude that in case of $\gamma_1^2 > 1$ the dispersion curve is concave and in case of $\gamma_1^2 < 1$

the dispersion curve is convex. In the case of $1 - \gamma_1^2 = 0$ there is no dispersion. Omitting the term u_{xxxx} in the equation (3.43), i.e., taking into account only microinertia, leads the evolution equation in the form

$$\alpha_\tau + \alpha_{\xi\xi\xi} = 0 \quad (3.45)$$

with a convex dispersion curve (downward cubic parabola). Omitting the term u_{xxtt} , i.e., concentrating on microelasticity, the evolution equation assumes the form

$$\alpha_\tau - \gamma_1^2 \alpha_{\xi\xi\xi} = 0 \quad (3.46)$$

with a concave dispersion curve (upward cubic parabola).

The special case $\gamma_1^2 = 1$ gives now the motivation to turn back from the evolution equation (3.44) to the original equation (3.43) and study in detail all three cases $\gamma_1^2 < 1$, $\gamma_1^2 = 1$ and $\gamma_1^2 > 1$.

Using the definition of (3.12)₁ the full and the reduced linear equations (3.40) and (3.43) can be rewritten as

$$u_{tt} = \bar{c}^2 u_{xx} - p^2 (u_{tt} - c_0^2 u_{xx})_{tt} + p^2 c_1^2 (u_{tt} - c_0^2 u_{xx})_{xx} \quad (3.47)$$

and

$$u_{tt} = \bar{c}^2 u_{xx} + p^2 c_A^2 (u_{tt} - c_1^2 u_{xx})_{xx}, \quad (3.48)$$

respectively. With the usual wave ansatz

$$u = \hat{u} \cos(kx - \omega t) \quad (3.49)$$

one obtains the dispersion relations

$$\omega^2 - \bar{c}^2 k^2 = p^2 (\omega^2 - c_0^2 k^2) (\omega^2 - c_1^2 k^2) \quad (3.50)$$

and

$$\omega^2 - \bar{c}^2 k^2 = -p^2 c_A^2 k^2 (\omega^2 - c_1^2 k^2), \quad (3.51)$$

respectively. These dispersion relations are graphically depicted in Figures 16–17 for different ratios c_1/\bar{c} . The full dispersion relation (3.50) when solved for ω^2 assumes the form

$$\omega^2 = \frac{1}{2p^2} \left\{ 1 + (c_0^2 + c_1^2) p^2 k^2 \pm \sqrt{1 + 2(c_0^2 + c_1^2 - 2\bar{c}^2) p^2 k^2 + (c_0^2 - c_1^2)^2 p^4 k^4} \right\} \quad (3.52)$$

and provides, for any wave number k , two values of the frequency ω . The upper one, starting at $\omega(0) = 1/p$, represents the optical branch, and the lower one, starting at the origin, represents the acoustical branch.

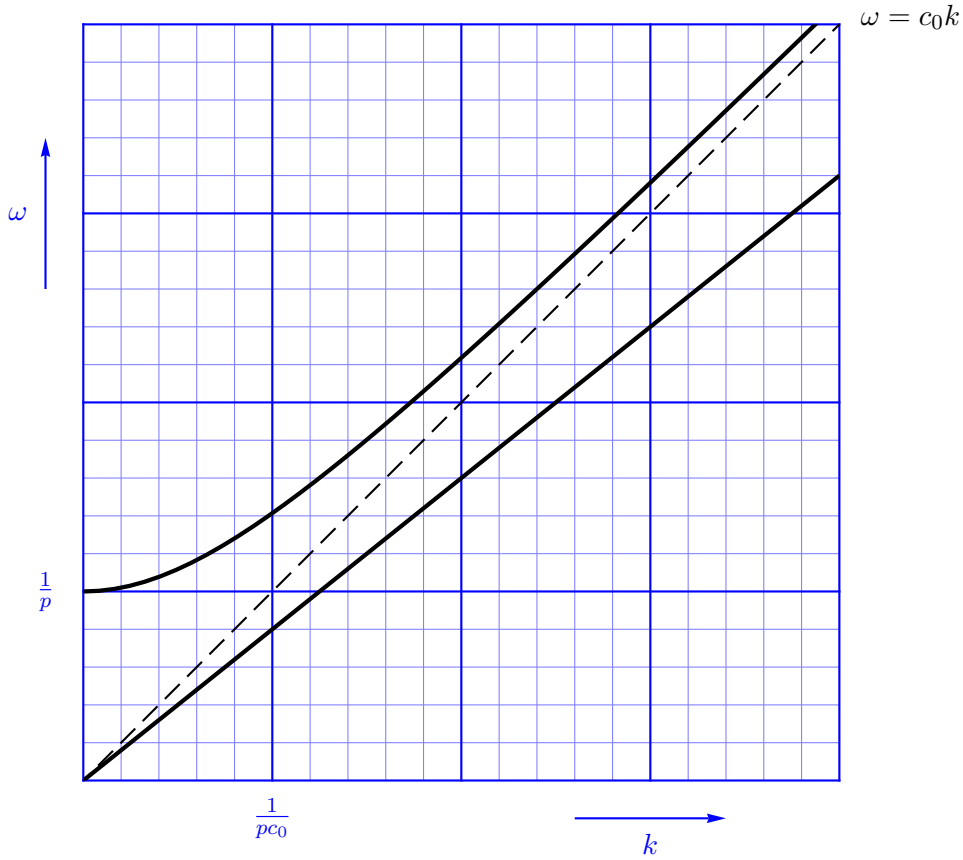


Figure 16: Dispersion diagram in the special case $c_1 = \bar{c}$ ($c_1 = \bar{c} = 0.8 c_0$)

The long-wave behaviour, which means small wave numbers, is obtained by omitting the highest power of k and making use of the well-known approximation formula $\sqrt{1 + \epsilon} \approx 1 + \frac{1}{2}\epsilon$. Thus from (3.52) one obtains the approximation

$$\omega^2 \approx \frac{1}{2p^2} \{1 + (c_0^2 + c_1^2)p^2k^2 \pm [1 + (c_0^2 + c_1^2 - 2\bar{c}^2)p^2k^2]\} \quad (3.53)$$

leading to

$$\omega \approx \begin{cases} \frac{1}{p} + \frac{1}{2} (c_0^2 + c_1^2 - \bar{c}^2) p k^2, \\ \bar{c}k. \end{cases} \quad (3.54)$$

The optical branch starts like a parabola with its vertex at $(0, 1/p)$, while the acoustical branch starts at the origin with the initial slope \bar{c} .

The short-wave behaviour, which means big wave numbers, is obtained by keeping only the highest powers of k , namely k^2 outside and k^4 inside the

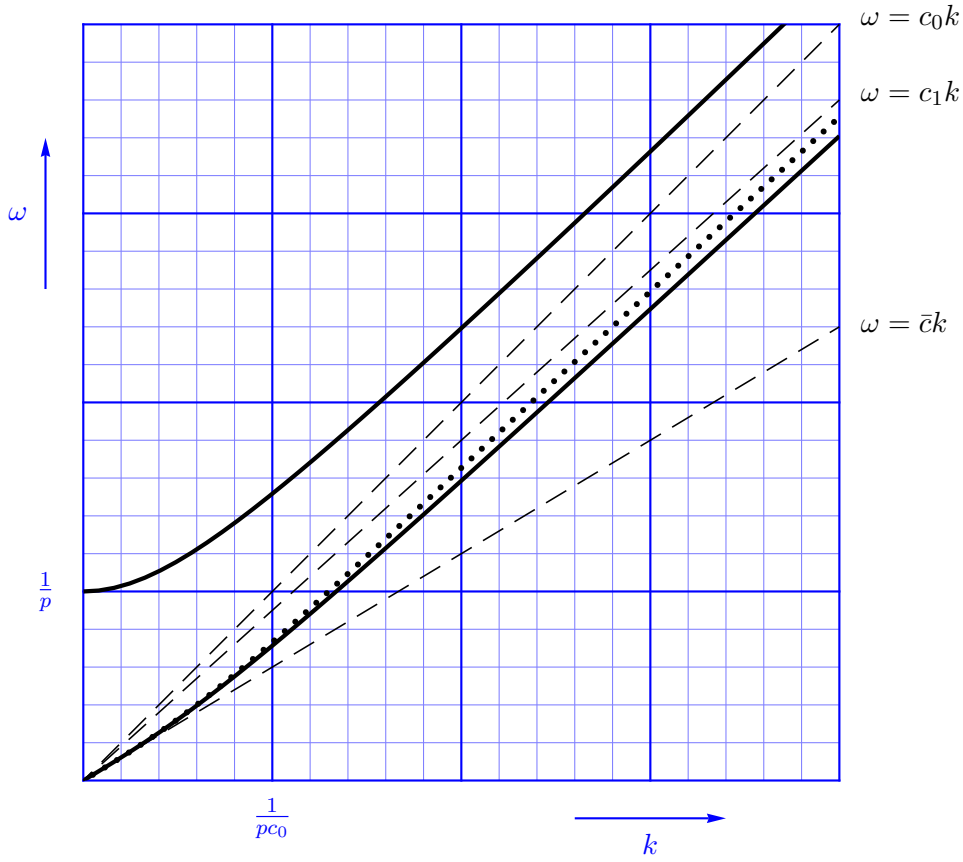


Figure 17: Dispersion diagram in the case $c_1 > \bar{c}$ ($c_1 = 0.9 c_0$, $\bar{c} = 0.6 c_0$)
 — full equation, reduced equation

square root. So one obtains

$$\omega^2 \approx \frac{1}{2p^2} \{ (c_0^2 + c_1^2) p^2 k^2 \pm (c_0^2 - c_1^2) p^2 k^2 \} \quad (3.55)$$

or

$$\omega \approx \begin{cases} c_0 k, \\ c_1 k. \end{cases} \quad (3.56)$$

Thus for short waves, the optical and acoustical branches approach asymptotically the straight lines with slopes c_0 and c_1 , respectively.

The reduced dispersion relation (3.51) when solved for ω^2 gives

$$\omega^2 = \frac{(\bar{c}^2 + c_A^2 c_1^2 p^2 k^2) k^2}{1 + c_A^2 p^2 k^2}. \quad (3.57)$$

For any value of the wave number k there is only one value of the frequency ω .

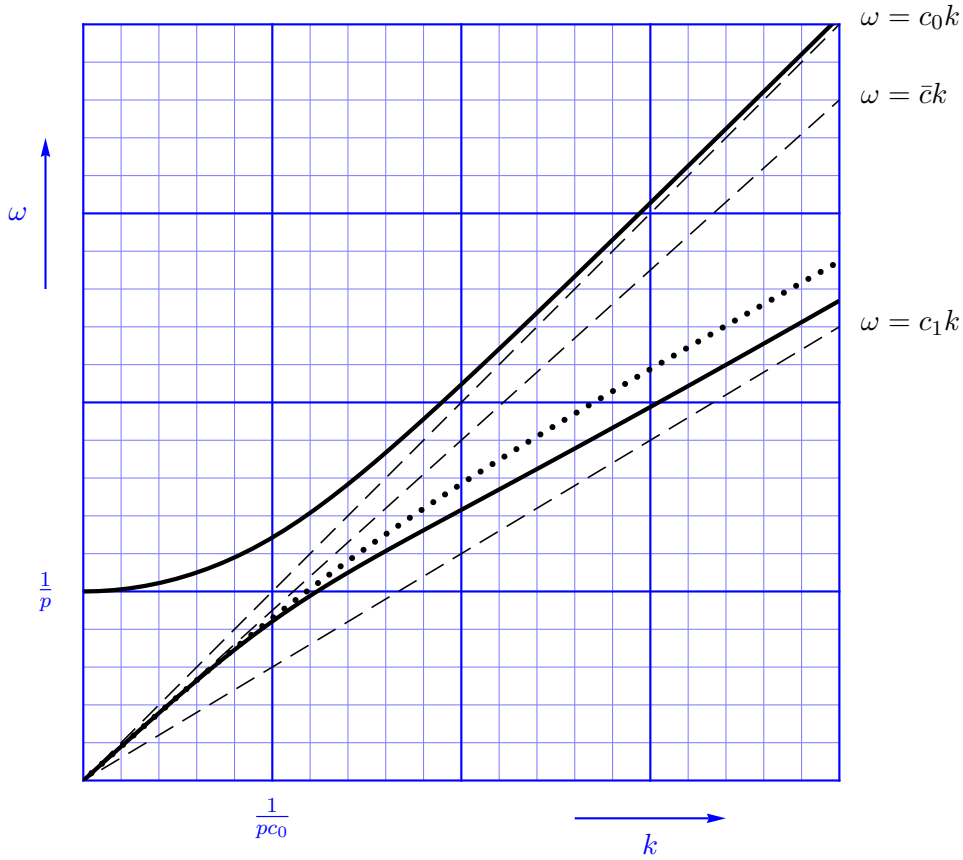


Figure 18: Dispersion diagram in the case $c_1 < \bar{c}$ ($c_1 = 0.6 c_0$, $\bar{c} = 0.9 c_0$)
 — full equation, reduced equation

Since $\omega(0) = 0$ it is the acoustical branch that is approximated by the reduced dispersion relation.

In the long-wave limit, i.e., for small wave numbers, one may omit the highest powers of k in numerator and denominator, obtaining

$$\omega \approx \bar{c}k. \quad (3.58)$$

So the dispersion curve starts with the slope $(3.54)_2$, which is the correct initial slope of the acoustical branch. Correspondingly for the short-wave limit, i.e., big wave numbers, one keeps only the highest powers of k in numerator and denominator and obtains

$$\omega \approx c_1 k, \quad (3.59)$$

which coincides with the correct asymptote of the acoustical branch $(3.56)_2$.

In general, one has either $c_1 < \bar{c}$ (Figure 18) or $c_1 > \bar{c}$ (Figure 17). Corresponding diagrams have been presented by Engelbrecht et al. [59]. In either

case, the acoustical branch of the dispersion diagram starts at the origin with the slope \bar{c} and, for $k \rightarrow \infty$, approaches the asymptote $\omega = c_1 k$. Necessarily there must be a point of inflection somewhere in between. The reduced equation yields an approximation of the acoustical branch, starting with the correct slope \bar{c} and also approaching the correct asymptote $\omega = c_1 k$. Only in between it deviates from the exact curve.

In the critical case $\gamma_1^2 = 1$, which, according to the definition (3.22)₁, means that $\bar{c}^2 = c_1^2$, the full and the reduced dispersion relations can be written as

$$(\omega^2 - c_1^2 k^2) [1 - p^2 (\omega^2 - c_0^2 k^2)] = 0 \quad (3.60)$$

and

$$(\omega^2 - c_1^2 k^2) (1 + p^2 c_A^2 k^2) = 0, \quad (3.61)$$

respectively. Both the full and the reduced dispersion relations show that there is a nondispersive wave propagating at the velocity $c_1 = \bar{c}$. The full equation additionally admits an optical branch which is clearly dispersive, see Figure 16. Since the reduced equation singles out only the acoustical branch, it does not give any dispersive effect. The dispersion “curve” according to the reduced equation looks the same as if it were governed by the simple wave equation $u_{tt} = \bar{c}^2 u_{xx}$, i.e., without any dispersion. The microstructure manifests itself only through the additional optical branch not predicted by the reduced equation. An optical branch of the dispersion relation is always dispersive, since it starts at a finite frequency, here $1/p$, in the long-wave limit $k = 0$. In the short-wave limit, $k \rightarrow \infty$, the waves of the optical branch propagate at the velocity c_0 .

4 Solutions of the extended KdV equation representing solitary waves

It is well known that the usual KdV equation admits solutions in the form of solitary waves, see Subsection 2.1. In this section it will be studied how these solitary waves are influenced by the presence of the micro-nonlinearity term of the extended KdV equation. This analysis is based on [55, 56] (Publications III and VI).

4.1 Extended KdV equation

The evolution equation (3.37) can be treated as an extended KdV equation, since if the influence of the micro-nonlinearity is omitted, it is reduced to the Korteweg–de Vries equation which admits solutions in the form of the sech^2 solitons.

Solutions of the KdV equation propagating without any distortion can be found in the form

$$q = q(\theta), \quad \theta = x - ct. \quad (4.1)$$

For the extended KdV equation (3.37) the ansatz (4.1) can be used unaltered. Inserting the ansatz into the extended KdV equation (3.37) yields the ordinary differential equation

$$-cq' + 3(q^2)' + q''' + 3\varepsilon(q'^2)'' = 0, \quad (4.2)$$

which can be integrated once resulting in

$$q'' + 3\varepsilon(q'^2)' = A + cq - 3q^2, \quad (4.3)$$

where A is a constant of integration.

Converting this second-order differential equation for the function $q(\theta)$ into a first-order differential equation for the function $q'(q)$ one obtains

$$q' (1 + 6\varepsilon q') \frac{dq'}{dq} = A + cq - 3q^2. \quad (4.4)$$

One further integration yields

$$\frac{1}{2}q'^2 + 2\varepsilon q'^3 = B + Aq + \frac{c}{2}q^2 - q^3. \quad (4.5)$$

The analysis will be restricted here to the special case of solitary waves. It is assumed that, as $\theta \rightarrow \pm\infty$, the function q tends uniformly to zero, i. e., $q \rightarrow 0$, $q' \rightarrow 0$, and $q'' \rightarrow 0$. Therefore, in (4.5) the constants A and B have to vanish. Thus equation (4.5) assumes the form

$$q'^2 + 4\varepsilon q'^3 = q^2(c - 2q). \quad (4.6)$$

In principle, this equation has to be solved for q' and then integrated.

4.2 Phase curves of solitary waves

Before turning to the last integration step, the cubic first-order differential equation (4.6) will be analyzed. Introducing the amplitude $a = c/2$ the equation is written as

$$q'^2 + 4\epsilon q'^3 = 2q^2(a - q). \quad (4.7)$$

It represents a curve in the (q, q') phase plane. A solitary wave $q = q(\theta)$ emerges asymptotically from the negative θ -axis, raises with positive slope until its peak $q(0) = a$, turns to negative slope and approaches asymptotically the θ -axis for $\theta \rightarrow +\infty$. The corresponding phase curve starts in the origin of the (q, q') plane with finite positive slope, follows a loop crossing the q -axis downward at $(a, 0)$, and bends back to the origin at finite slope.

To analyze the principal behaviour of the phase curve described by (4.7) let us define the two functions

$$f(q) = 2q^2(a - q) \quad \text{and} \quad g(q') = 4\epsilon q'^3 + q'^2 - f(q). \quad (4.8)$$

Their qualitative graphs are shown in Figures 19 and 20. If $\epsilon > 0$ the function g has a relative maximum

$$g(q'_1) = \frac{1}{108\epsilon^2} - f(q) \quad \text{at} \quad q'_1 = -\frac{1}{6\epsilon}. \quad (4.9)$$

If this relative maximum is above the q' -axis there are three zeros of the function $g(q')$, if it is below there is only one.

For any value q attained by the solitary wave there must be a positive and a negative slope q' , which means that the function $g(q')$ must have two zeros,

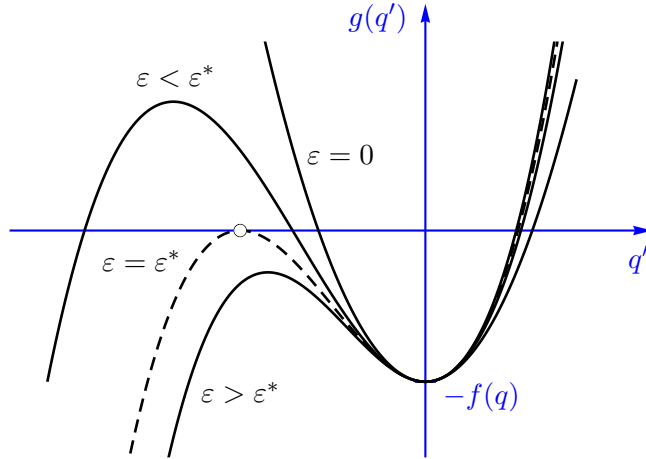


Figure 19: Graph of function $g(q')$

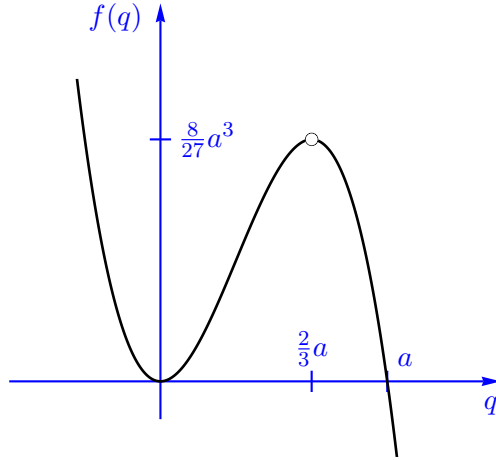


Figure 20: Graph of function $f(q)$

one positive and one negative, for any q in the range $0 < q < a$. In order that there are two zeros, or even three, the relative maximum (4.9)₁ must not be negative. Therefore the parameter ε is restricted by the inequality

$$\varepsilon \leq \varepsilon^* = \frac{1}{6\sqrt{3}f(q)} \quad (4.10)$$

which has to hold for any $q < a$. The inequality must hold even in the worst case, namely, if $f(q)$ attains its biggest value. The function $f(q)$, according to its definition (4.8)₂, has a relative maximum

$$f(q_2) = \left(\frac{2}{3}a\right)^3 \quad \text{at} \quad q_2 = \frac{2}{3}a. \quad (4.11)$$

Thus, for $q \geq 0$, we have

$$f(q) \leq \left(\frac{2}{3}a\right)^3. \quad (4.12)$$

The inequality (4.10) can, therefore, be extended to

$$\varepsilon \leq \frac{1}{6\sqrt{3}f(q_2)} = \frac{1}{4a\sqrt{2}a}. \quad (4.13)$$

To get rid of the square root one can express the peak value a in terms of the new parameter

$$\eta = \sqrt{\frac{a}{2}} = \frac{\sqrt{c}}{2}, \quad (4.14)$$

which is motivated by the equation (2.2) for KdV solitons. Introducing this parameter the inequality (4.13) assumes the form

$$\varepsilon \leq \frac{1}{16\eta^3}. \quad (4.15)$$

The extended KdV equation admits solitary waves of amplitude $a = 2\eta^2$ and velocity $c = 4\eta^2$ only up to this limit of the micro-nonlinearity parameter ε .

In order to plot the phase curve given by (4.7) without solving a cubic equation one can introduce the parameter

$$p = \frac{q'}{q} \quad (4.16)$$

which represents the slope of the position vector in the phase plane. Equation (4.7) can then be written in the form

$$p^2(1 + 4\varepsilon pq) = 2(a - q). \quad (4.17)$$

Solving this equation for q and recalling (4.16) one obtains a parametric representation of the phase curve in the form

$$q(p) = \frac{a - \frac{1}{2}p^2}{1 + 2\varepsilon p^3}, \quad q'(p) = pq(p). \quad (4.18)$$

The curve parameter p varies in the interval $-\sqrt{2a} \leq p \leq +\sqrt{2a}$. The advantage of this parametric representation is that one does not need to solve the cubic equation (4.7) for q' . Using the above parametric representation the phase curves are drawn in Figure 21 for different values of ε . For the maximum value

$$\varepsilon = \varepsilon_{\max} = \frac{1}{16\eta^3} \quad (4.19)$$

the parametric representation (4.18) becomes singular at $p = -(2\varepsilon)^{-1/3} = -2\eta$. A detailed analysis shows that the phase curve, in this limiting case, degenerates into a semi-ellipse and a straight line representing a diameter of the ellipse. The final step of integration can be performed explicitly in this case. This will be presented in Subsection 4.4.

4.3 Approximate solution of the extended KdV equation

In order to get the solution $q = q(\theta)$ the first-order differential equation (4.7) has to be solved for q' and integrated. Using the abbreviation (4.8)₂ it is written as

$$q'^2 + 4\varepsilon q'^3 = f(q). \quad (4.20)$$

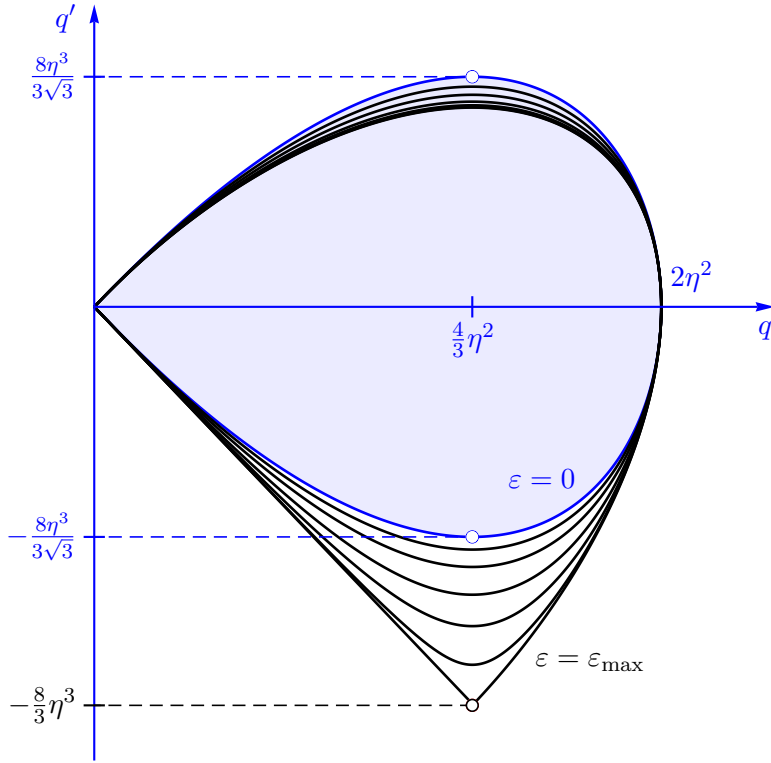


Figure 21: Phase curves of the extended KdV equation for different values of ε

Since it is unlikely that one finds an explicit solution after applying Cardano's formula on this cubic equation, an approximate solution by a series expansion in the small parameter ε is used. The corresponding formula is briefly derived in Subsubsection 4.3.1. This approach is justified by the fact that solitary wave solutions exist only for small values of the parameter ε satisfying the inequality (4.15).

It is assumed that the maximum value $a = c/2$ is attained at $\theta = 0$, from where the function $q(\theta)$ decreases as θ increases and vice versa. Applying the formula (4.31)₂ to the cubic equation (4.20) one obtains the approximation

$$q' = \mp \sqrt{f(q)} - 2\varepsilon f(q) \mp 10\varepsilon^2 [f(q)]^{3/2} - 64\varepsilon^3 [f(q)]^2 + O(\varepsilon^4), \quad (4.21)$$

where the upper and lower signs are valid for $\theta > 0$ and $\theta < 0$, respectively. For performing the integration also the reciprocal value is needed which, according to (4.33), is obtained as

$$\frac{d\theta}{dq} = \frac{1}{q'} = \frac{\mp 1}{\sqrt{f(q)}} + 2\varepsilon \pm 6\varepsilon^2 \sqrt{f(q)} + 32\varepsilon^3 f(q) + O(\varepsilon^4). \quad (4.22)$$

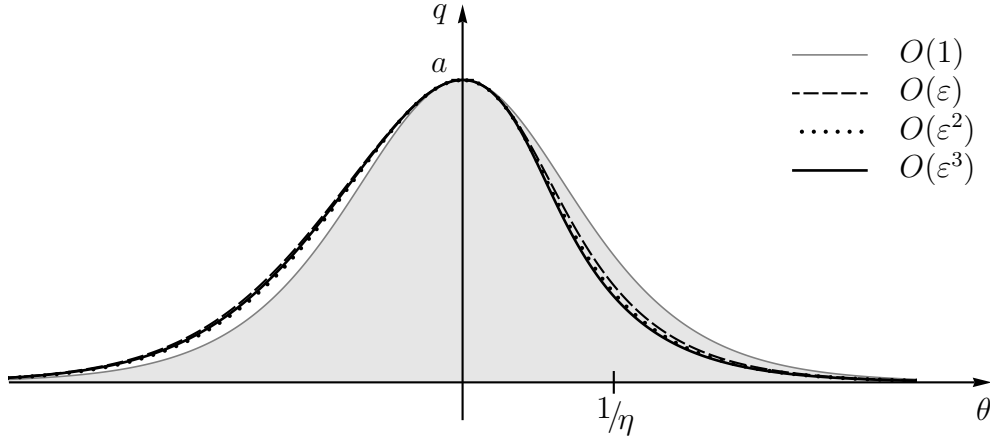


Figure 22: Solitary wave governed by the extended KdV equation ($\varepsilon = \varepsilon_{\max}$) in different approximations

The definite integration starts with the maximum value $q = a$ attained at $\theta = 0$. Thus one obtains

$$\theta = \int_a^q \left[\frac{\mp 1}{\sqrt{f(q)}} + 2\varepsilon \pm 6\varepsilon^2 \sqrt{f(q)} + 32\varepsilon^3 f(q) + O(\varepsilon^4) \right] dq. \quad (4.23)$$

Inserting the function $f(q)$ from (4.8)₂ and performing the definite integration yields

$$\begin{aligned} \theta = & \pm \sqrt{\frac{2}{a}} \operatorname{arcosh} \sqrt{\frac{a}{q}} - 2\varepsilon(a - q) \mp \frac{2}{5}\varepsilon^2(2a + 3q) [2(a - q)]^{3/2} - \\ & - \frac{16}{3}\varepsilon^3 (a^2 + 2aq + 3q^2) (a - q)^2 + O(\varepsilon^4). \end{aligned} \quad (4.24)$$

In principle, this equation has to be solved for q to unveil the function $q = q(\theta)$. The inversion cannot be performed in closed form. The graph, however, can also be drawn directly from (4.24).

Figure 22 shows subsequent approximations of a solitary wave governed by the extended KdV equation with a fixed value of the micro-nonlinearity parameter ε . Starting from the symmetric KdV soliton even the approximation of order ε exhibits the asymmetric behaviour of the solitary wave. The $O(\varepsilon^2)$ and $O(\varepsilon^3)$ approximations come out nearly identical.

The convergence behaviour is different on the left and on the right side. For $\theta > 0$ the limit is approached from one side while for $\theta < 0$ there is an alternating behaviour. A comparison of the approximation with the exact solution is provided in Subsection 4.4 for the limiting value of the parameter ε .

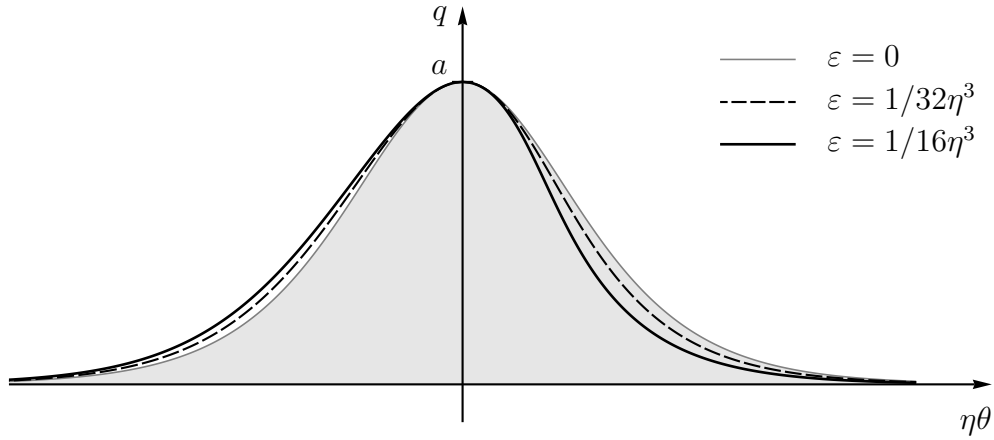


Figure 23: Approximate $O(\varepsilon^3)$ solutions for different values of the micro-nonlinearity parameter

The influence of the micro-nonlinearity parameter ε is shown in Figure 23. Starting from the symmetric KdV soliton ($\varepsilon = 0$) the solitary wave becomes more asymmetric as ε is increased.

To emphasise the relation to the KdV soliton, the arcosh function in (4.24) is inverted, leading to the implicit representation

$$q = a \operatorname{sech}^2 \eta \left[\theta + 2\varepsilon(a - q) \pm \frac{2}{5}\varepsilon^2(2a + 3q) [2(a - q)]^{3/2} + \frac{16}{3}\varepsilon^3 (a^2 + 2aq + 3q^2) (a - q)^2 + O(\varepsilon^4) \right]. \quad (4.25)$$

of the solitary wave. The dependent variable q appears in the argument of the sech function, and the equation cannot be solved explicitly for q .

4.3.1 Approximate solution of a cubic equation

In the analysis of the extended KdV equation (3.37) one comes across a cubic equation with a small coefficient at the cubic term. Instead of solving the equation exactly, an approximate solution is used.

The solutions of the cubic equation

$$\varepsilon x^3 + x^2 = a^2, \quad (4.26)$$

with a small coefficient ε , are assumed in the form

$$x = x_0 + \varepsilon x_1 + \varepsilon^2 x_2 + \varepsilon^3 x_3 + O(\varepsilon^4). \quad (4.27)$$

Restricting the expansion to the order ε^3 the square of the series (4.27) is obtained as

$$x^2 = x_0^2 + 2\varepsilon x_0 x_1 + \varepsilon^2 (2x_0 x_2 + x_1^2) + 2\varepsilon^3 (x_0 x_3 + x_1 x_2) + O(\varepsilon^4). \quad (4.28)$$

The third power is needed only up to the order ε^2 , since it will be multiplied by ε . Thus

$$x^3 = x_0^3 + 3\varepsilon x_0^2 x_1 + 3\varepsilon^2 (x_0^2 x_2 + x_0 x_1^2) + O(\varepsilon^3). \quad (4.29)$$

By inserting these series into the cubic equation (4.26) and equating coefficients of like powers of ε one obtains a set of equations for the coefficients x_k which finally lead to

$$x_0 = \pm a, \quad x_1 = -\frac{1}{2}a^2, \quad x_2 = \pm\frac{5}{8}a^3, \quad x_3 = -a^4. \quad (4.30)$$

Thus the roots of the cubic equation (4.26) are approximated by

$$\begin{aligned} x_{\pm} &= \pm a - \frac{1}{2}\varepsilon a^2 \pm \frac{5}{8}\varepsilon^2 a^3 - \varepsilon^3 a^4 + O(\varepsilon^4) = \\ &= \pm a \left[1 \mp \frac{1}{2}\varepsilon a + \frac{5}{8}\varepsilon^2 a^2 \mp \varepsilon^3 a^3 + O(\varepsilon^4) \right]. \end{aligned} \quad (4.31)$$

The roots (4.31) are those emerging from the two roots of the quadratic equation to which (4.26) reduces for $\varepsilon = 0$. For any $\varepsilon \neq 0$ there must be a third root, which can be expanded into the series

$$x_{\times} = -\frac{1}{\varepsilon} + \varepsilon a^2 + 2\varepsilon^3 a^4 + O(\varepsilon^4). \quad (4.32)$$

This third root, however, is of no relevance in our application.

Within the integration process of Subsection 4.3 also the reciprocal roots $1/x_{\pm}$ are needed, which are obtained from (4.31) by the well-known geometric series expansion as

$$\begin{aligned} \frac{1}{x_{\pm}} &= \pm \frac{1}{a} \left[1 \pm \frac{1}{2}\varepsilon a - \frac{3}{8}\varepsilon^2 a^2 \pm \frac{1}{2}\varepsilon^3 a^3 + O(\varepsilon^4) \right] = \\ &= \pm \frac{1}{a} + \frac{1}{2}\varepsilon \mp \frac{3}{8}\varepsilon^2 a + \frac{1}{2}\varepsilon^3 a^2 + O(\varepsilon^4). \end{aligned} \quad (4.33)$$

In principle, the expansions can be extended to higher orders in ε . The level of $O(\varepsilon^3)$ seems to be sufficient for the application here.

4.4 Analytical solution in the limiting case

It has been shown that bounded and closed phase curves $q'(q)$ are possible only if $\varepsilon\eta^3 \leq 1/16$. In addition to the case $\varepsilon = 0$, where one gets the well-known KdV soliton as an analytical representation, it can be shown that an analytical solution in closed form is also possible in the limiting case $\varepsilon\eta^3 = 1/16$.

After inserting the limiting value

$$\varepsilon = \frac{1}{16\eta^3} \quad (4.34)$$

the ordinary differential equation (4.7) can be written in the form

$$q'^2 - 4\eta^2 q^2 + \frac{1}{4\eta^3} (q'^3 + 8\eta^3 q^3) = 0. \quad (4.35)$$

The quadratic and cubic parts of this equation allow the factorizations

$$\begin{aligned} q'^2 - 4\eta^2 q^2 &= (q' + 2\eta q)(q' - 2\eta q), \\ q'^3 + 8\eta^3 q^3 &= (q' + 2\eta q)(q'^2 - 2\eta q q' + 4\eta^2 q^2). \end{aligned} \quad (4.36)$$

Thus (4.35) may be written as

$$(q' + 2\eta q) \left[q' - 2\eta q + \frac{1}{4\eta^3} (q'^2 - 2\eta q q' + 4\eta^2 q^2) \right] = 0. \quad (4.37)$$

The phase curve consists of two branches, namely the straight line

$$q' = -2\eta q \quad (4.38)$$

and the ellipse

$$q'^2 + 2\eta(2\eta^2 - q)q' - 4\eta^2 q(2\eta^2 - q) = 0, \quad (4.39)$$

see Figure 24. Solving the last equation for q' gives the solutions

$$\begin{aligned} q'_{1,2} &= \eta \left[-(2\eta^2 - q) \pm \sqrt{4\eta^4 + 4\eta^2 q - 3q^2} \right] \\ &= \eta \left[-(a - q) \pm \sqrt{a^2 + 2aq - 3q^2} \right], \end{aligned} \quad (4.40)$$

where, for convenience, the abbreviation $a = 2\eta^2$ has been introduced according to (4.14). Putting together these solutions in the proper order one has to start at the origin which is attained asymptotically for $\theta \rightarrow -\infty$. Then the wave profile will build up with positive slope (4.40), + sign, increasing up to $q'_{\max} = 4\eta^3/3$ at $q = 2a/3$. The peak value of the wave profile $a = 2\eta^2$ is

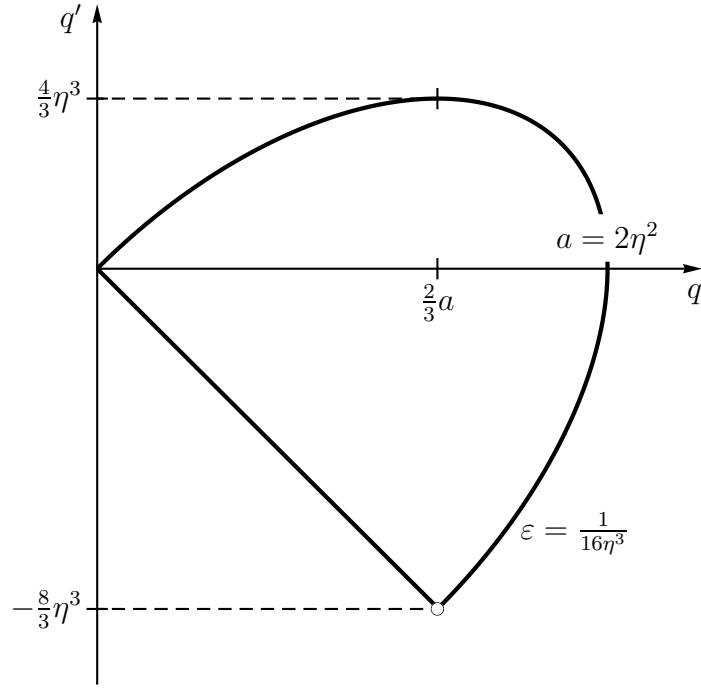


Figure 24: Phase curve of the extended KdV equation in the limiting case

assumed to be attained at $\theta = 0$. For $\theta > 0$ the wave profile will decrease, i.e., it assumes the negative slope (4.40), $-$ sign. At $q = 2a/3$ the steepest decline is reached with the slope $q' = -8\eta^3/3$. At this point the phase curve switches to the linear branch (4.38) until the origin is reached, again asymptotically for $\theta \rightarrow \infty$. Thus the phase curve, as shown in Figure 24, is represented by

$$\frac{q'}{\eta} = \begin{cases} \sqrt{a^2 + 2aq - 3q^2} - (a - q) & \text{for } \theta \leq 0 \quad \text{and} \quad 0 \leq q \leq a, \\ -\sqrt{a^2 + 2aq - 3q^2} - (a - q) & \text{for } \theta \geq 0 \quad \text{and} \quad a \geq q \geq \frac{2}{3}a, \\ -2q & \text{for } \theta \geq 0 \quad \text{and} \quad \frac{2}{3}a \geq q \geq 0. \end{cases} \quad (4.41)$$

The phase curve is traversed in clockwise sense, as always, since in the upper half-plane ($q' > 0$) the values of q must increase while in the lower half-plane ($q' < 0$) the values of q must decrease. The q axis is intersected at a right angle except in a point which is reached only asymptotically. Let the right-hand side of (4.41) be abbreviated by $f(q)$. Then the wave profile $q(\theta)$ is the solution of the initial-value problem

$$\frac{dq}{d\theta} = \eta f(q), \quad q(0) = a. \quad (4.42)$$

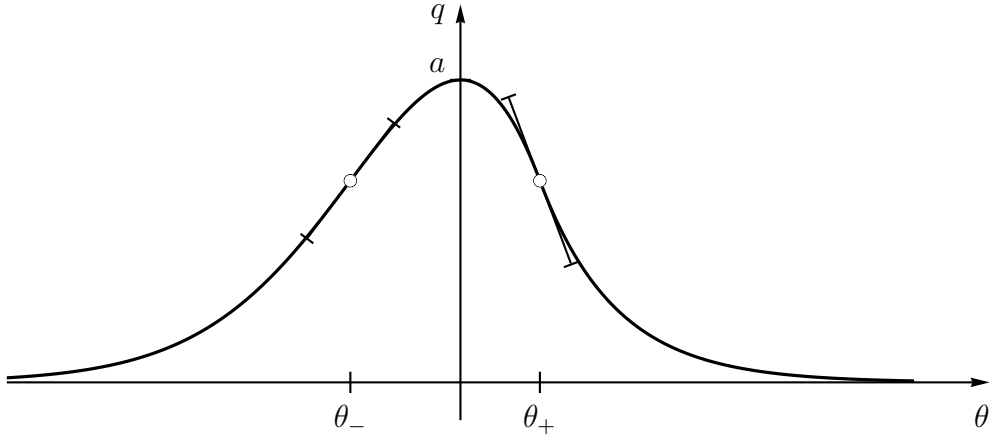


Figure 25: Profile of the solitary wave in the limiting case

By separation of variables and subsequent integration the solution is obtained as

$$\int_a^q \frac{dq}{f(q)} = \eta\theta. \quad (4.43)$$

The integral on the left-hand side has still to be evaluated.

For $\theta \leq 0$, the function f is given by (4.41)₁. Using the corresponding definite integral [55, Appendix B] with the upper sign, one obtains

$$\ln \frac{a(\sqrt{a^2 + 2aq - 3q^2} + a + q)}{2q^2} + \sqrt{3} \arccos \frac{3q - a}{2a} = -4\eta\theta. \quad (4.44)$$

The maximum slope

$$q'_{\max} = \frac{4}{3}\eta^3 \quad (4.45)$$

is attained, according to Figure 24, when the amplitude is $q = 2a/3$, i.e., at a value of

$$\theta_- = -\frac{1}{4\eta} \left(\ln 3 + \frac{\pi}{\sqrt{3}} \right) \quad (4.46)$$

of the independent variable θ . This branch of the curve ends with the peak value $q = a$ attained at $\theta = 0$, see Figure 25.

For $\theta \geq 0$ and $a \geq q \geq 2a/3$ the function f is given by (4.41)₂. The definite integral [55, Appendix B] with the lower sign yields

$$\ln \frac{\sqrt{a^2 + 2aq - 3q^2} + a + q}{2a} + \sqrt{3} \arccos \frac{3q - a}{2a} = 4\eta\theta. \quad (4.47)$$

The branch ends at

$$\theta_+ = \frac{1}{4\eta} \left(\ln \frac{4}{3} + \frac{\pi}{\sqrt{3}} \right) \quad (4.48)$$

with the minimum (or maximum negative) slope

$$q'_{\min} = -\frac{8}{3}\eta^3 \quad (4.49)$$

at the height $q = 2a/3$. The last branch starts at (4.48), and the function f is given by (4.41)₃. Thus one has to perform the definite integration

$$\int_{2a/3}^q \frac{dq}{q} = -2\eta \int_{\theta_+}^{\theta} d\theta, \quad (4.50)$$

which yields the solution

$$q = \frac{2a}{3} \exp[-2\eta(\theta - \theta_+)]. \quad (4.51)$$

At $\theta = \theta_+$ the branch starts with the slope

$$q'(\theta_+) = -\frac{4}{3}a\eta = -\frac{8}{3}\eta^3. \quad (4.52)$$

This means that the last branch is attached continuously differentiable to the preceding one. The whole wave profile is shown in Figure 25, where also the tangents at the inflectional points θ_{\mp} are indicated.

A comparison of this exact solution with the approximate solution (4.24) is depicted in Figure 26. In the left, flat part, the curves coincide excellently while on the steeper flank the approximation is slightly above the exact curve. It should be noted that this good coincidence pertains to the maximum value of the parameter ε allowing a solitary wave solution. For smaller values it should be even better.

4.5 Concluding remarks

From various studies it is known that in a microstructured material solitary waves can propagate if dispersion and nonlinearity are balanced appropriately. If the linear dispersion evoked by the microstructure is complemented only by macro-nonlinearity the dynamical behaviour is described by the Korteweg–de Vries equation, and the well-known symmetric solitary waves are possible solutions.

If also some nonlinearity in the microscale is included the evolution equation contains an additional nonlinear term which involves higher derivatives. This makes the shape of the solitary waves asymmetric. In Subsection 4.3, a formula has been provided, which describes the asymmetric solitary wave analytically, although in some approximation.

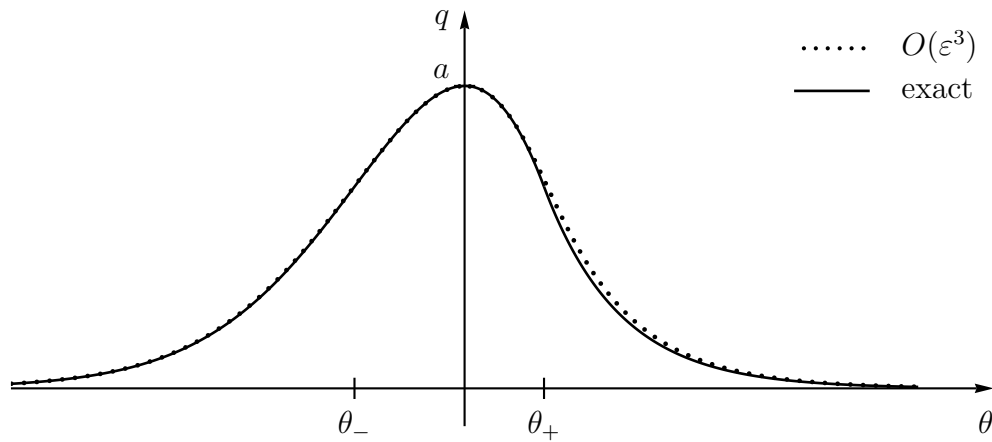


Figure 26: Exact and approximate solutions in the limiting case $\varepsilon = 1/16\eta^3$

It has been shown that solitary waves are possible only up to a certain limit of the micro-nonlinearity parameter. For this limit as a special case, the extended KdV equation can be solved explicitly and used as a reference. The approximate solution agrees quite well with the exact one in the limit case, and the coincidence must be even better for smaller values of the micro-nonlinearity parameter.

It is still an open question to what extent the presented solutions, which pertain to the extended KdV equation (3.37), are consistent with the original model (3.9). This should be analyzed by numerical studies of the full model equations which, however, are outside of the scope of this work.

5 Solutions of the extended KdV equation representing periodic waves

As in the KdV case also the extended KdV equation admits periodic solutions in addition to the solitary waves discussed in Section 4. The analysis of these periodic solutions is based on [67] (Publication IV).

5.1 Extended KdV equation

Again we are looking for solutions of the form

$$q = q(\theta), \quad \theta = x - ct \quad (5.1)$$

representing undistorted waves propagating at the velocity c within the moving reference frame. The function $q = q(\theta)$ will then satisfy an ordinary differential equation which can be integrated twice to result in a first-order differential equation of the form

$$q'^2 + 4\varepsilon q'^3 = f(q), \quad (5.2)$$

where $f(q)$ is a third-order polynomial of the form (2.13).

In principle, the equation (5.2) has to be solved for q' and then integrated. However, it is unlikely that this integration can be performed in closed form. Therefore we confine ourselves to an *approximate* solution, assuming the parameter ε to be small. Expanding the roots of the cubic equation (5.2) in powers of ε one obtains

$$q' = \pm \sqrt{f(q)} \left\{ 1 \mp 2\varepsilon \sqrt{f(q)} + 10\varepsilon^2 f(q) \mp 64\varepsilon^3 [f(q)]^{3/2} \right\} + O(\varepsilon^4), \quad (5.3)$$

where $f(q)$ is the cubic polynomial defined by (2.13). Although, at first glance, this differential equation for $q(\theta)$ seems even more complicated than the original one, it can be integrated in closed form.

5.2 Phase portrait

Before going on with the integration the behaviour of the phase curves $q'(q)$ will be analyzed in detail. The polynomial $f(q)$ involves three parameters. In order to get a one-parameter family of curves two constants should be fixed. Let us suppose that the minimum and the maximum of the polynomial are located at $q = 0$ and $q = d$, respectively, where d is an arbitrary but fixed value. Then the cubic polynomial admits the representation

$$f(q) = b^2 - (2q + d)(q - d)^2, \quad (5.4)$$

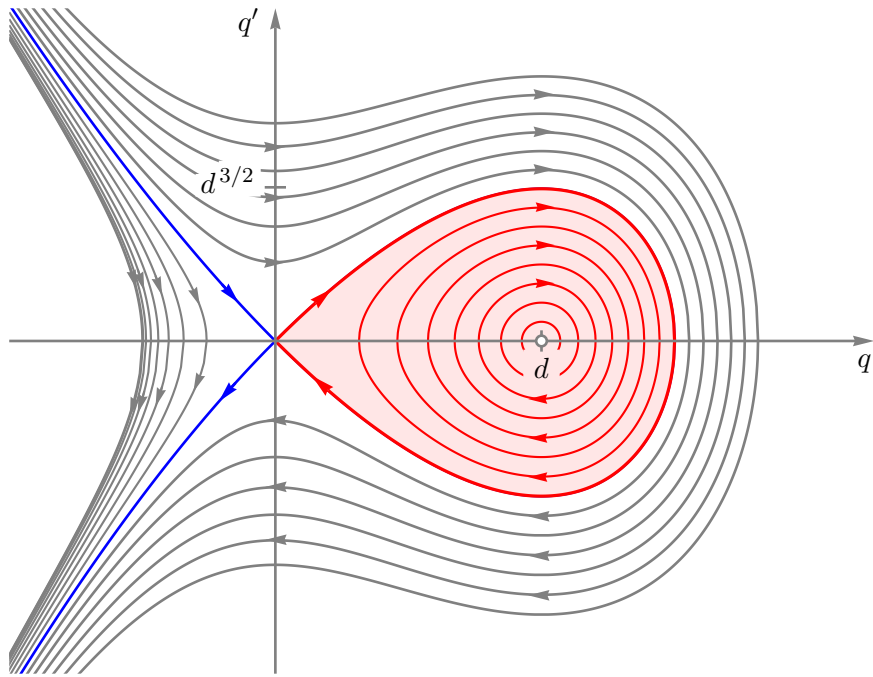


Figure 27: Phase portrait of the KdV equation ($\varepsilon = 0$)

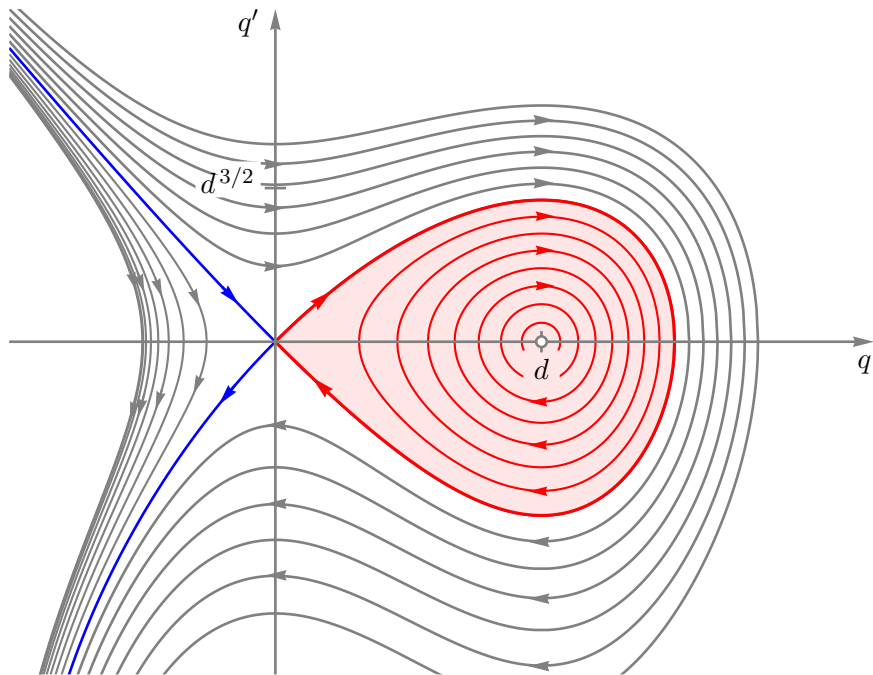


Figure 28: Phase portrait of the extended KdV equation ($\varepsilon = 0.5 \varepsilon_{\max}$)

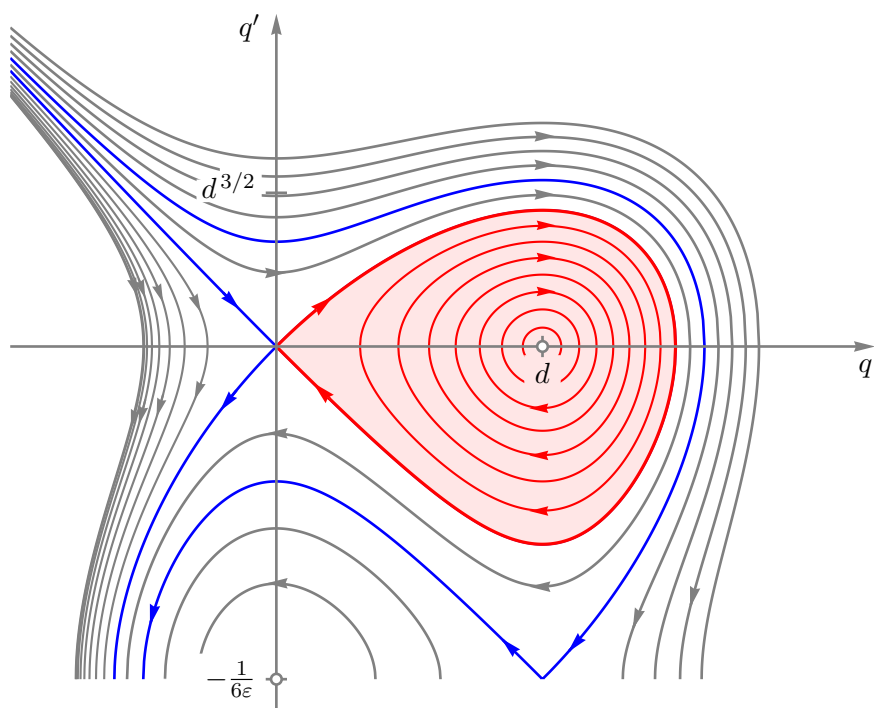


Figure 29: Phase portrait of the extended KdV equation ($\varepsilon = 0.8\varepsilon_{\max}$)

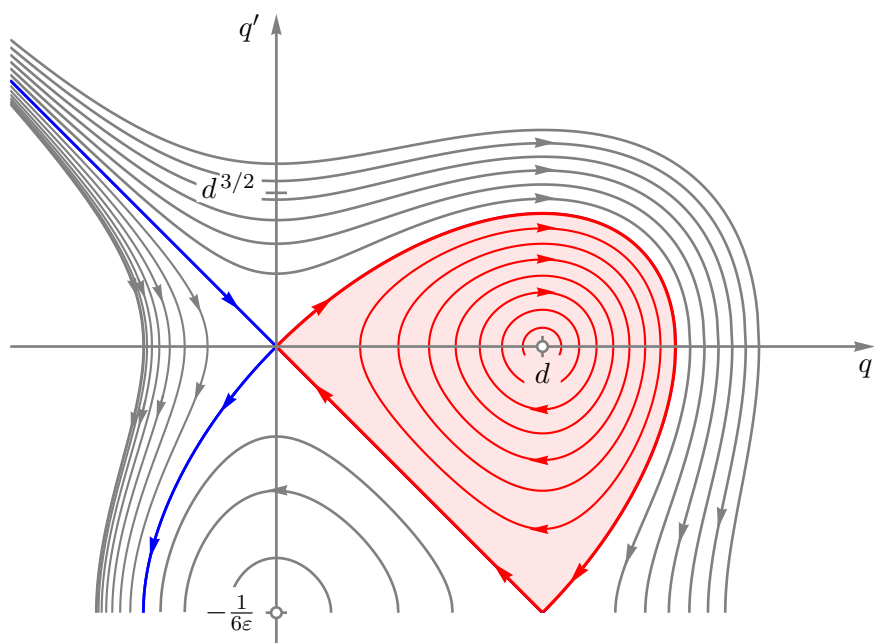


Figure 30: Phase portrait of the extended KdV equation ($\varepsilon = \varepsilon_{\max}$)

where b is considered as the only free parameter of the function. The *phase portrait* depicts the family of phase curves $q'(q)$ for different values of the parameter b while d and ε are kept fixed.

For $\varepsilon = 0$ the symmetric phase portrait of the KdV equation is retained, see Figure 27. Only the shaded part of the phase portrait is of relevance. The trajectories outside this area extend to infinity and do not represent finite solutions. The uppermost curve, for instance, represents a solution $q = q(\theta)$ that starts at $q = -\infty$ with infinite slope, gradually coming up to a maximum value of q with slope $q' = 0$, then symmetrically going back to $q = -\infty$ with infinite negative slope. The phase curves in the shaded region are closed cycles representing periodic waves, which, in the case of the KdV equation, are cnoidal waves. The limiting curve forms a homoclinic orbit starting and ending at the origin, which means that $q = q' = 0$ is attained asymptotically for $\theta \rightarrow \pm\infty$. This curve corresponds to the limiting solitary wave of height $a = 3d/2$.

With increasing values of the micro-nonlinearity parameter ε the phase portrait becomes more and more asymmetric with respect to the q -axis. According to (4.13), solitary waves are possible solutions of the extended KdV equation only if

$$\varepsilon \leq \varepsilon_{\max} = \frac{1}{2} (2a)^{-\frac{3}{2}} = \frac{1}{2} (3d)^{-\frac{3}{2}}. \quad (5.5)$$

The phase portraits for $\varepsilon = 0.5 \varepsilon_{\max}$, $\varepsilon = 0.8 \varepsilon_{\max}$, and $\varepsilon = \varepsilon_{\max}$ are depicted in Figures 28, 29, and 30, respectively. Also in these phase portraits only the phase curves in the shaded area represent finite solutions $q = q(\theta)$. Again the closed cycles represent periodic waves, which, however, are not symmetric anymore. At each level of q , one obtains a positive and a negative slope q' , where the negative slope is steeper than the positive slope. The asymmetry is also present in the solitary wave limit, which has been studied already in the preceding section.

At the maximum value $\varepsilon = \varepsilon_{\max}$ of the micro-nonlinearity parameter the limiting trajectory representing the solitary wave degenerates into a half ellipse and a straight line. This remarkable feature has opened the possibility to get an analytic solution $q = q(\theta)$ in that special case, as described in Subsection 4.4.

The phase portraits have been studied in [67]. Due to page limitations only the phase portrait for $\varepsilon = 0.8 \varepsilon_{\max}$ has been included in this paper.

The final integration uses the series expansion (5.3) rather than the exact phase curves $q'(q)$. In Figure 31 the exact solution of the cubic equation (5.2) is contrasted with the approximations (5.3) allowing for different powers of ε . The $O(1)$ approximation neglects the influence of micro-nonlinearity and gives the symmetric phase curves of the KdV case. Taking into account the corrections (5.3) with increasing powers of ε leads to the asymmetric phase

curves which are characteristic for the extended KdV equation.

The approximations converge to the exact solution. In the upper half-plane the convergence is alternating, in the lower the curves approach the limit from above. Even for $\varepsilon = \varepsilon_{\max}$ the approximation is acceptable for the periodic waves. It is still poor at the kink of the phase curve representing the solitary wave. This, however, is the worst case.

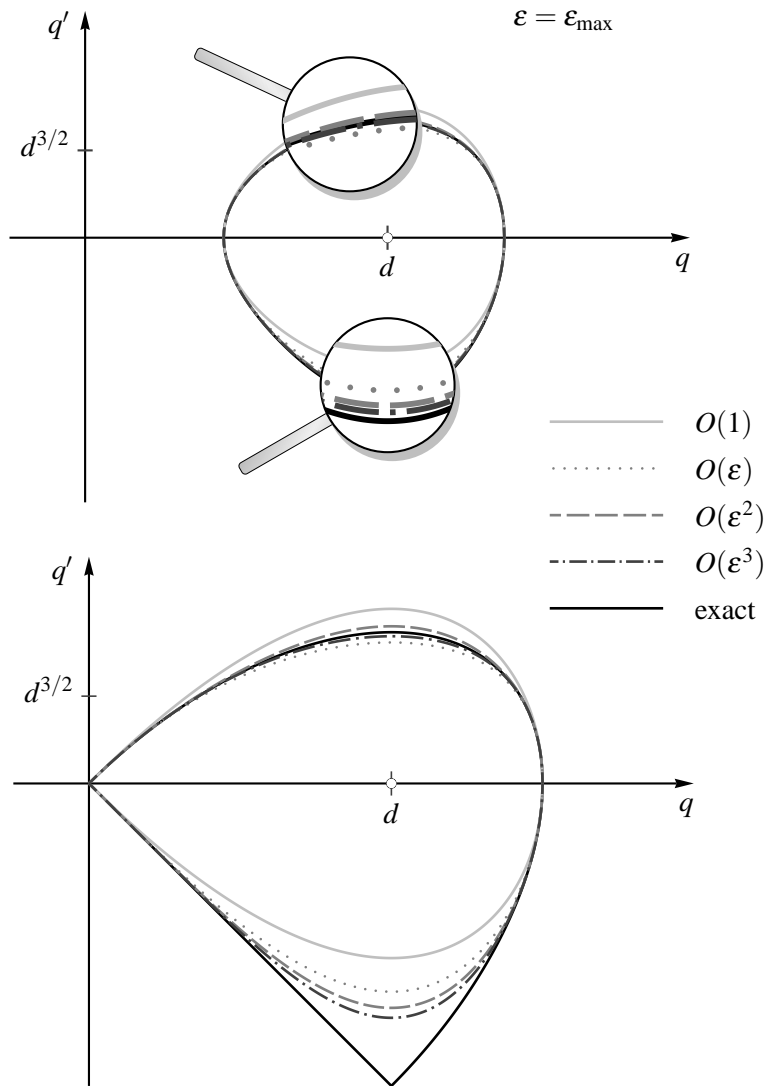


Figure 31: Approximate phase curves of the extended KdV equation with maximal micro-nonlinearity parameter. Upper: periodic wave (with magnified areas). Lower: limiting solitary wave.

5.3 Asymmetric periodic waves

The final integration will be performed using the approximation of q' by the power series (5.3). Without loss of generality one may assume that q attains its maximum value q_3 at $\theta = 0$. Using this as initial condition for the definite integration, the values of q will decrease as θ increases. Therefore the lower signs in (5.3) are chosen. For performing the integration one needs the reciprocal value $1/q'$ which is obtained as

$$\frac{d\theta}{dq} = \frac{1}{q'} = -\frac{1}{\sqrt{f(q)}} \left[1 - 2\varepsilon\sqrt{f(q)} \right] + O(\varepsilon^2) = -\frac{1}{\sqrt{f(q)}} + 2\varepsilon + O(\varepsilon^2). \quad (5.6)$$

The analysis is restricted here to the $O(\varepsilon)$ approximation but can easily be extended to higher orders. Using the initial condition $q(0) = q_3$ the integration yields

$$\theta = \int_{q_3}^q \left[\frac{-1}{\sqrt{f(q)}} + 2\varepsilon \right] dq. \quad (5.7)$$

Following the analysis of cnoidal waves in Subsection 2.2, the integral is evaluated explicitly by using the substitution (2.17)

$$q = q_2 + (q_3 - q_2) \cos^2 \varphi, \quad (5.8)$$

see Figure 9 about the geometrical interpretation of the new variable φ . Performing the integration gives the result

$$\theta = \frac{1}{\eta} F(\varphi; k) - 2\varepsilon(q_3 - q), \quad (5.9)$$

where F denotes the incomplete elliptic integral of the first kind and the constants

$$\eta = \sqrt{\frac{q_3 - q_1}{2}} \quad \text{and} \quad k = \sqrt{\frac{q_3 - q_2}{q_3 - q_1}} \quad (5.10)$$

have been introduced. Solving (5.9) for the auxiliary variable φ and resubstituting this into the transformation formula (5.8) yields

$$q = q_2 + (q_3 - q_2) \text{cn}^2 \eta [\theta + 2\varepsilon(q_3 - q)]. \quad (5.11)$$

This is an implicit representation of the periodic wave solutions of the extended KdV equation (3.32), though only in a first approximation. For $\varepsilon = 0$ it passes into the cnoidal wave solution of the KdV equation studied in Subsection 2.2. Figure 32 shows a family of periodic waves together with their limiting solitary wave, as described by (5.11). The waves look very much like corresponding cnoidal waves, but are inclined to the right.

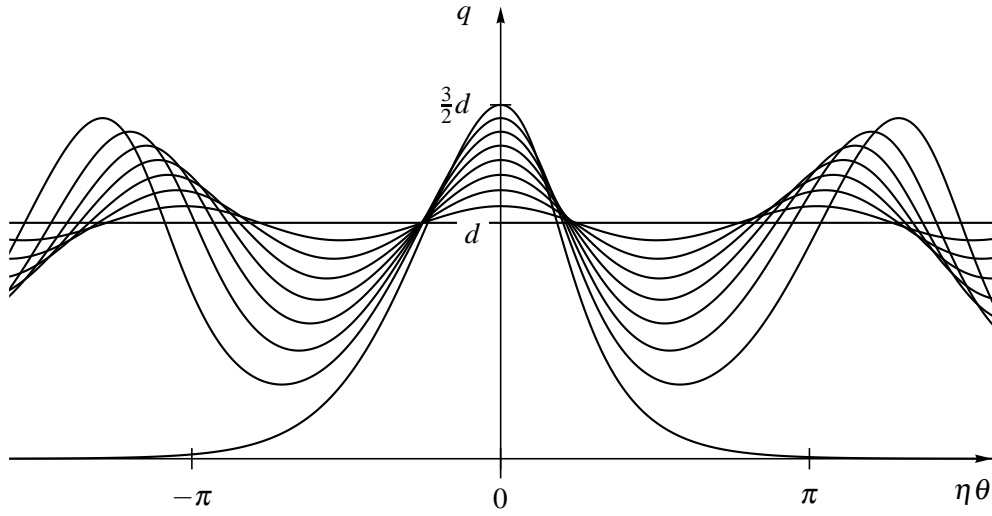


Figure 32: Periodic waves and solitary wave governed by the extended KdV equation

5.4 Concluding remarks

As shown in [55, 56, 68], the propagation of one-dimensional deformation waves in a nonlinear microstructured solid leads to an evolution equation which has the form of an extended Korteweg–de Vries equation. Janno and Engelbrecht [10] have demonstrated that due to the nonlinearity of the microscale the solitary wave profile becomes asymmetric. The same effect appears in the case of the respective evolution equation which has been solved approximately by Randrüüt and Braun [55]. Although solitary waves constitute the most interesting type of solutions, the same procedure has been applied here to the more general case. Solitary waves can be considered as the long-wave limit of periodic solutions which, in the KdV case, have the form of cnoidal waves.

It is shown that, due to the nonlinearity in microscale, the cnoidal waves stay periodic but become inclined in the same manner as the solitary waves. Compared with the classical cnoidal waves ($\varepsilon = 0$), the periodic waves for $\varepsilon > 0$ have steeper slope at the leading flank while the trailing flank falls off gentler. Qualitatively the behaviour is like expected from the solitary-wave limit.

6 Numerical simulation

The main goals of the numerical analysis are (i) to find numerical solutions for the evolution equation (3.32), (ii) to study the influence of the micro-nonlinearity parameter, and (iii) to compare the results with those of the two-wave equation. The numerical analysis presented here is based on [68, 69] (Publications II and V).

The evolution equation (3.32) can be written in the form

$$\alpha_\tau + s\alpha\alpha_\xi + z\alpha_{\xi\xi\xi} + w(\alpha_\xi\alpha_{\xi\xi\xi} + \alpha_{\xi\xi}^2) = 0, \quad (6.1)$$

where the parameters

$$s = \frac{c_N^2}{\bar{c}^2}, \quad z = \frac{\bar{c}^2 - c_1^2}{\bar{c}^2}, \quad w = \epsilon \frac{c_M^2}{\bar{c}^2}, \quad (6.2)$$

characterise nonlinearity of the macroscale, dispersion, and nonlinearity of the microscale, respectively. Equalizing the micro-nonlinearity parameter w to zero yields the well-known Korteweg–de Vries (KdV) equation. Thus, compared with the standard KdV equation, (6.1) includes an additional complicated term which reflects the nonlinearity of the macroscale.

The evolution equation (6.1) is solved under localised and harmonic initial conditions

$$\alpha(\xi, 0) = A_0 \operatorname{sech}^2 \frac{\xi - \xi_0}{\sqrt{12z/A_0}} \quad \text{and} \quad \alpha(\xi, 0) = \sin \xi, \quad (6.3)$$

respectively, where A_0 denotes the amplitude, ξ_0 the initial phase-shift, and $\sqrt{12z/A_0}$ the width of the initial pulse. For numerical integration the FFT-based pseudospectral method is used and periodic boundary conditions are applied [70].

The crucial question is the proper choice of parameters because not much is known about the values of physical constants of Mindlin's model [1]. We choose here the values of parameters comparable with the standard KdV equation which has been studied in detail (see, for example [71, 72]). One of the important features of the standard KdV equation is the emergence of a soliton train. The number of solitons in a train depends on the values of s and z . Widely used values are $s = 1$ and $z = 10^{-2.5}$ [71, 72]. Then the soliton train develops at $\tau \approx 30$. Another important feature for the KdV equation is the existence of a single stable soliton.

On the basis of the argumentation above, we take here $s = 1$ and vary the other parameters in the following domains: $10^{-2.5} \leq z \leq 1$ and $0 \leq w \leq 1$. The localised initial wave (6.3)₂ is the analytical solution for equation (6.1) in the case of $w = 0$, i.e., it represents the KdV soliton.

6.1 Localised initial excitation

Janno and Engelbrecht [10] have shown that for the two-wave equation (3.21) there exists an asymmetric travelling wave solution, i.e., the nonlinearity in microscale leads to asymmetry of the wave profile. Numerical experiments by Salupere et al. [73, 74] have demonstrated, that in the case of equation (3.21), an initially symmetric localised wave is deformed to an asymmetric wave during propagation. Here we demonstrate that the same effect takes place in the case of the evolution equation (6.1).

The evolution of the initial symmetric sech^2 pulse can be traced in Figure 33. It can be seen that the shape of the wave is altered during propagation and an oscillating tail is formed. In Figure 34, the initial wave-profile and the altered shape of the wave profile at the end of the integration interval are plotted against ξ . In order to characterise the asymmetry of the last wave-profile more explicitly, α_ξ is plotted against α in Figure 35.

Applying localised initial conditions the value of micro-nonlinearity parameter $w = 10^{-2.5}$ is chosen quite big compared to the macro-nonlinearity parameter s and dispersion parameter z in order to demonstrate the effect of asymmetry more pronouncedly.

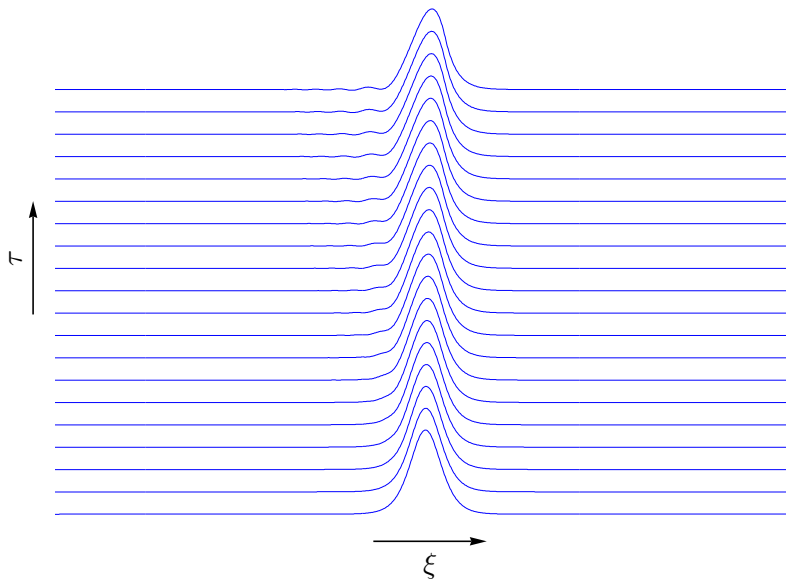


Figure 33: Time-slice plot for $z = 10^{-2}$, $w = 10^{-2.5}$.

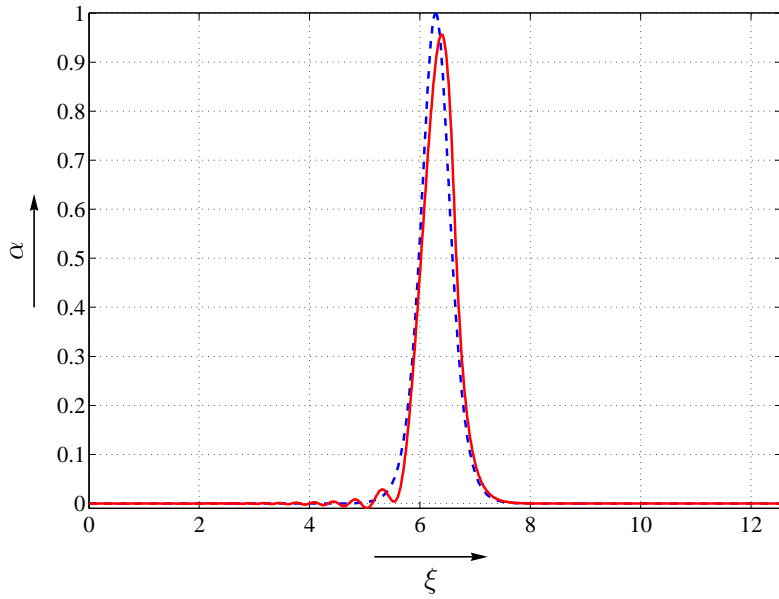


Figure 34: The initial (dashed line) and the deformed (solid line) wave profile from Figure 33 ($z = 10^{-2}$, $w = 10^{-2.5}$).

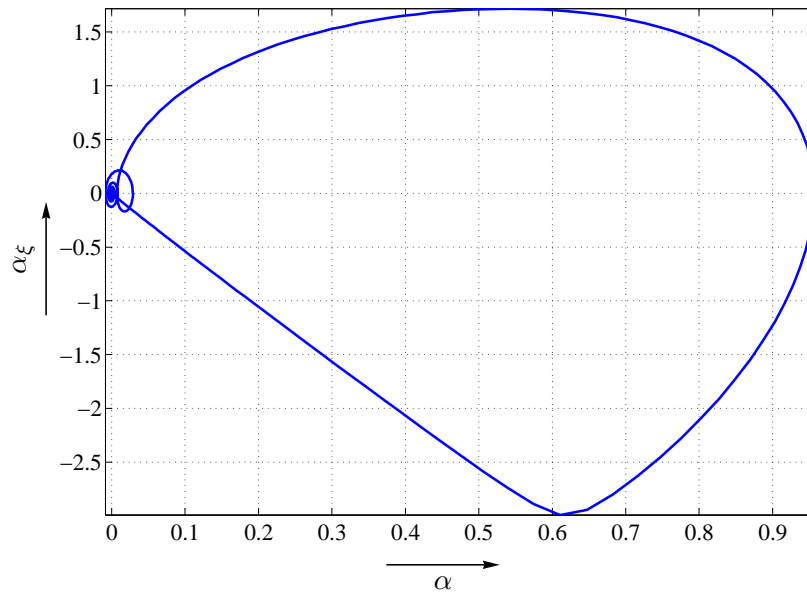


Figure 35: Asymmetry of the wave profile at the end of integration interval: α_ξ against α for $z = 10^{-2}$, $w = 10^{-2.5}$.

6.2 Harmonic initial excitation

Solving the evolution equation (6.1) under harmonic initial conditions (6.3)₂ the following results are obtained, which are concentrated on three cases of different values of dispersion parameter z and micro-nonlinearity parameter w . Also the comparison with the corresponding KdV cases is presented.

Figures 36 and 38 represent the time-slice plot and pseudocolour plot, respectively, over two space periods in the KdV case for $z = 10^{-0.5}$, i.e., the micro-nonlinearity is neglected. The corresponding plots for $w = 10^{-0.9936}$ are shown in Figures 37 and 39. The difference of these plotted patterns compared to the KdV case can easily be observed. Similarly to the case of localised initial conditions, the emerged solitons (Figure 40) are asymmetric as can be seen from the phase plane, i.e., the (α, α_ξ) -plot, see Figure 41. This is a clear sign of influence of the micro-nonlinearity.

For the next value of the dispersion parameter under consideration, $z = 10^{-1.5}$, it is again of interest to start with the case $w = 0$ which corresponds to the standard KdV equation. Typically to the KdV case, from a harmonic initial excitation a train of solitons will emerge (Figure 42). The interaction picture is complicated but solitons preserve their shape and speed over long time intervals. The soliton amplitudes fluctuate in the interval that is dictated by the interaction rules [71, 72]. When the micro-nonlinearity ($w = 10^{-2.6210}$) is taken into account the interaction pattern is altered, e.g., speeds of solitons are higher compared with the KdV case (Figures 42, 43 and Figures 44, 45). Again, like in the case of localised initial conditions, emerged solitons (Figure 46) are asymmetric, as shown in the phase plane (Figure 47) expressing the influence of the micro-nonlinearity. The chosen time instant $\tau = 14.3$ corresponds to the formation of the soliton train at given values of z and w .

Figures 48 and 50 represent the time-slice plot and pseudocolour plot, respectively, over two space periods in the KdV case for $z = 10^{-2.5}$, i.e., the micro-nonlinearity is neglected. The corresponding plots for $w = 10^{-4.1775}$ are shown in Figures 49 and 51. When the micro-nonlinearity is taken into account the interaction pattern is altered similarly to the case discussed just above and the difference compared to the KdV case is clearly visible.

6.3 Comparison of analytical and numerical results

In order to compare the analytical results of Section 4 and the numerical results of Section 6 one first needs to establish the relations between the different sets of parameters used in the formulations of the extended KdV equation. The extended Korteweg–de Vries equation has been presented in different, but equivalent forms, see (3.32) and (6.1).

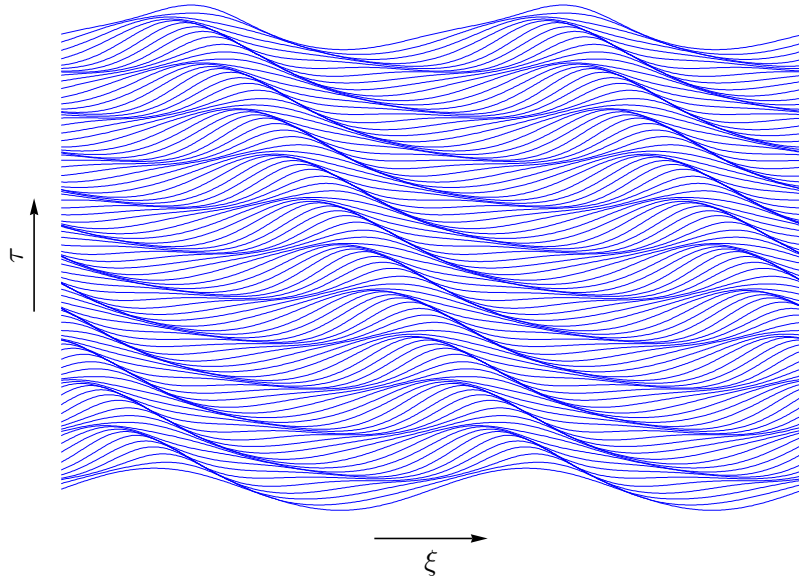


Figure 36: Time-slice plot over two space periods for KdV case, $z = 10^{-0.5}$, $w = 0$.

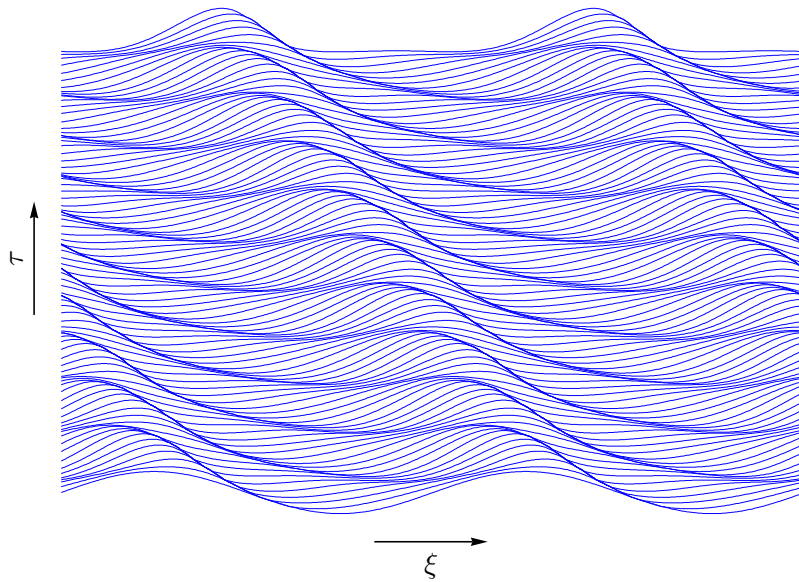


Figure 37: Time-slice plot over two space periods for $z = 10^{-0.5}$, $w = 10^{-0.9936}$.

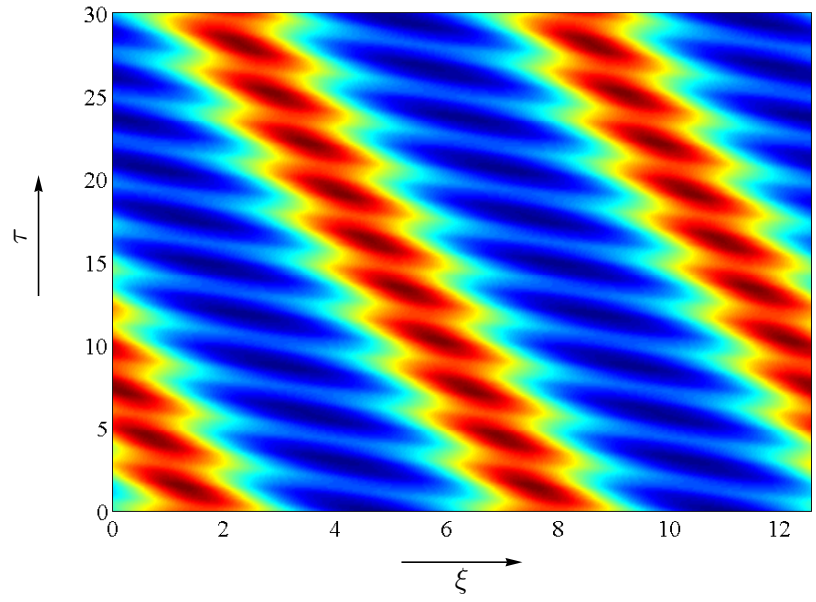


Figure 38: Pseudocolour plot over two space periods for KdV case, $z = 10^{-0.5}$, $w = 0$.

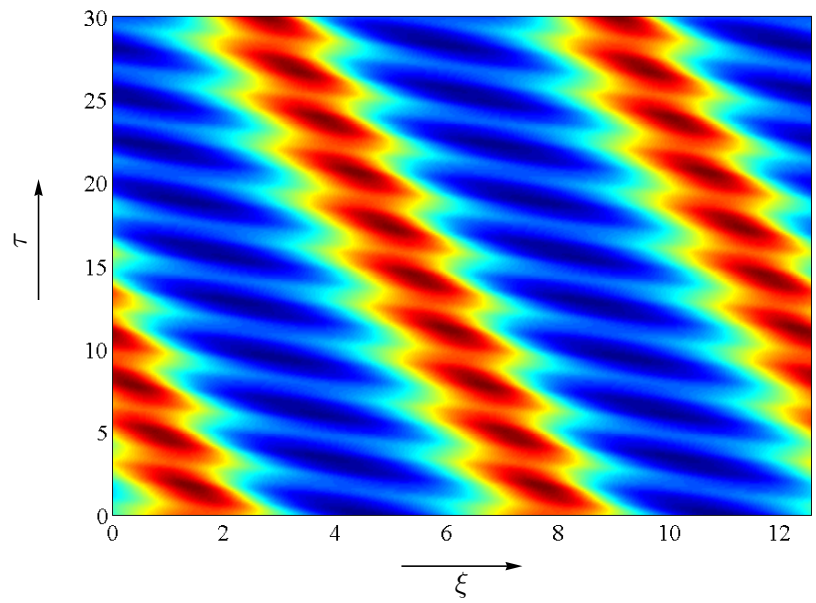


Figure 39: Pseudocolour plot over two space periods for $z = 10^{-0.5}$, $w = 10^{-0.9936}$.

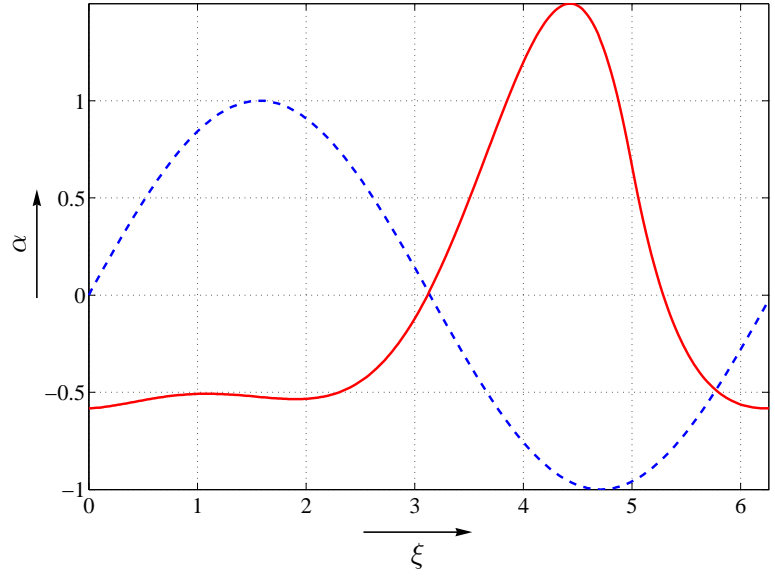


Figure 40: Initial harmonic wave (dashed line) and wave profile (solid line) at $\tau = 20.6$ for $z = 10^{-0.5}, w = 10^{-0.9936}$.

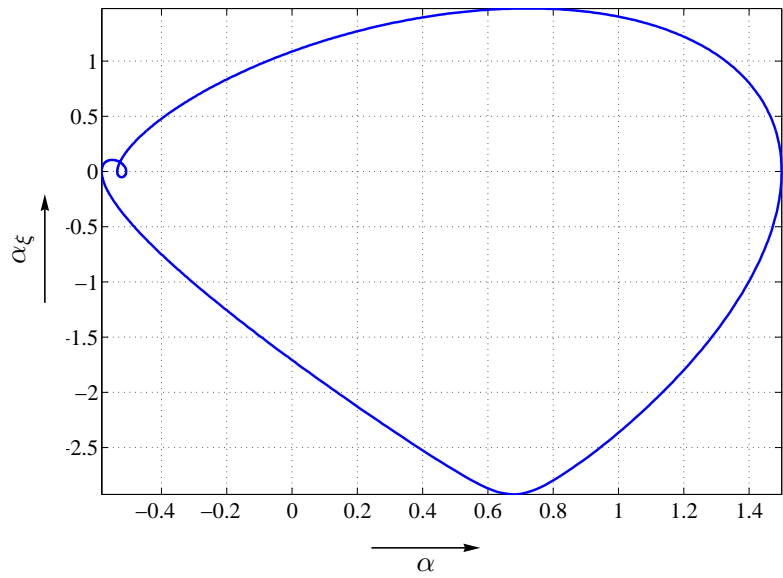


Figure 41: Asymmetry of solitons: α_ξ against α at $\tau = 20.6$ for $z = 10^{-0.5}, w = 10^{-0.9936}$.

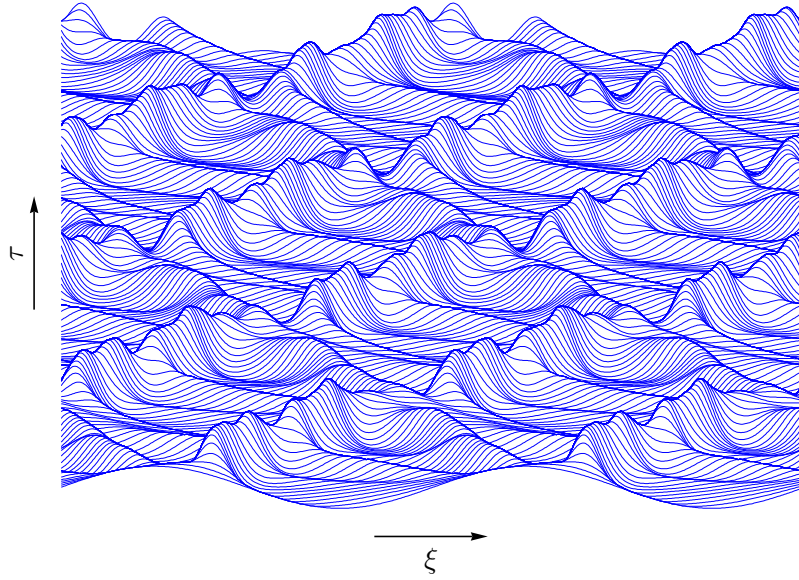


Figure 42: Time-slice plot over two space periods for KdV case, $z = 10^{-1.5}$, $w = 0$.

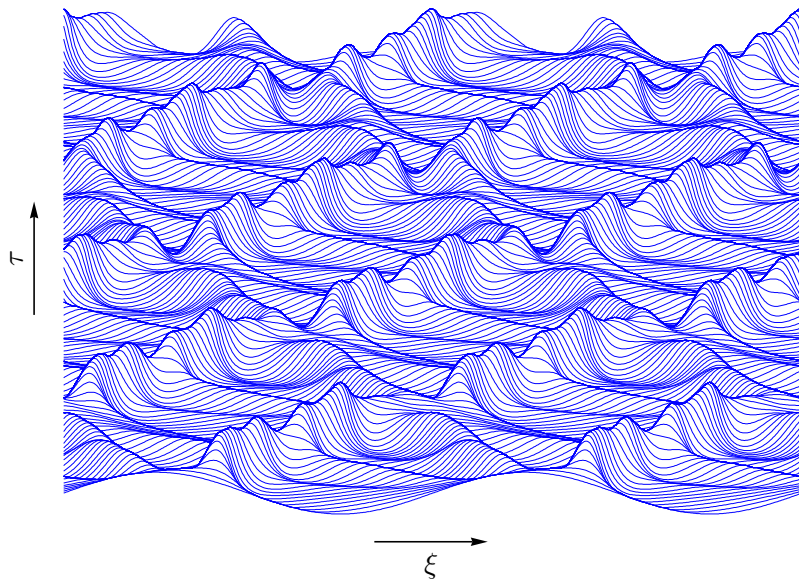


Figure 43: Time-slice plot over two space periods for $z = 10^{-1.5}$, $w = 10^{-2.621}$.

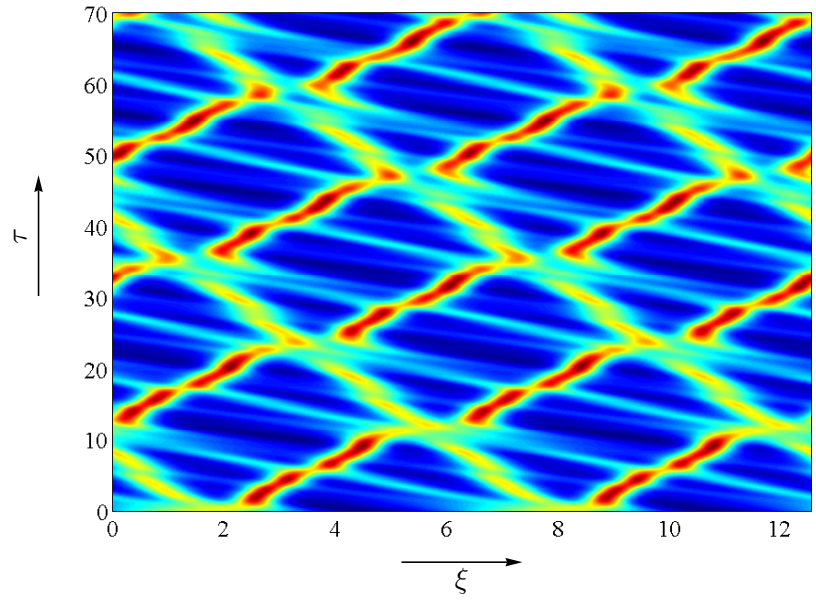


Figure 44: Pseudocolour plot over two space periods for KdV case, $z = 10^{-1.5}$, $w = 0$.

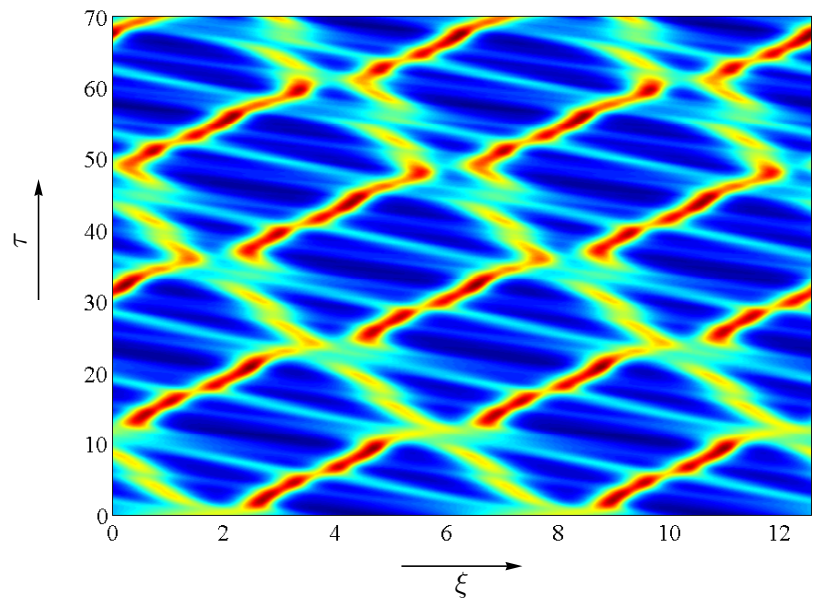


Figure 45: Pseudocolour plot over two space periods for $z = 10^{-1.5}$, $w = 10^{-2.6210}$.

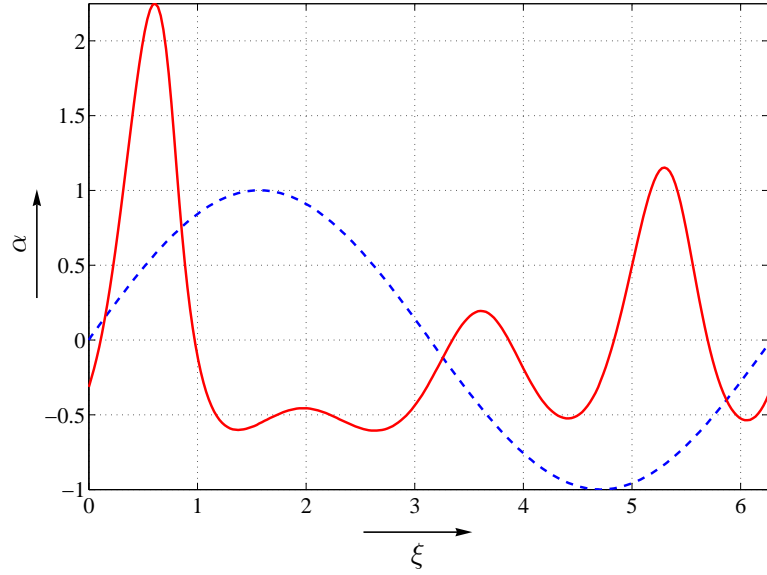


Figure 46: Initial harmonic wave (dashed line) and wave profile (solid line) at $\tau = 14.3$ for $z = 10^{-1.5}, w = 10^{-2.621}$.

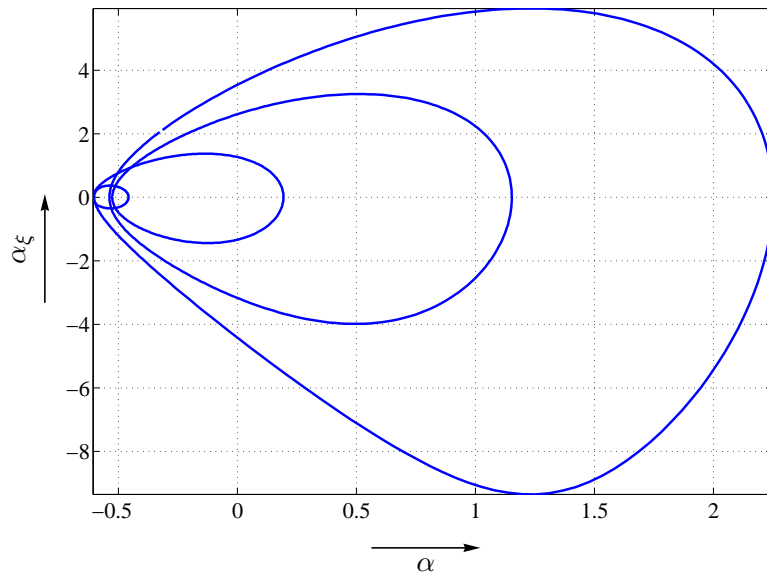


Figure 47: Asymmetry of solitons: α_ξ against α at $\tau = 14.3$ for $z = 10^{-1.5}, w = 10^{-2.621}$.

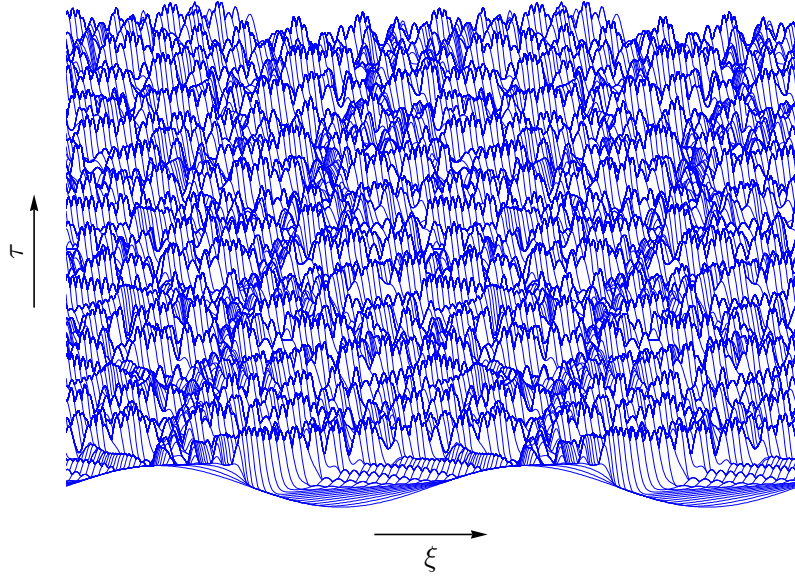


Figure 48: Time-slice plot over two space periods for KdV case, $z = 10^{-2.5}$, $w = 0$.

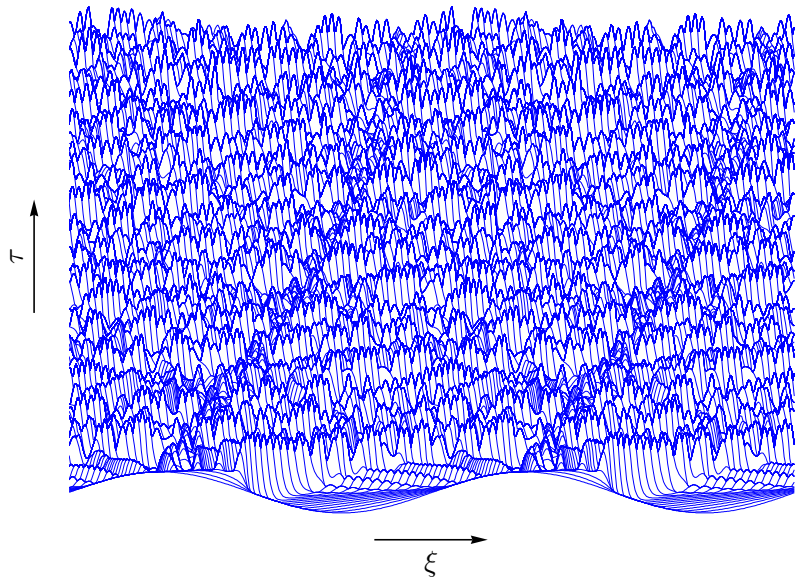


Figure 49: Time-slice plot over two space periods for $z = 10^{-2.5}$, $w = 10^{-4.1775}$.

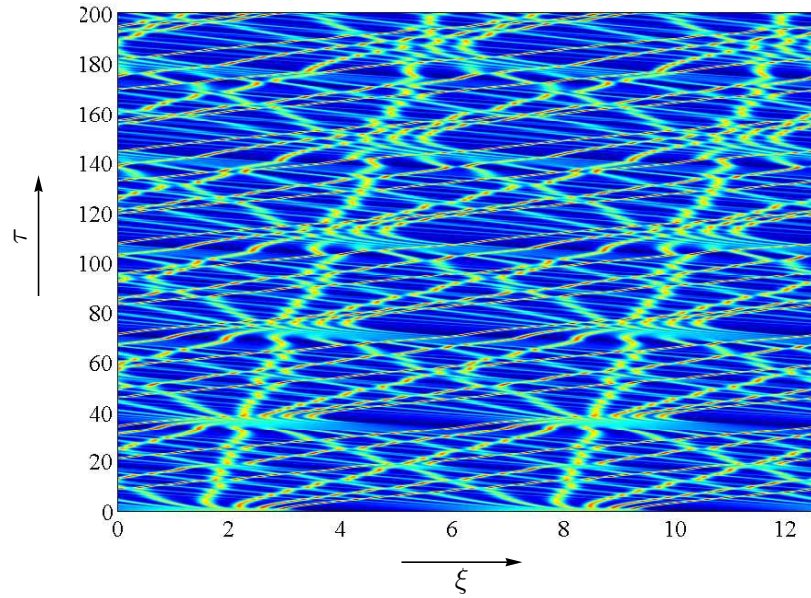


Figure 50: Pseudocolour plot over two space periods for KdV case, $z = 10^{-2.5}$, $w = 0$.

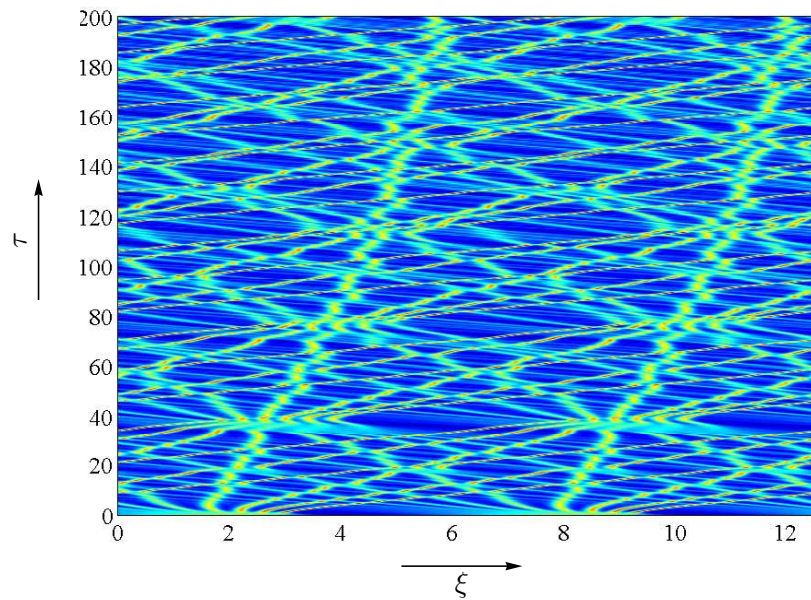


Figure 51: Pseudocolour plot over two space periods for $z = 10^{-2.5}$, $w = 10^{-4.1775}$.

Numerical calculations are performed on the basis of the equation (6.1), which can also be written as

$$\alpha_\tau + \frac{s}{2} (\alpha^2)_\xi + z \alpha_{\xi\xi\xi} + \frac{w}{2} (\alpha_\xi^2)_{\xi\xi} = 0. \quad (6.4)$$

Apart from the coefficients this equation coincides with the version (3.32), which forms the basis of the analytical treatment of the extended KdV equation. The two sets of coefficients are related by

$$s = \gamma_N^2, \quad z = 1 - \gamma_1^2, \quad w = \epsilon \gamma_M^2. \quad (6.5)$$

The standardized form of the extended KdV equation (3.37) is obtained from either (6.1) or (6.4) by the transformation formulas (3.36)

$$\alpha = \frac{6}{\gamma_N^2} (1 - \gamma_1^2)^{1/3} q = \frac{6}{s} z^{1/3} q, \quad \xi = (1 - \gamma_1^2)^{1/3} x = z^{1/3} x, \quad \tau = t. \quad (6.6)$$

There is only one parameter left, namely the micro-nonlinearity parameter

$$\varepsilon = \frac{\epsilon \gamma_M^2}{(1 - \gamma_1^2) \gamma_N^2} = \frac{w}{sz}, \quad (6.7)$$

cf. (3.38).

The standardized KdV equation, i.e., (3.37) with $\varepsilon = 0$, admits solutions that represent solitary waves, even solitons, of the form (2.2)

$$q = 2\eta^2 \operatorname{sech}^2 \eta (x - 4\eta^2 t). \quad (6.8)$$

Both the amplitude $2\eta^2$ and the propagation speed $4\eta^2$ are related to the width parameter η . Turning to the non-standardized KdV equation (6.4) with $w = 0$ the soliton (6.8), by use of the transformation (6.6), is transformed to

$$\alpha = \frac{12}{s} z^{1/3} \eta^2 \operatorname{sech}^2 \eta z^{-1/3} (\xi - 4\eta^2 z^{1/3} \tau). \quad (6.9)$$

Denoting the α -amplitude by A we have

$$A = \frac{12}{s} z^{1/3} \eta^2 \quad \text{or} \quad \eta = z^{-1/6} \sqrt{\frac{As}{12}}. \quad (6.10)$$

Using the amplitude A rather than η as the primary parameter, the width parameter and the propagation speed associated with the coordinate ξ are

$$\eta z^{-1/3} = \sqrt{\frac{As}{12z}} \quad \text{and} \quad 4\eta^2 z^{1/3} = \frac{s}{3} A, \quad (6.11)$$

respectively. Thus the standard KdV soliton satisfying (6.4) for $w = 0$ is

$$\alpha(\xi, \tau) = A \operatorname{sech}^2 \sqrt{\frac{As}{12z}} \left(\xi - \frac{s}{3} A \tau \right), \quad (6.12)$$

where A denotes the amplitude of the soliton. The profile $\alpha(\xi, 0)$, with $s = 1$, has been used in (6.3)₁ as an initial condition for the extended KdV equation (6.4). At least qualitatively it seems that an asymmetric solitary wave develops, followed by some small undulations.

The numerical results cannot be strictly compared with the approximate or analytical solutions presented in Section 4. The latter are restricted to the propagation of undistorted waves, while the numerics allows for arbitrary time-dependent wave profiles. Nevertheless, one can try at least to match the results.

It has been shown that the standardized extended KdV equation admits solitary waves only if the micro-nonlinearity parameter ε and the wave number η satisfy the inequality (4.15). By inserting (6.7) and (6.10)₂ one obtains

$$\varepsilon \eta^3 = \frac{1}{8} w \sqrt{s} \left(\frac{A}{3z} \right)^{\frac{3}{2}} \leq \frac{1}{16} \quad (6.13)$$

or, finally,

$$w \leq w_{\max} = \frac{1}{2\sqrt{s}} \left(\frac{3z}{A} \right)^{\frac{3}{2}}. \quad (6.14)$$

The non-standardized extended KdV equation (6.4) admits solutions in the form of asymmetric solitary waves only if its parameters s , z , w and the wave amplitude A satisfy the inequality (6.14).

The numerical result depicted in Figure 35 is obtained from numerical integration using the parameters

$$s = 1, \quad z = 0.01, \quad w = 10^{-2.5} \approx 0.00316. \quad (6.15)$$

The simulation started with the amplitude $A_0 = 1$. When the asymmetric solitary wave has fully developed the amplitude has dropped to $A \approx 0.95$. According to (6.14), the maximum micro-nonlinearity parameter that permits undistorted solitary waves would be

$$w_{\max} \approx 0.00281. \quad (6.16)$$

The phase curve in Figure 35 suggests that the solitary wave corresponds to a macro-nonlinearity close to the maximum value, because the trailing flank is nearly a straight line. Actually the macro-nonlinearity parameter of the numerical simulation is above the theoretical maximum. There can be several

reasons for this effect. First it must be taken into account that the numerical result does not represent an exact undistorted solitary wave. Rather there are some undulations at its trailing flank. Secondly the numerical simulation is performed on a finite ξ -interval using periodic boundary conditions. Periodic waves, however, are still possible at values of the micro-nonlinearity above the limit (6.14). Finally there is always some computational inaccuracy. The value of w is at least not too far from the theoretical limit (6.16).

Also some other properties of the limiting solitary wave are reflected only approximately by the numerical result. According to Figure 24, the maximum and minimum values of α_ξ should be located at $2/3$ of the amplitude, and the downward slope should be twice the upward slope. Approximately this can be realized in the numerical result Figure 35, although the maximum and the minimum are not exactly at the same value of α . This might be again due to the tail of the wave, which gives rise to the irregular behaviour of the phase curve at the origin.

The second numerical example, see Subsection 6.2, starts from a harmonic initial wave train and eventually develops a solitary wave extending below the α -axis, see Figures 40 and 46. Therefore theory must be generalised to allow for solitary waves with non-zero limits for $\xi \rightarrow \pm\infty$.

It can be proved that if $\alpha = \alpha(\xi, \tau)$ is some solution of the non-standardized extended KdV equation (6.4), then the function

$$\bar{\alpha}(\xi, \tau) = \alpha_0 + \alpha(\xi - s\alpha_0\tau, \tau) \quad (6.17)$$

is also a solution of (6.4) for any constant α_0 . In the case of undistorted waves, the wave profile is raised by the constant value α_0 and the propagation velocity is increased by $s\alpha_0$. Correspondingly, for a negative value of α_0 , the wave profile is lowered and the propagation speed is reduced.

6.4 Concluding remarks

The evolution equation (6.1) that governs one-wave propagation in microstructured solids according to Mindlin's model is derived and solved numerically under localised and harmonic initial conditions. Analysis of numerical results demonstrates that (i) for both the governing equation and the evolution equation nonlinearity in microscale leads to asymmetry of the wave profile [10, 68]; and (ii) the stronger the influence of micro-nonlinearity, the more the solutions of the evolution equation (6.1) differ from those of the KdV model.

In conclusion, the derived evolution equation (6.1), notwithstanding that it is a simplified model equation compared with the two-wave equation (3.21), is able to grasp essential effects of microinertia and elasticity of a microstructure. The values of parameters used above, are chosen for the comparison

with the standard KdV equation in order to demonstrate the influence of the microstructure.

In general the solitary waves exhibit the qualitative and quantitative properties predicted by the analytical results.

7 Conclusion

This thesis focuses on wave propagation in microstructured solids with the main aim to analyse dynamical properties of 1D microstructured solids as described by a Mindlin-type model.

Materials used nowadays in highly developed engineering applications are often characterised by their complex structure satisfying many requirements in practice. This concerns ceramic composites, alloys, polycrystalline solids, functionally graded materials, etc. The continua (materials) we are focused on, contain irregularities with one or more internal scales and therefore the notion “microstructured materials” is used. The complex dynamic behaviour of such materials cannot be explained by the classical theory of continua.

The embedding of a microstructure in an elastic material is reflected in an inherent length scale causing dispersion of propagating waves. The scale dependence involves dispersive effects as shown already in [2]. Nonlinear effects, if taken into account, will counteract dispersion. A suitable balance of nonlinearity and dispersion may permit the propagation of solitary waves. The Korteweg–de Vries equation describes how waves evolve under these two competing but comparable effects. Examples of nonlinear and dispersive behaviour of solid materials are provided by Samsonov [75] who has verified experimentally and explained theoretically the existence of solitary waves in solids, see also Porubov [76, 77] and the extensive literature cited therein. However, besides the solitary waves the KdV equation admits a whole family of periodic solutions, the so-called cnoidal waves [30], of which the solitary wave is just the limit if the period tends to infinity. It should be stressed that both solitons and cnoidal waves propagate without distortion, while in general, solutions of the KdV equation represent waves changing their shape during propagation.

A linear theory of microstructured solids has been proposed by Mindlin [1] in 1964. Mindlin’s model has recently been extensively studied [9, 59, 61], mostly in the 1D setting which explicitly explains the main features of the process. It has been shown that such modelling describes well the influence of microstructure on dispersion and the existence of wave hierarchies. The model permits, for example, to understand the emergence of solitary waves in microstructured materials, both analytically [10] and numerically [73, 74]. In addition, there is a wide area of possible applications in nondestructive testing by solving the corresponding inverse problem for determining the material properties [62, 78].

The model equation, in studies mentioned above, in the 1D case is a typical hierarchical wave equation with the leading operator of the 2nd order and the higher-order operators describing the influence of the microstructure [59, 61]. This is the two-wave equation, i.e., it describes waves propagating in two di-

rections. The powerful analytic methods [63] show explicitly how in this case evolution equations could be derived that govern the propagation of one wave only. The best example of such an evolution equation is the celebrated KdV equation. If we are interested in wave propagation along a certain coordinate without reflection from boundaries then the concept of evolution equations is preferable. However, the transformations from a two-wave model to an evolution equation should bring over all the essential features that could influence the velocities or the distortions of the wave profile.

The main result of the thesis is derivation and analysis of the extended KdV equation as the evolution equation of waves propagating in microstructured solids. More specifically, the results are as follows:

Evolution equation

- For the nonlinear MEP model an evolution equation has been derived, which describes the slow change of the profile of a wave propagating in one direction with the basic propagation speed \bar{c} . In the special case of the linear system it is shown that the same evolution equation is obtained from both the full and the reduced equation.
- The evolution equation has the form of an extended KdV equation, in which the additional term originates from the micro-nonlinearity of the original system of equations. If this is neglected the evolution equation is reduced to the standard KdV equation.
- The coefficients of the evolution equation can be traced back to the material parameters of the model. Moreover, the evolution equation can be standardised by rescaling the moving space and time coordinates such that there is only a single dimensionless parameter ε left. It is a measure for the influence of the micro-nonlinearity compared to the combined effects of dispersion and macro-nonlinearity.

Undistorted waves

- The evolution equation describes the slow change in time of an arbitrary wave profile. There exist special wave profiles whose shape does not change in time. This constant profile may still move slowly relative to the frame travelling at the basic propagation speed \bar{c} . The undistorted waves are solutions of a nonlinear ordinary differential equation derived from the evolution equation by a wave ansatz.

Existence of solitary waves

- Special emphasis has been put on solitary waves. In contrast to periodic waves, solitary waves are localised, i.e., outside some moving space interval they fade away rapidly.
- By discussing the properties of the phase curves it is shown that, in the case of the extended KdV equation, solitary waves exist if the micro-nonlinearity parameter ε does not exceed some maximum value ε_{\max} which depends on the width parameter η . This confirms a result of Janno and Engelbrecht.

Approximate and exact solutions representing solitary waves

- The nonlinear evolution equation as an extended KdV equation is solved approximately by a series expansion in a small parameter representing the micro-nonlinearity. Already the first approximation indicates the asymmetry of the solitary waves.
- In the limiting case $\varepsilon = \varepsilon_{\max}$ the phase curve degenerates into a semi-ellipse and a straight line. This makes it possible to get an exact analytical solution representing the corresponding solitary wave. Since this solution is available just for the “worst” case, the quality of the approximate solutions can be assessed.

Generalisation to periodic waves

- The classical sech^2 soliton can be considered as the long-wave limit of the cnoidal waves. In the same way the asymmetric solitary waves governed by the extended KdV equation are the limits of periodic wave trains when their wave length tends to infinity.
- Periodic waves emerging from the cnoidal waves of the KdV equation are studied using the same perturbation procedure as for the solitary waves. Compared with the cnoidal waves, these more general periodic waves are asymmetric, i.e., inclined to the direction of propagation.
- The behaviour of the periodic waves is also studied in the phase plane. They are represented by regular orbits, along which the representative point circles once per wave length. As the wave length tends to infinity the phase curve, now representing a solitary wave, develops a saddle point.

Numerical solutions of the evolution equation

- While all the analytical results mentioned above are related to undistorted waves some numerical calculations have been performed with the evolution equation as a partial differential equation. The evolution equation is integrated numerically both under harmonic and localised initial conditions making use of the pseudospectral method.
- From both initial conditions solitary waves develop, followed by some disturbances. Analysis of numerical results demonstrates that (i) for both the governing equation and the evolution equation nonlinearity in microscale leads to asymmetry of the wave profile; and (ii) the stronger the influence of micro-nonlinearity, the more the solutions of the evolution equation differ from those of the KdV model.
- In general the solitary waves exhibit the qualitative and quantitative properties predicted by the analytical results.

Further prospects

Wave propagation in microstructured materials is an attractive research topic which opens a wide field of further studies. The results presented in this thesis do not give a complete picture of the wave propagation in microstructured materials. Even if the basic idea of the MEP model is kept there remains a lot of open questions which could be studied in the future. Among them are the following points, which might be of special interest:

- To compare solutions of the original system of partial differential equations with the solutions of the evolution equation at fixed values of the material parameters to justify the application of the reductive perturbation method.
- To find a physical interpretation of the model parameters A , B , C , etc. in terms of the mechanical and geometrical properties of the microstructured material.
- Generalisation of the model to two (and three) dimensions. Representation of the corresponding constitutive equations for isotropic microstructured materials or materials with specified anisotropy. Also, to find possible applications in nondestructive testing.
- If applied to the linear model, the evolution equation is related to the acoustical branch of the dispersion diagram. There should be also a corresponding evolution equations related to the optical branch. Does

its nonlinear version also allow solitary waves and, if so, what is their relevance?

- Are there *exact* solutions of the original system representing solitary waves? If so, how good is the coincidence with the approximate theory using the evolution equation?
- For the KdV equation the interaction of two (and more) solitons can be described analytically. Can one analyse the interaction of two asymmetric solitary waves governed by the extended KdV equation at least approximately?

Abstract

The focus of the thesis is on wave propagation in microstructured solids. The main aim of the investigation is to analyse dynamical properties of 1D microstructured solids as described by a Mindlin-type model. The embedding of a microstructure in an elastic material is reflected in an inherent length scale causing dispersion of propagating waves. Nonlinear effects, if taken into account, will counteract dispersion. A suitable balance between nonlinearity and dispersion may permit the propagation of solitary waves.

Using the reductive perturbation method, for the nonlinear Mindlin–Engelbrecht–Pastrone model an evolution equation is derived, which describes the slow change of the profile of a wave propagating in one direction with the basic propagation speed. This evolution equation enlarges the class of the KdV-type equations by including two types of nonlinearities. In the special case of the linear system it is shown that the same evolution equation is obtained from both the full and the reduced equation.

The nonlinear evolution equation as an extended Korteweg–de Vries equation is solved approximately by a series expansion in a small parameter representing the micro-nonlinearity. Already the first approximation indicates the asymmetry of the solitary waves. It is shown that solitary waves will propagate only if the micro-nonlinearity does not exceed some upper bound. For the limiting case, an analytical solution of the extended Korteweg–de Vries equation can be provided and used as a reference for the approximate solutions.

The classical sech^2 soliton can be considered as the long-wave limit of the cnoidal waves. In the same way the asymmetric solitary waves governed by the extended KdV equation are the limits of periodic wave trains when their wave length tends to infinity. Periodic waves emerging from the cnoidal waves of the KdV equation are studied using the same perturbation procedure as for the solitary waves. Compared with the cnoidal waves, these more general periodic waves are asymmetric, i.e., inclined to the direction of propagation.

The evolution equation is integrated numerically both under harmonic and localised initial conditions making use of the pseudospectral method. It is demonstrated that the derived evolution equation is able to grasp essential effects of microinertia and elasticity of a microstructure. The influence of these effects can result in the emergence of asymmetric solitary waves. In general the solitary waves exhibit the qualitative and quantitative properties predicted by analytical results.

Main results of the thesis have been summarised in seven presentations, five of them at international conferences. Also the results have been published in six academic papers, four of them in journals indexed by ISI Web of Science.

Kokkuvõte

Doktoritöö käsitleb lainelevi mikrostruktuuriga tahkistes. Töö põhieesmärk on analüüsida mikrostruktuuriga materjalide dünaamilisi omadusi ühedimensioonilisel juhtumil, kasutades Mindlini tüüpi mudelit. Mikrostruktuur elastises materjalis kui materjali sisemine skaala põhjustab selles materjalis levivate lainete dispersiooni. Mittelineaarsete efektide mõju on aga seotud katkevuste tekkega, st profiili järsenemisega. Dispersiooni- ja mittelineaarsete efektide tasakaalu korral on võimalik üksiklainete levi.

Asümptootilise häiritusmeetodi abil on tuletatud mittelineaarsetele Mindlini–Engelbrechti–Pastrone mudelile vastav evolutsioonivõrrand, mis kirjeldab põhikiirusega liikuva laineprofiili aeglast muutumist ajas. See evolutsioonivõrrand laiendab tuntud KdV-tüüpi võrrandite klassi, sisaldades kahte tüüpi mittelineaarset liikmeid. Lineaarsel juhtumil on näidatud, et nii täisvõrrand kui aproksimeeritud hierarhiline võrrand viivad identsete evolutsioonivõrranditeni.

Mittelineaarne evolutsioonivõrrand kui üldistatud Kortewegi–de Vriesi võrrand on lahendatud ligikaudselt, kasutades rittaarendust mikrotasandi mittelineaarsust iseloomustava väikese parameetri järgi. Juba esimest järku lähendus osutab üksiklaine profiili ebasümmeetriale. Ilmneb, et üksiklaineline lahend eksisteerib vaid siis, kui mikro-mittelineaarsus ei ületa teatavat ülemist piiri. Nimetatud piirjuhtumil on saadud üldistatud KdV-võrrandile täpne lahend, mille põhjal on võimalik hinnata, kui head vastavad ligikaudsed lahendid on.

Klassikalisi sech^2 -solitone võib vaadelda kui lõpmatusele läheneva lainepikkusega knoidaalseid laineid. Samuti on ebasümmeetrilised üksiklained kui üldistatud KdV-võrrandi lahendid vaadeldavad lõpmatusele läheneva lainepikkusega perioodiliste lainetena. Knoidaalsete lainetega võrreldes on üldistatud KdV-võrrandi perioodilistel lahenditel vastavalt liikumise suunale profiili esikülj järsema kaldega kui tagumine. Selgub, et mittelineaarsete lisaliikme mõju perioodilistele lahenditele on samasugune kui üksiklainelisele lahendile, põhjustades laineprofiili ebasümmeetria.

Evolutsioonivõrrand on lahendatud numbriliselt lokaliseeritud ja harmooniliste algtingimuste korral, rakendades pseudospektraalmeetodit. Tulemuste analüüs näitab, et evolutsioonivõrrand säilitab endas olulised mikrostruktuuri efektid, nagu mikroinerts ja elastsus. Nende efektide koosmõjul saavad tekkida ebasümmeetrilised üksiklained. Üldiselt langevad numbrilise analüüsi tulemused nii kvalitatiivselt kui kvantitatiivselt kokku analüütiliste tulemustega.

Töö põhitulemusi on esitletud seitsmes ettekandes, millest viis rahvusvahelistel konverentsidel, ja avaldatud kuues teadusartiklis, millest neli on ilmunud rahvusvaheliselt tunnustatud erialaajakirjades (indekseeritud ISI Web of Science'i poolt).

References

- [1] Raymond D. Mindlin: Microstructure in linear elasticity. *Archive for Rational Mechanics and Analysis* **16** (1964) 51–78.
- [2] C.-T. Sun, Jan D. Achenbach, and George Herrmann: Continuum theory for a laminated medium. *Journal of Applied Mechanics, Transactions of the American Society of Mechanical Engineering*, **35** (1968) 467–475.
- [3] George Herrmann and Jan D. Achenbach: Application of theories of generalized Cosserat continua to the dynamics of composite materials. In: Ekkehard Kröner (editor), *Mechanics of Generalized Continua*. Springer, Berlin 1968, 69–79.
- [4] Ahmet Cemal Eringen: Linear theory of micropolar elasticity. *Journal of Applied Mathematics and Mechanics* **15** (1966) 909–923.
- [5] Gérard A. Maugin: *Material Inhomogeneities in Elasticity*. Chapman and Hall, London 1993.
- [6] Ahmet Cemal Eringen: *Microcontinuum Field Theories I: Foundations and Solids*. Springer, New York 1999.
- [7] Jerald LaVerne Ericksen and Clifford Truesdell: Exact theory of stress and strain in rods and shells. *Archive for Rational Mechanics and Analysis* **1** (1958) 295–323.
- [8] Eugene Cosserat and François Cosserat: *Théorie des Corps Déformables*. Hermann & Fils, Paris 1909.
- [9] Jüri Engelbrecht and Franco Pastrone: Waves in microstructured solids with strong nonlinearities in microscale. *Proceedings of the Estonian Academy of Sciences. Physics, Mathematics* **52** (2003) 12–20.
- [10] Jaan Janno and Jüri Engelbrecht: Solitary waves in nonlinear microstructured materials. *Journal of Physics A: Mathematical and General* **38** (2005) 5159–5172.
- [11] Donald E. Hall: *Musical Acoustics: An Introduction*. Wadsworth Publishing Company, Belmont 1980.
- [12] Gerald B. Whitham: *Linear and Nonlinear Waves*. John Wiley & Sons, New York 1974.
- [13] Clifford Truesdell and Walter Noll: *The Non-Linear Field Theories of Mechanics*. Springer–Verlag, New York 1965.

- [14] John Billingham and Andrew C. King: *Wave Motion*. Cambridge University Press, Cambridge 2000.
- [15] Michael A. Slawinski: Seismic waves and rays in elastic media. In: Klaus Helbig and Sven Treitel (editors), *Handbook of Geophysical Exploration: Seismic Exploration*, Vol. 34. Elsevier 2003.
- [16] Karl F. Graff: *Wave Motion in Elastic Solids*. Dover Publications, Inc., New York 1991.
- [17] Jan D. Achenbach: *Wave Propagation in Elastic Solids*. North-Holland Publishing Company, Amsterdam, London; American Elsevier Publishing Company, Inc., New York 1973.
- [18] Philip G. Drazin: *Solitons*. Cambridge University Press, Cambridge 1985.
- [19] Yuan-Cheng Fung and Ping Tong: *Classical and Computational Solid Mechanics*. World Scientific Publishing Co., Singapore 2001.
- [20] Allan F. Bower: *Applied Mechanics of Solids*. CRC Press, Boca Raton 2010.
- [21] Stephen A. Thau: Linear dispersive waves. In: Sidney Leibovich and A. Richard Seebass (editors), *Nonlinear Waves*. Cornell University Press, Ithaca, London 1974, 44–81.
- [22] Augustus Edward Hough Love: *A Treatise on the Mathematical Theory of Elasticity*. Cambridge University Press, Cambridge 1927.
- [23] Alwyn Scott (editor): *Encyclopedia of Nonlinear Science*. Routledge, New York, London 2005.
- [24] Jüri Engelbrecht: Deformation waves in solids. In: Ewald Quak and Tarmo Soomere (editors), *Applied Wave Mathematics. Selected Topics in Solids, Fluids, and Mathematical Methods*. Springer–Verlag, Berlin Heidelberg 2009.
- [25] Jüri Engelbrecht: *Nonlinear Wave Dynamics. Complexity and Simplicity*. Kluwer, Dordrecht 1997.
- [26] Jüri Engelbrecht: Nonlinear wave motion and evolution equations. In: Alan Jeffrey and Jüri Engelbrecht (editors), *Nonlinear Waves in Solids*. CISM Courses and Lectures No. 341, International Centre for Mechanical Sciences. Springer–Verlag, Wien, New York 1994.
- [27] Mysore N. L. Narasimhan: *Principles of Continuum Mechanics*. John Wiley & Sons, Inc., New York 1993.

- [28] Ray W. Ogden: *Non-linear Elastic Deformations*. Dover Publications, Mineola, New York 1997, 118–119.
- [29] Jüri Engelbrecht: *Nonlinear Wave Processes of Deformation in Solids*. Pitman, Boston 1983.
- [30] Gustav de Vries: *Bijdrage tot de kennis der lange golven*. Doctoral dissertation, University of Amsterdam, Amsterdam 1894.
- [31] Enrico Fermi, John R. Pasta, and Stanislaw Marcin Ulam: Studies of nonlinear problems. Los Alamos report LA-1940 (1955), published later in: E. Segré (editor), *Collected Papers of Enrico Fermi*. University of Chicago Press, Chicago 1965.
- [32] Diedrik Johannes Korteweg and Gustav de Vries: On the change of form of long waves advancing in a rectangular canal, and on a new type of long stationary waves. *Philosophical Magazine*, 5th series, **39** (1895) 422–443.
- [33] Norman J. Zabusky and Martin D. Kruskal: Interaction of “solitons” in a collisionless plasma and the recurrence of initial states. *Physical Review Letters* **15** (1965) 240–243.
- [34] Philip G. Drazin and Robin Stanley Johnson: *Solitons: An Introduction*. Cambridge University Press, Cambridge 2002, 13–14.
- [35] Milton Abramowitz, Irene A. Stegun (editors): *Handbook of Mathematical Functions*. Dover Publications, New York 1965.
- [36] Wolfgang Gröbner, Nikolaus Hofreiter (Herausgeber): *Integraltafel. Erster Teil: Unbestimmte Integrale*. Fünfte, verbesserte Auflage. Springer-Verlag, Wien, New York 1975.
- [37] Manfred Braun: Nonlinear progressive waves in elastic materials. *Rheologica Acta* **16** (1977) 146–154.
- [38] John K. Hunter and Jurgen Scheurle: Existence of perturbed solitary wave solutions to a model equation for water waves. *Physica D: Nonlinear Phenomena* **32**(2) (1988) 253–268.
- [39] Vladimir I. Karpman and Jean-Marc Vanden-Broeck: Stationary solitons and stabilization of the collapse described by KdV-type equations with high nonlinearities and dispersion. *Physics Letters A* **200**(6) (1995) 423–428.
- [40] Tsunehiko Kakutani and Hiroaki Ono: Weak non-linear hydromagnetic waves in a cold collision-free plasma. *The Journal of the Physical Society of Japan* **26** (1969) 1305–1318.

- [41] Olari Ilison and Andrus Salupere: Propagation of sech^2 -type solitary waves in higher-order KdV-type systems. *Chaos Solitons Fractals* **26**(2) (2005) 453–465.
- [42] Olari Ilison and Andrus Salupere: On the propagation of solitary pulses in microstructured materials. *Chaos Solitons Fractals* **29**(1) (2006) 202–214.
- [43] Andrus Salupere, Gérard A. Maugin, and Jüri Engelbrecht: Solitons in systems with a quartic potential and higher-order dispersion. *Proceedings of the Estonian Academy of Sciences. Physics, Mathematics.* **46** (1997) 118–127.
- [44] Peter E. Holloway, Efim Pelinovsky, Tatiana Talipova: Internal tide transformation and oceanic internal solitary waves. In: Roger Grimshaw (editor), *Environmental Stratified Flows*. Kluwer Academic Publishers, Boston 2001, 29–60.
- [45] Roger Grimshaw: Internal solitary waves. In: Roger Grimshaw (editor), *Environmental Stratified Flows*. Kluwer Academic Publishers, Boston 2001, 1–28.
- [46] Roger Grimshaw, Efim Pelinovsky, Tatiana Talipova and Andrey Kurkin: Simulation of the transformation of internal solitary waves on oceanic shelves. *Journal of Physical Oceanography* **34** (2004) 2774–2779.
- [47] Alexey V. Porubov, Gérard A. Maugin, Vitaly V. Gursky, Valeria V. Krzhizhanovskaya: On some localized waves described by the extended KdV equation. *C. R. Mecanique* **333**(7) (2005) 528–533.
- [48] Timothy R. Marchant: Solitary wave interaction for the extended BBM equation. *Proceedings of the Royal Society of London, Series A* **456** (2000) 433–453.
- [49] Jüri Engelbrecht and Manfred Braun: Nonlinear waves in nonlocal media. *Applied Mechanics Reviews* **51** (1998) 475–488.
- [50] Arnold M. Kosevich and Serge E. Savotchenko: Features of dynamics of one-dimensional discrete systems with non-neighbouring interactions, and role of higher-order dispersion in solitary wave dynamics. *Low Temperature Physics* **25** (1999) 737–747.
- [51] Shunji Kawamoto: Solitary wave solutions of the Korteweg–de Vries equation with higher order nonlinearity. *The Journal of the Physical Society of Japan* **53**(11) (1984) 3729–3731.

- [52] Yu Tan, Jianke Yang, Dmitry E. Pelinovsky: Semi-stability of embedded solitons in the general fifth-order KdV equation. *Wave Motion* **36**(3) (2002) 241–255.
- [53] Nikolai A. Kudryashov and Dmitry I. Sinelshchikov: Nonlinear waves in bubbly liquids with consideration for viscosity and heat transfer. *Physics Letters A* **374**(19–20) (2010) 2011–2016.
- [54] Pasquale Giovine and Francesco Oliveri: Dynamics and wave propagation in dilatant granular materials. *Meccanica* **30** (1995) 341–357.
- [55] Merle Randrüüt and Manfred Braun: On one-dimensional solitary waves in microstructured solids. *Wave Motion* **47**(4) (2010) 217–230.
- [56] Merle Randrüüt and Manfred Braun: On solitary waves in one-dimensional microstructured solids. *PAMM. Proceedings in Applied Mathematics and Mechanics* **9**(1) (2010) 495–496.
- [57] Roger Grimshaw, Efim Pelinovsky, Tatiana Talipova: Damping of large-amplitude solitary waves. *Wave Motion* **37**(4) (2003) 351–364.
- [58] Hilmi Demiray: A note on the solution of perturbed Korteweg–de Vries equation. *Applied Mathematics and Computation* **132**(2–3) (2002) 643–647.
- [59] Jüri Engelbrecht, Arkadi Berezovski, Franco Pastrone, and Manfred Braun: Waves in microstructured materials and dispersion. *Philosophical Magazine* **85**(33–35) (2005) 4127–4141.
- [60] Richard A. Toupin: Elastic materials with couple-stresses. *Archive for Rational Mechanics and Analysis* **11** (1962) 385–414.
- [61] Jüri Engelbrecht, Franco Pastrone, Manfred Braun, and Arkadi Berezovski: Hierarchies of waves in nonclassical materials. In: Pier Paolo Delsanto (editor), *The Universality of Nonclassical Nonlinearity: Applications to Non-destructive Evaluations and Ultrasonics*. Springer 2006, 29–48.
- [62] Jaan Janno and Jüri Engelbrecht: Waves in microstructured solids: Inverse problems. *Wave Motion* **43** (2005) 1–11.
- [63] Tosiya Taniuti and Kazuhiro Nishihara: *Nonlinear Waves*. Pitman, London 1983.
- [64] Jüri Engelbrecht: *An Introduction to Asymmetric Solitary Waves*. Longman, Harlow 1991.

- [65] Alan C. Newell: *Solitons in Mathematics and Physics*. Society for Industrial and Applied Mathematics, Philadelphia 1985.
- [66] Tanel Peets, Merle Randrüüt, and Jüri Engelbrecht: On modelling dispersion in microstructured solids. *Wave Motion* **45**(4) (2008) 471–480.
- [67] Manfred Braun and Merle Randrüüt: On periodic waves governed by the extended Korteweg–de Vries equation. *Proceedings of the Estonian Academy of Sciences* **59**(2) (2010) 133–138.
- [68] Merle Randrüüt, Andrus Salupere, and Jüri Engelbrecht: On modelling wave motion in microstructured solids. *Proceedings of the Estonian Academy of Sciences* **58**(4) (2009) 241–246.
- [69] Andrus Salupere, Merle Randrüüt, and Kert Tamm: Emergence of soliton trains in microstructured materials. In: J. Denier, M. Finn, T. Mattner (editors), *XXII International Congress of Theoretical and Applied Mechanics ICTAM 2008*, CD-ROM Proceedings, August 24–29, Adelaide, Australia 2008.
- [70] Bengt Fornberg: *Practical Guide to Pseudospectral Methods*. Cambridge University Press, Cambridge 1998.
- [71] Andrus Salupere, Jüri Engelbrecht, and Pearu Peterson: Long-time behaviour of soliton ensembles. Part I – Emergence of ensembles. *Chaos, Solitons & Fractals* **14** (2002) 1413–1424.
- [72] Andrus Salupere, Jüri Engelbrecht, and Pearu Peterson: Long-time behaviour of soliton ensembles. Part II – Periodical patterns of trajectories. *Chaos, Solitons & Fractals* **15** (2003) 29–40.
- [73] Andrus Salupere, Kert Tamm, and Jüri Engelbrecht: Numerical simulation of interaction of solitary deformation waves in microstructured solids. *International Journal of Non-Linear Mechanics* **43** (2008) 201–208.
- [74] Andrus Salupere, Kert Tamm, Jüri Engelbrecht, and Pearu Peterson: On interaction of deformation waves in microstructured solids. *Proceedings of the Estonian Academy of Sciences. Physics, Mathematics*. **56**(2) (2007) 93–99.
- [75] Alexander M. Samsonov: *Strain Solitons in Solids and How to Construct Them*. Chapman & Hall/CRC, Boca Raton 2001.
- [76] Alexey V. Porubov: *Amplification of Nonlinear Strain Waves in Solids*. World Scientific, New Jersey 2003.

- [77] Алексей В. Порубов: *Локализация нелинейных волн деформации*. Физматлит, Москва 2009.
- [78] Jaan Janno and Jüri Engelbrecht: An inverse solitary wave problem related to microstructured materials. *Inverse Problems* **21** (2005) 2019–2034.

APPENDIX A

PUBLICATIONS

PUBLICATION I

Tanel Peets, **Merle Randrüüt**, and Jüri Engelbrecht: On modelling dispersion in microstructured solids. *Wave Motion* **45**(4) (2008) 471–480.[‡]

[‡]Reprinted with permission from Elsevier.

On modelling dispersion in microstructured solids

T. Peets ^{*,1}, M. Randrüüt ¹, J. Engelbrecht

Centre for Nonlinear Studies, Institute of Cybernetics at Tallinn University of Technology, Akadeemia tee 21, 12618 Tallinn, Estonia

Received 13 April 2007; received in revised form 21 September 2007; accepted 27 September 2007

Available online 6 October 2007

Abstract

The Mindlin-type model is used for describing the longitudinal deformation waves in microstructured solids. A simplified hierarchical model is derived in one-dimensional setting which is a two-wave equation. In addition, the evolution equations (one-wave equations) are derived for both the full and simplified models. It is shown that the simplified model as well as evolution equations grasp main effects of dispersion in a wide range of physical parameters.

© 2007 Elsevier B.V. All rights reserved.

Keywords: Dispersion; Microstructure; Hierarchy of waves

1. Introduction

In contemporary materials science and structural mechanics much attention is given to microstructured materials possessing internal scales. Microstructured materials like alloys, crystallites, ceramics, functionally graded materials, etc have gained wide application in modern technology because combining the mechanical properties of different constituencies as in functionally graded materials or composites yields better (optimal) properties of solids. Very often they are used in severe loading conditions including impact, which means generation of stress/deformation waves. The modelling of wave propagation in such materials should be able to account for various scales of microstructure. The scale dependence involves dispersive effects and if in addition the material behaves nonlinearly then dispersive and nonlinear effects may be balanced. As widely known, in this case solitary waves may emerge as a result of such a balance.

Clearly the classical theory of continuous media is not able to describe the influence of microstructure which is needed for explain dispersive and dissipative effects. There are many studies in this field, starting from the papers of Mindlin [1] and Eringen [2] several decades ago. Now we have a solid theoretical background, see for example [3,4], but another problem has arisen: the governing equations tend to be rather complicated and the number of material parameters needed to describe the stress field, is rather high. Therefore there is an

* Corresponding author. Tel.: +372 6204169; fax: +372 6204151.

E-mail addresses: tanelp@cens.ioc.ee (T. Peets), merler@cens.ioc.ee (M. Randrüüt), je@ioc.ee (J. Engelbrecht).

¹ These authors contributed equally to this work.

urgent need to find simplified governing equations but the physical effects should still be described with the needed accuracy.

The problem is not only in the mathematical complexity of governing equations but also in the number of waves. If in the linear theory, for example, longitudinal and shear waves can be easily separated then in the nonlinear theory the coupling can affect both waves considerably. In a general case of a complicated system of equations the main question is to understand to which wave which physical effects are related both quantitatively and qualitatively.

One of the possibilities to overcome such difficulties in contemporary mathematical physics is to introduce the notion of evolution equations governing just one single wave. Physically it means the separation (if possible) of a multi-wave process into separate waves. The waves are then governed by the so-called evolution equations every one of which describe the distortion of a single wave along a properly chosen characteristics (ray).

In this paper the attention is focused to the analysis of dispersion described by Mindlin-type models [1]. Engelbrecht et al. [5,6] have derived the one-dimensional mathematical model for longitudinal waves in microstructured materials. Based on the separation of macro- and microstructure of a material, this model is characterised by a clear physical structure of the governing equation. The analysis of the full-dispersion relation of this model compared with others is briefly presented in [5] (see also references therein). Our question here is the following: if we use asymptotic methods to simplify the model then can we describe still the physics with acceptable accuracy? We shall use two asymptotic approaches: (i) the slaving principle [7] in order to get a hierarchical asymptotic Whitham-type model from the basic one and (ii) the perturbative reduction method [8,9] in order to get evolution equations. Although nonlinearity is an important factor, here we deal only with dispersive effects and nonlinear waves will be analysed in our further publications.

The paper is organized as follows: the basic model following [5,6] is presented in Section 2. In Section 3, the asymptotic models are derived following two approaches resulting in a hierarchical simplified equation and in evolution equations. Section 4 is devoted to the dispersion analysis of the basic and the simplified models. In Section 5, final remarks are presented. It has been shown that the simplified model as well as evolution equations grasp main effects of dispersion in a wide range of physical parameters.

2. Basic model

The basic model is that of Mindlin [1] and we follow the presentation of that in [5,6]. The main idea is to distinguish between macro- and microdisplacements $u_i(x_i, t)$ and $u'_j(x'_i, t)$, respectively. Assuming that microdisplacement is defined in coordinates x'_k moving with microvolume, we define

$$u'_j = x'_k \varphi_{kj}(x_i, t), \quad (1)$$

where φ_{kj} is an arbitrary function. It is clear that actually it is microdeformation while

$$\partial u'_j / \partial x'_i = \partial'_i u'_j = \varphi_{ij}. \quad (2)$$

Further we consider the simplest 1D case and drop the indices i and j .

Now the fundamental balance laws can be formulated separately for macroscopic and microscopic scales. Introducing the Lagrangian $L = K - W$, formed from the kinetic and potential energies

$$\begin{cases} K = \frac{1}{2} \rho u_t^2 + \frac{1}{2} I \varphi_t^2 \\ W = W(u_x, \varphi, \varphi_x), \end{cases} \quad (3)$$

where ρ and I denote the macroscopic density and the microinertia, respectively, we can derive the corresponding Euler–Lagrange equations:

$$\begin{cases} \left(\frac{\partial L}{\partial u_t} \right)_t + \left(\frac{\partial L}{\partial u_x} \right)_x - \left(\frac{\partial L}{\partial u} \right) = 0 \\ \left(\frac{\partial L}{\partial \varphi_t} \right)_t + \left(\frac{\partial L}{\partial \varphi_x} \right)_x - \left(\frac{\partial L}{\partial \varphi} \right) = 0. \end{cases} \quad (4)$$

Here and further, the indices x and t denote differentiation.

The partial derivatives

$$\sigma = \partial W / \partial u_x, \quad \eta = \partial W / \partial \varphi_x, \quad F = \partial W / \partial \varphi \tag{5}$$

are recognized as the macrostress, the microstress and the interactive force, respectively.

The equations of motion are now

$$\rho u_{tt} = \sigma_x, \quad I \varphi_{tt} = \eta_x - F. \tag{6}$$

The simplest potential energy function describing the influence of a microstructure is a quadratic function

$$W = \frac{1}{2} a u_x^2 + A \varphi u_x + \frac{1}{2} B \varphi^2 + \frac{1}{2} C \varphi_x^2, \tag{7}$$

where a, A, B, C denote material constants. Introducing Eq. (7) into Eq. (5) we get finally

$$\begin{cases} \rho u_{tt} = a u_{xx} + A \varphi_x \\ I \varphi_{tt} = C \varphi_{xx} - A u_x - B \varphi. \end{cases} \tag{8}$$

This is the governing system of two second-order equations that can also be represented in the form of one fourth-order equation

$$u_{tt} = (c_0^2 - c_A^2) u_{xx} - p^2 (u_{tt} - c_0^2 u_{xx})_{tt} + p^2 c_1^2 (u_{tt} - c_0^2 u_{xx})_{xx}, \tag{9}$$

where material parameters

$$c_0^2 = a/\rho, \quad c_1^2 = C/I, \quad c_A^2 = A^2/\rho B, \quad p^2 = I/B \tag{10}$$

are introduced. The parameters c_0, c_1, c_A are velocities while p is a time parameter. This is the basic linear equation governing 1D longitudinal waves in microstructured solids.

3. Approximations

3.1. Slaving principle

This idea (see [7]) is used in [5,9] for deriving a hierarchical asymptotic model starting from Eq. (9). It is supposed that the inherent length-scale l is small compared with the wavelength L of the excitation. The following dimensionless variables and parameters are introduced

$$U = u/U_0, \quad X = x/L, \quad T = c_0 t/L, \quad \delta = (l/L)^2, \quad \varepsilon = U_0/L, \tag{11}$$

where U_0 is the amplitude of the excitation. In addition, it is assumed that $I = \rho l^2 I^*$ and $C = l^2 C^*$, where I^* is dimensionless and C^* has the dimension of stress.

Next, the system Eq. (8) is rewritten in its dimensionless form and the slaving principle [7] is applied. It is supposed that

$$\varphi = \varphi_0 + \delta \varphi_1 + \delta^2 \varphi_2 + \dots \tag{12}$$

The dimensionless form of Eq. (8b) yields

$$\varphi = -\varepsilon \frac{A}{B} U_X - \frac{\delta}{B} (a I^* \varphi_{TT} - C^* \varphi_{XX}) \tag{13}$$

from which the successive terms

$$\varphi_0 = -\varepsilon \frac{A}{B} U_X, \quad \varphi_1 = \varepsilon \frac{A}{B^2} (a I^* U_{XTT} - C^* U_{XXX}), \dots \tag{14}$$

of the expansion Eq. (12) are obtained. Inserting them into Eq. (8a) in its dimensionless form, we finally get

$$U_{TT} = \left(1 - \frac{c_A^2}{c_0^2} \right) U_{XX} + \frac{c_A^2}{c_B^2} \left(U_{TT} - \frac{c_1^2}{c_0^2} U_{XX} \right)_{XX}, \tag{15}$$

where $c_B^2 = L^2/p^2 = BL^2/I$. Note that c_B involves the scales L and l and c_A includes the interaction effects through the parameter A . Eq. (15) is valid up to $O(\delta)$ because higher order terms are neglected. In addition, in general $\varepsilon \gg \delta^2$.

Now it is possible to restore the dimensions in order to compare the result with Eq. (9). Eq. (15) yields

$$u_{tt} = (c_0^2 - c_A^2)u_{xx} + p^2 c_A^2 (u_{tt} - c_1^2 u_{xx})_{xx}. \tag{16}$$

This is an example of the Whitham-type [10] hierarchical equation.

The dimensionless form of the basic linear Eq. (9) is

$$U_{TT} = \left(1 - \frac{c_A^2}{c_0^2}\right)U_{XX} - \frac{c_0^2}{c_A^2}\delta\beta U_{TTTT} + \left(\frac{c_0^2}{c_A^2} + \frac{c_1^2}{c_A^2}\right)\delta\beta U_{XXTT} - \frac{c_1^2}{c_A^2}\delta\beta U_{XXXX}, \tag{17}$$

where $\delta\beta = c_A^2/c_B^2$.

3.2. Evolution equations

Another idea to simplify the model is to use instead of the two-wave equation (16) an evolution equation that describes just one wave [8,9].

Here we follow [9] and apply the asymptotic (reductive perturbation) method. We can represent Eq. (15) in the matrix form

$$I \frac{\partial \mathbf{V}}{\partial T} + \tilde{A} \frac{\partial \mathbf{V}}{\partial X} + \tilde{B} \frac{\partial^3 \mathbf{V}}{\partial T \partial X^2} + \tilde{C} \frac{\partial^3 \mathbf{V}}{\partial X^3} = 0, \tag{18}$$

where

$$\mathbf{V} = \begin{pmatrix} \partial U / \partial T \\ \partial U / \partial X \end{pmatrix} \tag{19}$$

and I, \tilde{A}, \tilde{B} and \tilde{C} are following matrices

$$I = \begin{pmatrix} 1 & 0 \\ 0 & 1 \end{pmatrix}, \quad \tilde{A} = \begin{pmatrix} 0 & -(1 - n^2) \\ -1 & 0 \end{pmatrix},$$

$$\tilde{B} = \begin{pmatrix} -\delta\beta & 0 \\ 0 & -1 \end{pmatrix}, \quad \tilde{C} = \begin{pmatrix} 0 & \delta\beta m^2 \\ 1 & 0 \end{pmatrix},$$

where

$$n^2 = c_A^2/c_0^2 \neq 1, \quad m^2 = c_1^2/c_0^2. \tag{20}$$

It is possible to develop vector \mathbf{V} into the power series in a small parameter

$$\mathbf{V} = \mathbf{V}_0 + \varepsilon \mathbf{V}_1 + \varepsilon^2 \mathbf{V}_2 + \dots = \sum_{i=0} \varepsilon^i \mathbf{V}_i. \tag{21}$$

The space-space transformation is used:

$$\begin{cases} \xi = cT - X \\ \tau = \varepsilon X, \end{cases} \tag{22}$$

i.e.

$$\{X, T\} \rightarrow \{\xi, \tau\}, \tag{23}$$

where $c = \left(1 - \frac{A^2}{aB}\right)^{1/2} = \left(1 - \frac{c_A^2}{c_0^2}\right)^{1/2}$.

According to the asymptotic method [9] we get the sequence of equations of various powers in ε . Assuming that ε and δ are small parameters of the same order, we get finally the approximate linear evolution equation in the form

$$\frac{\partial \alpha}{\partial \tau} + \frac{\delta(\gamma - \beta c^2)}{2\epsilon c^2} \frac{\partial^3 \alpha}{\partial \xi^3} = 0, \tag{24}$$

where $\beta = \frac{A^2 I^*}{B^2}$, $\gamma = \frac{A^2 C^*}{aB^2}$ and $\alpha = \frac{\partial U}{\partial T} = -c \frac{\partial U}{\partial X}$ is the unknown amplitude factor.

Similarly, applying the asymptotic method [9] for the basic linear Eq. (17) we first represent it in the matrix form

$$I \frac{\partial \mathbf{V}}{\partial T} + \tilde{A} \frac{\partial \mathbf{V}}{\partial X} + \tilde{D} \frac{\partial^3 \mathbf{V}}{\partial T^3} + \tilde{E} \frac{\partial^3 \mathbf{V}}{\partial T \partial X^2} + \tilde{F} \frac{\partial^3 \mathbf{V}}{\partial X^3} = 0, \tag{25}$$

where $I, \tilde{A}, \tilde{D}, \tilde{E}$ and \tilde{F} are following matrices

$$\begin{aligned} I &= \begin{pmatrix} 1 & 0 \\ 0 & 1 \end{pmatrix}, & \tilde{A} &= \begin{pmatrix} 0 & -(1 - n^2) \\ -1 & 0 \end{pmatrix}, \\ \tilde{D} &= \begin{pmatrix} \frac{1}{n^2} \delta\beta & 0 \\ 0 & 0 \end{pmatrix}, & \tilde{E} &= \begin{pmatrix} -(\frac{1}{n^2} \delta\beta + n_1^2 \delta\beta) & 0 \\ 0 & -1 \end{pmatrix}, \\ \tilde{F} &= \begin{pmatrix} 0 & n_1^2 \delta\beta \\ 1 & 0 \end{pmatrix}, \end{aligned}$$

where

$$n_1^2 = c_1^2 / c_A^2, \tag{26}$$

and write the evolution equation in the form

$$\frac{\partial \alpha}{\partial \tau} + \frac{\delta(\gamma - \beta c^2)}{2\epsilon c^2} \frac{\partial^3 \alpha}{\partial \xi^3} = 0. \tag{27}$$

This means, that the approximate Eq. (15) and the basic Eq. (17) yield the evolution equations in the same form, see Eqs. (24) and (27). Consequently, using the idea of evolution equations there is no difference whether we begin the derivation from the basic Eq. (17) with the addition term U_{TTTT} or from the approximate Eq. (15) with terms U_{XXTT} and U_{XXXX} . However, note that the parameters of Eqs. (15) and (16) are different.

The character of dispersion in the case of microstructured materials is analysed in [5] on the basis of the approximate Eq. (15). It has been shown that both of the effects – inertia of the microstructure (described by term U_{TTXX}) and elasticity of the microstructure (described by term U_{XXXX}) have influence on dispersive relations and corresponding dispersion curves. If only inertia of the microstructure (term U_{TTXX}) is taken into account then the dispersion curve is concave, if only elasticity of the microstructure (term U_{XXXX}) is taken into account then the dispersion curve is convex. With both terms (double dispersion) the curve tends from one asymptote to another.

In the case of the evolution equation these two effects are described by a single term (term $\alpha_{\xi\xi\xi}$) but the sign of this term (the sign of its coefficient) depends on the ratio of the double dispersion effects.

It is possible to conclude that in case of $\gamma > \beta c^2$ (elastic effects prevailing) the dispersion curve is convex and in case of $\gamma < \beta c^2$ (inertial effects prevailing) the dispersion curve is concave. So the evolution equation keeps the main characteristics of the process. In case of $\gamma - \beta c^2 = 0$ there is no microstructure and the dispersion curve is linear, as expected.

4. Dispersion analysis

4.1. Dispersion relations

Internal scales of microstructured solids lead to dispersive effects. This is also quite clear from the governing equations derived in previous sections. The presence of higher-order derivatives in the governing equations indicates dispersion.

In order to derive dispersion relations, we assume the solution in the form of a wave

$$u(x, t) = \hat{u} \exp[i(kx - \omega t)], \quad (28)$$

with wave number k , frequency ω and amplitude \hat{u} .

Introducing Eq. (28) into Eq. (9) the dispersion relation

$$\omega^2 = (c_0^2 - c_A^2)k^2 + p^2(\omega^2 - c_0^2k^2)(\omega^2 - c_1^2k^2) \quad (29)$$

is obtained. The parameters involved are a time constant p and three characteristic velocities c_0, c_1, c_A . Instead of c_A the velocity $c_R^2 = c_0^2 - c_A^2$ could be introduced as a parameter, since it has an obvious meaning for the given wave process. Waves of very low frequencies ($\omega \ll p^{-1}$) propagate at the velocity c_R . The auxiliary velocity c_A does not occur explicitly as a limit velocity. The phase speed of the wave is defined as $c_p = \omega/k$ and can be obtained directly from the dispersion relation.

In order to reduce the number of independent variables we normalise the wave number, the frequency and the relative propagation speeds defining

$$\kappa = pc_0k, \quad \eta = p\omega, \quad n = c_A/c_0, \quad m = c_1/c_0. \quad (30)$$

Using these new quantities the full-dispersion relation (29) assumes the form

$$\eta^2 = (1 - n^2)\kappa^2 + (\eta^2 - \kappa^2)(\eta^2 - m^2\kappa^2). \quad (31)$$

The dimensionless phase speed is defined as $\gamma_p = c_p/c_0 = \eta/\kappa$.

For convenience we also use the parameter $c = c_R/c_0 = (1 - n^2)^{1/2}$ (see Eq. (22)).

In the same way, the approximate differential equation (16) yields the dispersion relation

$$\omega^2 = (c_0^2 - c_A^2) - p^2c_A^2(\omega^2 - c_1^2k^2)k^2. \quad (32)$$

Introducing Eq. (30) into Eq. (32) we obtain

$$\eta^2 = (1 - n^2)\kappa^2 - n^2(\eta^2 - m^2\kappa^2)\kappa^2. \quad (33)$$

4.2. The range of parameters

The numerical simulation is done with the dimensionless Eqs. (31) and (33) and with the dimensionless parameters n and m . Since $c^2 = 1 - n^2$ then $n < 1$, which makes physically sense because the velocity c_0 is interpreted as the maximum possible velocity. Therefore also $m < 1$.

We also assume that $n \neq m \neq 0$. If $n = 0$ then also $A = 0$ and then the governing Eq. (8) will have the form where there is no interaction between the macro- and the microstructure.

Therefore we will consider the parameters in the following ranges

$$0 < n < 1, \quad 0 < m < 1. \quad (34)$$

4.3. The results

The characteristic dispersion curves are shown in Fig. 1 from which the following can be concluded. The full-dispersion relation (31), which is represented by the continuous lines, represents two branches which in general are distinct. The upper, or ‘optical’ branch starts at $\eta = 1$ with zero slope and in the short wave limit the branch asymptotically approaches to the line $\eta = \kappa$. Lower, or ‘acoustical’, branch starts at the origin with a slope $\eta = c\kappa$ and in the short wave limit the branch approaches to the asymptotic line $\eta = m\kappa$. Here the dotted lines show asymptotic values.

The approximate dispersion relation (33), which is represented by the dashed line, provides an approximation of the acoustical branch only.

It is clear that the dispersion relations (31) and (33) differ and our intention is to analyse the ranges of parameters where the results coincide. This is dictated by the values of parameters n and m . Fig. 2 illustrates the ranges of the parameters where the values obtained from the both relations agree within 5% error (the area between the dashed lines) and within 10% error (the area between the continuous lines) at the point $\kappa = 1.5$.

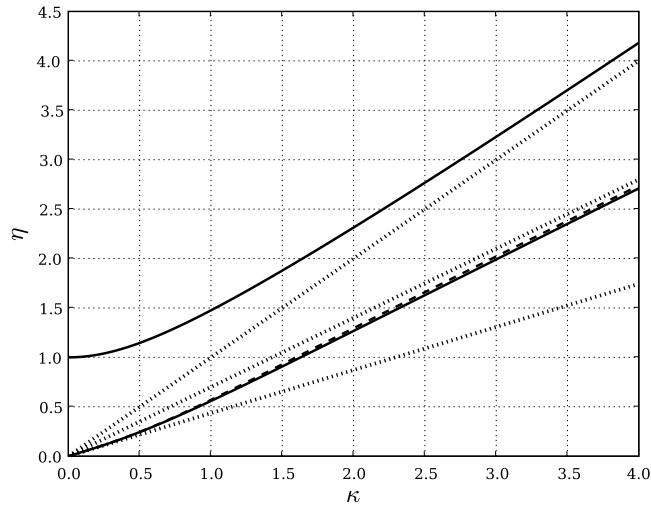


Fig. 1. The characteristic dispersion curves ($n = 0.9, m = 0.7$). See explanation in the text.

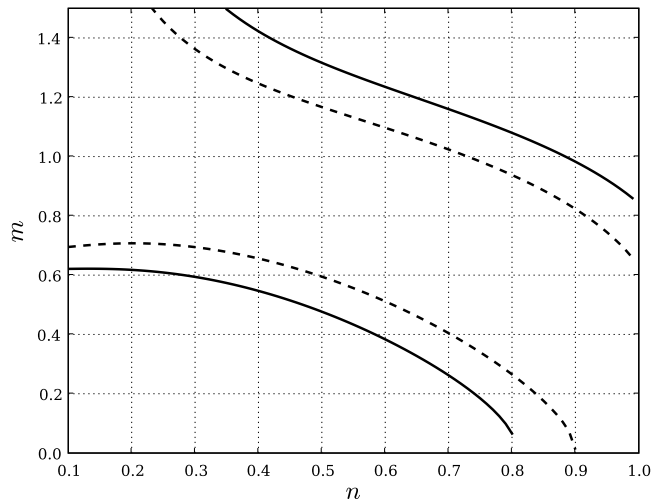


Fig. 2. The ranges of parameters. See explanation in the text.

The ranges for other values of κ behave similarly, only for $\kappa > 1.5$ the area of good agreement is narrower and for $\kappa < 1.5$ the area is wider.

Fig. 3 shows an example where the approximate dispersion relation (33) agrees very well with the full-dispersion relation (31). In Fig. 3a, $c_R < c_1$ and in Fig. 3b, $c_R > c_1$. The continuous lines correspond to the full and the dashed lines to the approximate dispersion relation.

Figs. 4 and 5 are examples of the combination of the parameters where the approximate Eq. (33) and the full-dispersion relation (31) do not coincide well. Fig. 4 is an example of $m < 1$, but not in a good approximation range (see Fig. 2). The continuous line corresponds again to the full and the dashed line to the approximate dispersion relation.

This result can be understood by examining the approximate dispersion relation (33). The strength of the second term in the approximate dispersion relation depends on the parameter n and if parameter n is close to 0 then the influence of the second term is diminished.

Fig. 5 is an example of the situation when c_1 becomes larger than c_0 ($m > 1$). Now the behaviour of the dispersion curves is changed. The full-dispersion relation (31) (represented by the continuous lines) still represents

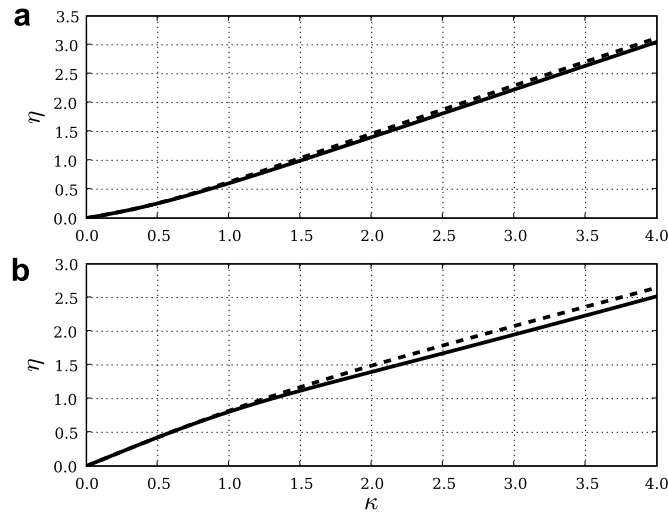


Fig. 3. The behaviour of the acoustic branches (a) $n = 0.9$, $m = 0.8$, (b) $n = 0.5$, $m = 0.6$. See explanation in the text.

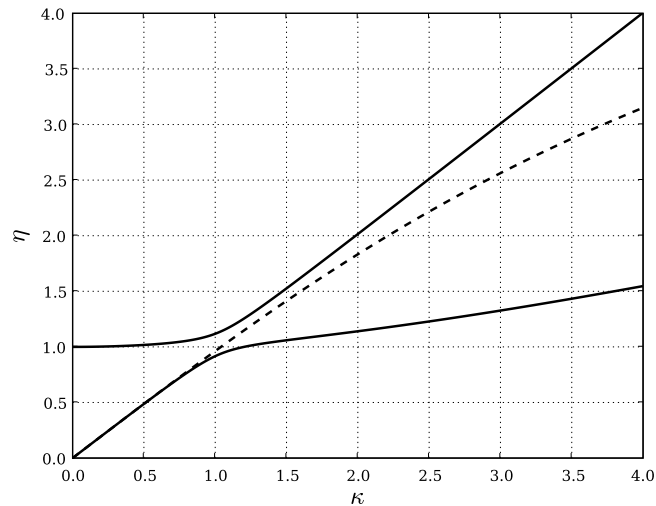


Fig. 4. The behaviour of the dispersion curves ($n = 0.2$, $m = 0.3$). See explanation in the text.

two branches but now the upper branch approaches to the asymptotic line $\eta = m\kappa$. Lower branch starts with a slope $\eta = c\kappa$ and in the short wave limit it approaches to the asymptotic line $\eta = \kappa$.

The approximate relation (33) (represented by the dashed line) also starts with a slope $\eta = c\kappa$, but in the short wave limit it approaches the asymptotic line $\eta = m\kappa$ and does not approach the acoustical branch.

5. Final remarks

Mindlin [1] has derived the dispersion relations for long wave-length (and very long wave-length) approximation and shown a similarity of dispersive effects with those in plates. While Mindlin [1] has used a concept of unit cells embedded in a surrounding medium, then many materials, especially composites, have clearly a defined layered structure. Sun et al. [12,13] have shown that an effective stiffness theory can be derived for describing waves in layered media. Actually, their result is a continuum [13] that bears clear resemblance to Mindlin's material, especially in a 1D case. It has also been shown that gradient elasticity theories [14] need both elastic and inertial effects to be taken into account. This shows again validity of the Mindlin idea. In addi-

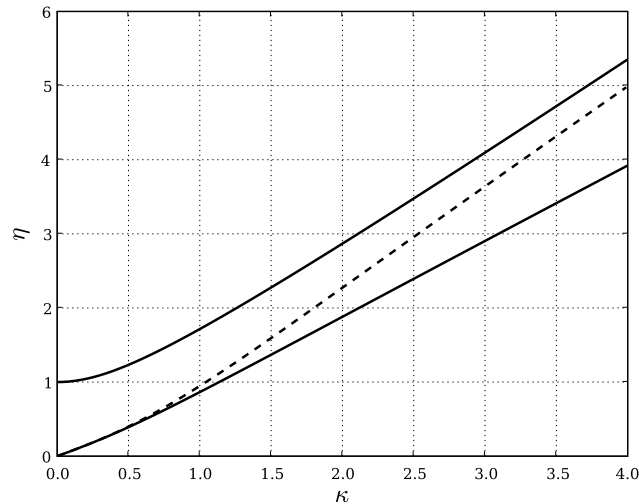


Fig. 5. The behaviour of the dispersion curves ($n = 0.7$, $m = 1.3$). See explanation in the text.

tion, the functionally graded materials (FGMs) which are widely used in contemporary technology [15], can be described by the Mindlin theory and the corresponding models presented above. The straight-forward numerical calculation of wave fields in FGMs [16] has shown explicitly the influence of microstructure for velocities as predicted by Mindlin-type models.

Here, we have derived hierarchical Mindlin-type models (Eqs. (9) and (16)) which describe well dispersive effects. In the wide range of parameters (see Fig. 2), the hierarchical asymptotic model is sufficient for grasping the real behaviour. The hierarchical model itself is certainly simpler and well-grounded physically. In addition, its similarity to discrete models [11] permits to bridge both types (continuous and discrete) models although some deeper analysis is needed in order to clarify the relations of model parameters. The full model (Eq. (9)) and its approximation (Eq. (16)) yield the same type of the evolution equation (cf. Eqs. (24) and (27)). This is not surprising because the proper scaling should lead to a result where the leading properties are accounted for. Even more, the evolution equation obtained in such a way shows clearly that for a homogeneous material (no microstructure) the dispersive effects disappear (here $\gamma = \beta c^2$, i.e. $c_1 = c$). In addition the convexity or concavity of the dispersion curve derived for cases $\gamma \neq \beta c^2$ depends clearly upon the influence of the material parameters. When in the microstructure elastic effects are stronger then $\gamma > \beta c^2$ and the dispersion curve is convex. When however the inertial effects in the microstructure are prevailing then $\gamma < \beta c^2$ and the dispersion curve is concave. The same effect follows from the analysis of full models.

This result is important even qualitatively for Nondestructive Testing (NDT). The concavity/convexity of the dispersion curve shows explicitly the influence of the basic material properties.

The main results of this paper shows that the asymptotic models, both hierarchical two-wave equation (15) (or (17)) and evolution equation (24) (or (27)) are able to grasp dispersive effects in microstructured solids within the wide range of parameters. As said in Section 1, the further studies should introduce nonlinearities like Pastrone [17].

Acknowledgements

Support of the Estonian Science Foundation under Contract Nos. 7037 (T.P.) and 7035 (M.R.) is gratefully acknowledged. The authors acknowledge the referees' valuable comments.

References

- [1] R.D. Mindlin, Microstructure in linear elasticity, Arch. Rat. Mech. Anal. 16 (1964) 51–78.
- [2] A.C. Eringen, Linear theory of micropolar elasticity, J. Math. Mech. 15 (1966) 909–923.

- [3] G.A. Maugin, *Material Inhomogeneities in Elasticity*, Chapman and Hall, London, 1993.
- [4] A.C. Eringen, *Microcontinuum Field Theories. I. Foundations and Solids*, Springer, New York, 1999.
- [5] J. Engelbrecht, A. Berezovski, F. Pastrone, M. Braun, Waves in microstructured materials and dispersion, *Philos. Mag.* 85 (33–35) (2005) 4127–4141.
- [6] J. Engelbrecht, F. Pastrone, M. Braun, A. Berezovski, Hierarchies of waves in nonclassical materials, in: P.-P. Delsanto (Ed.), *The Universality of Nonclassical Nonlinearity: Applications to Non-Destructive Evaluations and Ultrasonics*, Springer, Berlin, 2006, pp. 29–48.
- [7] P.L. Christiansen, V. Muto, S. Rionero, Solitary wave solution to a system of Boussinesq-like equations, *Chaos Solitons Fractals* 2 (1992) 45–50.
- [8] T. Taniuti, K. Nishihara, *Nonlinear Waves*, Pitman, London, 1983, in Japanese, 1977.
- [9] J. Engelbrecht, *Nonlinear Wave Processes of Deformation in Solids*, Pitman, Boston, London, Melbourne, 1983.
- [10] G.B. Whitham, *Linear and Nonlinear Waves*, J. Wiley, New York, 1974.
- [11] G.A. Maugin, *Nonlinear Waves in Elastic Crystals*, Oxford University Press, Oxford, 1999.
- [12] C.-T. Sun, J.D. Achenbach, G. Herrmann, Time-harmonic waves in a stratified medium propagating in the direction of the layering, *J. Appl. Mech. Trans. ASME* 35 (1968) 408–411, June.
- [13] C.-T. Sun, J.D. Achenbach, G. Herrmann, Continuum theory for a laminated medium, *J. Appl. Mech. Trans. ASME* 35 (3) (1968) 467–475.
- [14] H. Askes, E.C. Aifantis, Gradient elasticity theories in statics and dynamics – a unification of approaches, *Int. J. Fract.* 139 (2006) 297–304.
- [15] S. Suresh, A. Mortensen, *Fundamentals of Functionally Graded Materials*, The Institute of materials, London, 1998.
- [16] A. Berezovski, J. Engelbrecht, G.A. Maugin, Numerical simulation of two-dimensional wave propagation in functionally graded materials, *Eur. J. Mech. A-Solids* 22 (2003) 257–265.
- [17] F. Pastrone, Wave propagation in microstructured solids, *Math. Mech. Solids* 10 (2005) 349–357.

PUBLICATION II

Merle Randrüüt, Andrus Salupere, and Jüri Engelbrecht: On modelling wave motion in microstructured solids. *Proceedings of the Estonian Academy of Sciences* **58**(4) (2009) 241–246.



On modelling wave motion in microstructured solids

Merle Randrüüt*, Andrus Salupere, and Jüri Engelbrecht

Centre for Nonlinear Studies, Institute of Cybernetics at Tallinn University of Technology, Akadeemia tee 21, 12618 Tallinn, Estonia; salupere@ioc.ee, je@ioc.ee

Received 15 June 2009, revised 10 July 2009, accepted 3 August 2009

Abstract. The Mindlin-type model is used for describing the longitudinal deformation waves in microstructured solids. The evolution equation (one-wave equation) is derived for the hierarchical governing equation (two-wave equation) in the nonlinear case using the asymptotic (reductive perturbation) method. The evolution equation is integrated numerically under harmonic as well as localized initial conditions making use of the pseudospectral method. Analysis of the results demonstrates that the derived evolution equation is able to grasp essential effects of microinertia and elasticity of a microstructure. The influence of these effects can result in the emergence of asymmetric solitary waves.

Key words: nonlinear wave motion, microstructure, hierarchy of waves, evolution equations.

1. INTRODUCTION

In general terms, macrobehaviour of materials depends on properties of the material structure. This is extremely important in contemporary materials science where functionally graded materials, alloys, ceramics, composites, granular materials, etc. are widely used. Proper modelling brings in the scales and hierarchies [6], and the conventional theory of continuous homogeneous media should be considerably enlarged [2,4,11]. The scale dependence involves dispersive effects as shown already in [19]. The hierarchical behaviour in the Whitham sense means that, depending on the ratio of wave characteristics (wavelength) to scales in the material (characteristic scale of a microstructure), the weight of wave operators will be shifted from one to another [21].

One of the ideas to describe the effects of the microstructure is based on Mindlin's model [12]. This model has recently been extensively studied [2,3], mostly in the 1D setting which explicitly explains the main features of the process. It has been shown that such modelling describes well the influence of the microstructure on dispersion and the existence of hierarchies [2,3]. The model permits, for example, understanding the emergence of solitary waves in

microstructured materials, both analytically [9] and numerically [17,18]. In addition, there is a wide area of possible applications in nondestructive testing by solving the corresponding inverse problem for determining the material properties [8,10].

Our final interest is to analyse 2D problems. However, a common approach when solving multi-dimensional hyperbolic problems is to apply dimensional splitting, i.e., to iterate on 1D problems and to understand the accuracy of possible approximations.

The model equation in the studies mentioned above is in the 1D case a typical hierarchical wave equation with the leading operator of the 2nd order and the higher-order operators (4th, 6th orders) describing the influence of the microstructure [2,3]. This is the two-wave equation, i.e., it describes waves propagating in two directions. The powerful analytic methods [20] show explicitly how in this case evolution equations that govern the propagation of one wave only could be derived. The best example of such an evolution equation is the celebrated Korteweg–de Vries (KdV) equation. The evolution equations may also include hierarchies like in granular materials [7]. If we are interested in wave propagation along a certain coordinate without

* Corresponding author, merler@cens.ioc.ee

reflection from boundaries, then the concept of evolution equations is preferable. However, the transformations from a two-wave model to an evolution equation should bring over all the essential features that could influence the velocities or the distortions of the wave profile. It is of great interest to understand how the hierarchies in basic Mindlin-type models are reflected in the corresponding evolution equations and how the solutions describe the dispersive effects. It must be stressed that once we use nonlinear models, the balance between nonlinearity and dispersion is of interest.

The main goals of the present paper are (i) to derive the evolution equation that governs one-wave propagation for Mindlin’s model; (ii) to find numerical solutions to the evolution equation, and (iii) to compare the results with those of the two-wave equation.

2. BASIC MODEL AND THE EVOLUTION EQUATION

One-dimensional wave propagation in a microstructured material has been studied by Engelbrecht et al. [1–3] on the basis of Mindlin’s model [12], augmented by nonlinear terms. The motion is described by two scalar functions, the macrodisplacement $u(x,t)$ and the micro-deformation $\varphi(x,t)$, both depending on the material coordinate x and time t . The functions u and φ are governed by two coupled partial differential equations of the form

$$\begin{aligned} \rho u_{tt} &= au_{xx} + A\varphi_x + \frac{1}{2}N(u_x^2)_x, \\ I\varphi_{tt} &= C\varphi_{xx} - Au_x - B\varphi + \frac{1}{2}M(\varphi_x^2)_x, \end{aligned} \quad (2.1)$$

where ρ and I denote the macrodensity and the micro-inertia, respectively, and the constants a , A , B , C , N , and M are material parameters specifying the strain energy function. The last two constants, N and M , are responsible for nonlinear effects on the macro- and microscale, respectively.

The main interest is focused on longitudinal waves modified by the presence of the microstructure. For this purpose a single partial differential equation is extracted from the system (2.1), which describes a motion in which the macrodisplacement prevails and the influence of the microstructure is retained in a first approximation. The so-called ‘slaving principle’ is explained in detail in papers [1–3]. A modified version leading to the same result is presented in [14]. By keeping the original variables and parameters, the resulting equation has the form

$$\begin{aligned} \rho u_{tt} &= \left(a - \frac{A^2}{B}\right) u_{xx} + \frac{1}{2}N(u_x^2)_x + \frac{A^2}{B^2} (Iu_{tt} - Cu_{xx})_{xx} \\ &\quad + \frac{1}{2}M\frac{A^3}{B^3} (u_{xx}^2)_{xx}. \end{aligned} \quad (2.2)$$

It is an *approximate* equation extracted from the original system (2.1) by means of the slaving principle.

Equation (2.2) can still be condensed by introducing normalized variables and parameters. First, a reference length l is chosen. From the original material constants an inherent length can be extracted, which represents the size of the microstructure. It is considered to be small compared to the reference length l and is introduced by

$$(\delta l)^2 = \frac{IA^2}{\rho B^2}, \quad (2.3)$$

where the small number $\delta \ll 1$ characterizes the smallness of the microstructure. In addition, the characteristic velocities c , c_1 , c_N , and c_M are defined by

$$c^2 = \frac{1}{\rho} \left(a - \frac{A^2}{B}\right), \quad c_1^2 = \frac{C}{I}, \quad c_N^2 = \frac{N}{\rho}, \quad c_M^2 = \frac{MA}{IBI} \quad (2.4)$$

in terms of the basic model parameters and, in the case of c_M^2 , also of the standard length l .

The original variables x , t , u are finally replaced by nondimensional variables

$$X = \frac{x}{l}, \quad T = \frac{ct}{l}, \quad \varepsilon U = \frac{u}{l}. \quad (2.5)$$

The normalization of the displacement uses another small number $\varepsilon \ll 1$, which emphasizes that the displacement u is small compared to the reference length l . Using the new dimensionless variables, the governing equation (2.2) assumes the form

$$\begin{aligned} U_{TT} &= U_{XX} + \frac{1}{2}\varepsilon \frac{c_N^2}{c^2} (U_X^2)_X \\ &\quad + \delta^2 \left(U_{TT} - \frac{c_1^2}{c^2} U_{XX} + \frac{1}{2}\varepsilon \frac{c_M^2}{c^2} U_{XX} \right)_{XX}. \end{aligned} \quad (2.6)$$

If omitting dispersive and nonlinear terms in the governing equation (2.6), a simple wave equation would remain, whose general solution would be a left- or right-going wave of arbitrary shape travelling undisturbed. Due to the normalization, their speed would be unity. Let us concentrate on waves propagating to the right. To include the influence of the additional terms of the governing equation, we allow the wave profile to change slowly in time.

In selecting a right-going wave, the solution of the evolution equation is assumed in the form as suggested in [13, p. 6]:

$$U = f(\xi, \tau), \quad \xi = X - T, \quad \tau = \frac{1}{2}\varepsilon T, \quad (2.7)$$

where ξ and τ denote moving space and time coordinates, respectively. Inserting this ansatz into the recent form of the governing equation (2.6) and discarding the higher-order terms, one obtains the equation

$$-f_{\xi\xi\tau} = \frac{c_N^2}{2c^2} (f_{\xi\xi}^2)_{\xi} + \frac{\delta^2}{\varepsilon} \left(f_{\xi\xi\xi} - \frac{c_1^2}{c^2} f_{\xi\xi\xi} + \frac{1}{2}\varepsilon \frac{c_M^2}{c^2} f_{\xi\xi\xi}^2 \right)_{\xi\xi\xi}. \quad (2.8)$$

Evidently, the influences of dispersion and macro-nonlinearity, controlled by the two small parameters δ and ε , are balanced only if the quotient δ^2/ε is of the order of unity. Without loss of generality we may assume that ε is equal to δ^2 .

If we denote $f_\xi = \alpha$, the evolution equation assumes the form

$$\alpha_\tau + q(\alpha^2)_\xi + z\alpha_{\xi\xi\xi} + w(\alpha_\xi^2)_{\xi\xi} = 0, \quad (2.9)$$

where the parameters

$$q = \frac{c_N^2}{2c^2}, \quad z = \frac{c^2 - c_1^2}{c^2}, \quad w = \varepsilon \frac{c_M^2}{2c^2} \quad (2.10)$$

characterize the nonlinearity of macroscale, the dispersion, and the nonlinearity of microscale, respectively. Equalizing the micro-nonlinearity parameter w to zero yields the well-known KdV equation. Thus, compared with the standard KdV equation, equation (2.9) includes an additional complicated term which reflects the nonlinearity on the macroscale.

3. NUMERICAL SIMULATION

The evolution equation (2.9) is solved under harmonic and localized initial conditions

$$\alpha(\xi, 0) = \sin \xi, \quad \alpha(\xi, 0) = A_0 \operatorname{sech}^2 \frac{\xi - \xi_0}{\sqrt{12z/A_0}}, \quad (3.1)$$

respectively, where A_0 is the amplitude, ξ_0 the initial phase-shift, and $\sqrt{12z/A_0}$ the width of the initial pulse. For numerical integration the FFT-based pseudospectral method is used and the periodic boundary conditions are applied [5].

The crucial question is the proper choice of parameters because not much is known about the values of physical constants of Mindlin's model [12]. We choose here the values of parameters comparable with the standard KdV equation which has been studied in detail (see, for example [15,16]). One of the important features of the standard KdV equation is the emergence of a soliton train. The number of solitons in a train depends on the values of q and z . Widely used values are $q = 1$ and $z = 10^{-2.5}$ [15,16]. Then the soliton train develops at $\tau \approx 30$. Another important feature for the KdV equation is the existence of a single stable soliton.

On the basis of the argumentation above, we take here $q = 1$ and vary the other parameters in the following domains: $10^{-2.5} \leq z \leq 1$ and $0 \leq w \leq 1$. The localized initial wave (3.1)₂ is the analytical solution for equation (2.9) in the case of $w = 0$, i.e., it represents the KdV soliton.

3.1. Localized initial excitation

Janno and Engelbrecht [9] have shown that for the two-wave equation (2.6) there exists an asymmetric travelling wave solution, i.e., the nonlinearity in microscale leads to asymmetry of the wave profile. Numerical experiments by Salupere et al. [17,18] have demonstrated that in the case of equation (2.6), an initially symmetric localized wave is deformed to an asymmetric wave during propagation. Here we show that the same effect takes place in the case of the evolution equation (2.9).

The evolution of the initial symmetric sech^2 pulse can be traced in Fig. 1. It is clear that the shape of the wave is altered during propagation and an oscillating tail is formed. In Fig. 2 the initial wave profile and the altered shape of the wave profile at the end of the integration interval are plotted against ξ . In order to characterize the asymmetry of the last wave profile more explicitly, α_ξ is plotted against α in Fig. 3.

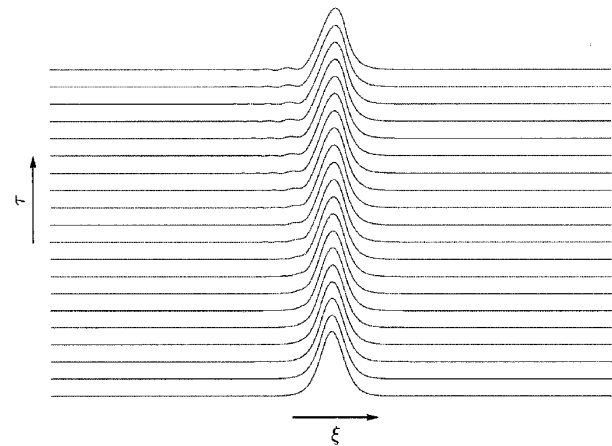


Fig. 1. Time-slice plot for $z = 10^{-2}$, $w = 10^{-2.5}$.

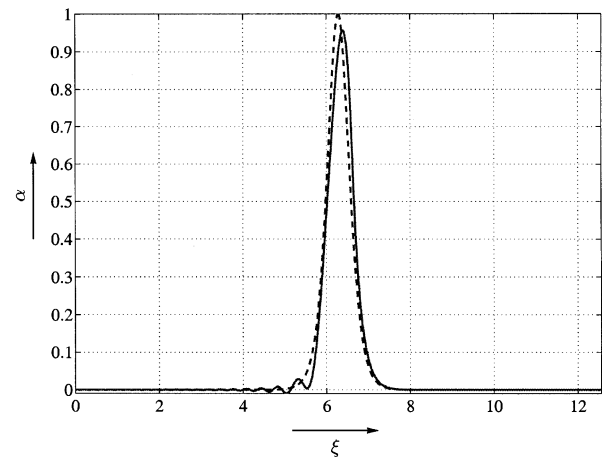


Fig. 2. The initial (dashed line) and the deformed (solid line) wave profile from Fig. 1 ($z = 10^{-2}$, $w = 10^{-2.5}$).

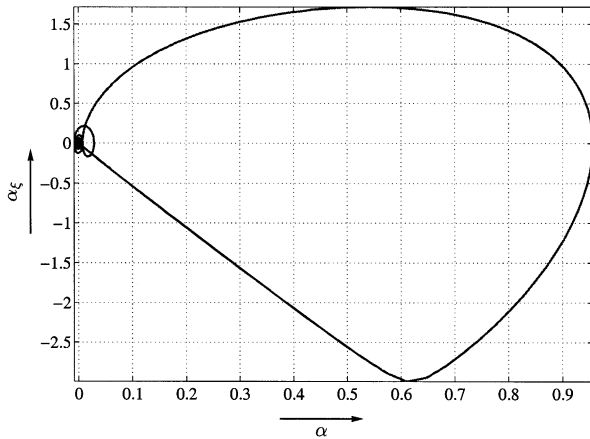


Fig. 3. Asymmetry of the wave profile at the end of the integration interval: α_ξ against α for $z = 10^{-2}$, $w = 10^{-2.5}$.

In applying localized initial conditions the value of the micro-nonlinearity parameter $w = 10^{-2.5}$ is chosen quite big compared to the macro-nonlinearity parameter q and the dispersion parameter z in order to demonstrate the effect of asymmetry more clearly.

3.2. Harmonic initial excitation

It is of interest to start with the case $w = 0$ which corresponds to a standard KdV equation. This means that micro-nonlinearity is neglected. As typical of the KdV case, a train of solitons will emerge from a harmonic initial excitation (Fig. 4.) The interaction picture is complicated but solitons preserve their shape and speed over long time intervals. The soliton amplitudes fluctuate in the interval that is dictated by the interaction rules [15,16]. When the micro-nonlinearity is taken into account, the interaction pattern is altered – speeds of solitons are higher than in the KdV case (cf. Figs 4 and 5). Like in the case of localized initial conditions,

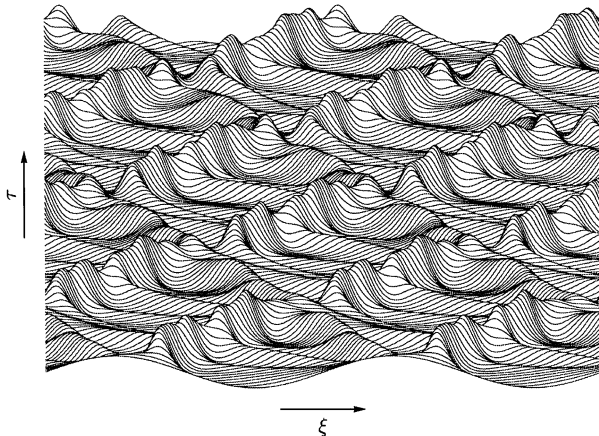


Fig. 4. Time-slice plot over two space periods for the KdV case, $z = 10^{-1.5}$, $w = 0$.

the emerged solitons (Fig. 6) are asymmetric, as can be observed from the phase plane, i.e., the (α, α_ξ) plot (Fig. 7). This is a clear sign of the influence of

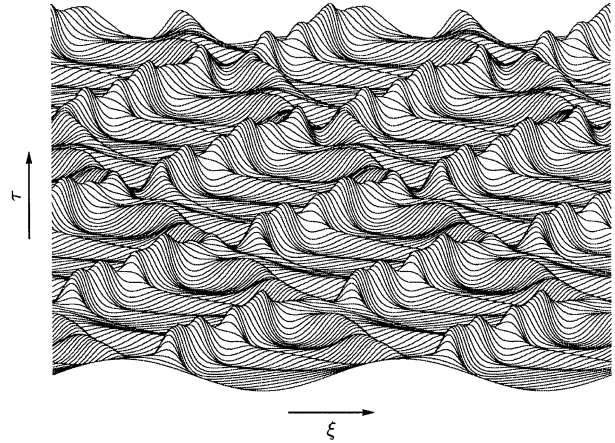


Fig. 5. Time-slice plot over two space periods for $z = 10^{-1.5}$, $w = 10^{-2.621}$.

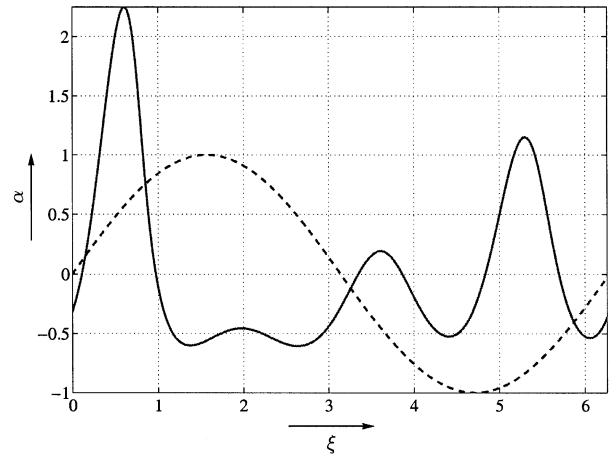


Fig. 6. Initial harmonic wave (dashed line) and wave profile (solid line) at $\tau = 14.3$ for $z = 10^{-1.5}$, $w = 10^{-2.621}$.

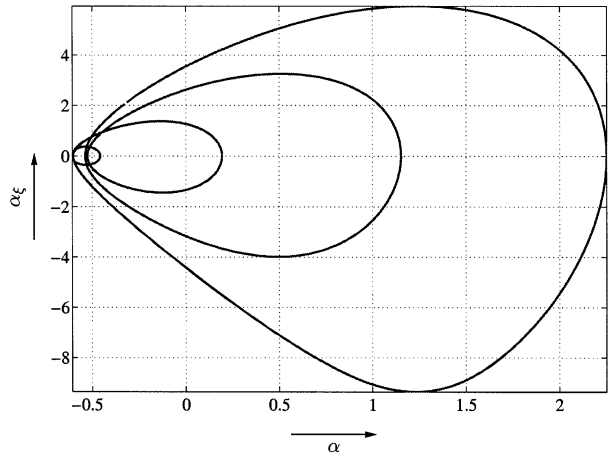


Fig. 7. Asymmetry of solitons: α_ξ against α at $\tau = 14.3$ for $z = 10^{-1.5}$, $w = 10^{-2.621}$.

micro-nonlinearity. The chosen time instant $\tau = 14.3$ corresponds to the formation of the soliton train at given values of z and w .

4. CONCLUDING REMARKS

The evolution equation (2.9) that governs one-wave propagation in microstructured solids according to Mindlin's model is derived and solved numerically under harmonic and localized initial conditions. Analysis of numerical results demonstrates that (i) for both the governing equation and the evolution equation nonlinearity in microscale leads to asymmetry of the wave profile; and (ii) the stronger the influence of micro-nonlinearity, the more the solutions of the evolution equation differ from those of the KdV model. In conclusion, the derived evolution equation (2.9) – notwithstanding that it is a simplified model equation compared to the two-wave equation (2.6) – is able to grasp essential effects of microinertia and elasticity of a microstructure. However, we stress that the values of parameters used above are chosen for the comparison with the standard KdV equation in order to demonstrate the influence of the microstructure. Studies with other parameters are in progress. A real challenge is to find an analytical solution to equation (2.9).

ACKNOWLEDGEMENT

The research was supported by the Estonian Science Foundation (grant No. 7035).

REFERENCES

- Engelbrecht, J. and Pastrone, F. Waves in microstructured solids with strong nonlinearities in microscale. *Proc. Estonian Acad. Sci. Phys. Math.*, 2003, **52**, 12–20.
- Engelbrecht, J., Berezovski, A., Pastrone, F., and Braun, M. Waves in microstructured materials and dispersion. *Phil. Mag.*, 2005, **85**, 4127–4141.
- Engelbrecht, J., Pastrone, F., Braun, M., and Berezovski, A. Hierarchies of waves in nonclassical materials. In *The Universality of Nonclassical Nonlinearity: Applications to Non-Destructive Evaluations and Ultrasonics* (Delsanto, P. P., ed.). Springer, Berlin, 2006, 29–48.
- Eringen, A. *Microcontinuum Field Theories. I Foundations and Solids*. Springer, New York, 1999.
- Fornberg, B. *Practical Guide to Pseudospectral Methods*. Cambridge University Press, Cambridge, 1998.
- Gates, T. S., Odegard, G. M., Frankland, S. J. V., and Clancy, T. C. Computational materials: multiscale modeling and simulation of nanostructured materials. *Compos. Sci. Technol.*, 2005, **65**, 2416–2434.
- Giovine, P. and Oliveri, F. Dynamics and wave propagation in dilatant granular materials. *Meccanica*, 1995, **30**, 341–357.
- Janno, J. and Engelbrecht, J. An inverse solitary wave problem related to microstructured materials. *Inverse Probl.*, 2005, **21**, 2019–2034.
- Janno, J. and Engelbrecht, J. Solitary waves in nonlinear microstructured materials. *J. Phys. A: Math. Gen.*, 2005, **38**, 5159–5172.
- Janno, J. and Engelbrecht, J. Waves in microstructured solids: inverse problems. *Wave Motion*, 2005, **43**, 1–11.
- Maugin, G. *Nonlinear Waves in Elastic Crystals*. Oxford University Press, Oxford, 1999.
- Mindlin, R. D. Micro-structure in linear elasticity. *Arch. Rat. Mech. Anal.*, 1964, **16**, 51–78.
- Newell, A. C. *Solitons in Mathematics and Physics*. Society for Industrial and Applied Mathematics, Philadelphia, 1985.
- Randrüüt, M. and Braun, M. On one-dimensional solitary waves in microstructured solids. *Wave Motion* (submitted).
- Salupere, A., Engelbrecht, J., and Peterson, P. Long-time behaviour of soliton ensembles. Part I – Emergence of ensembles. *Chaos Solitons Fractals*, 2002, **14**, 1413–1424.
- Salupere, A., Engelbrecht, J., and Peterson, P. Long-time behaviour of soliton ensembles. Part II – Periodical patterns of trajectories. *Chaos Solitons Fractals*, 2003, **15**, 29–40.
- Salupere, A., Tamm, K., and Engelbrecht, J. Numerical simulation of interaction of solitary deformation waves in microstructured solids. *Int. J. Non-Linear Mech.*, 2008, **43**, 201–208.
- Salupere, A., Tamm, K., Engelbrecht, J., and Peterson, P. On the interaction of deformation waves in microstructured solids. *Proc. Estonian Acad. Sci. Phys. Math.*, 2007, **56**, 93–99.
- Sun, C. T., Achenbach, J. D., and Herrmann, G. Continuum theory for a laminated medium. *J. Appl. Mech. Trans. ASME*, 1968, **35**(3), 467–475.
- Taniuti, T. and Nishihara, K. *Nonlinear Waves*. Pitman, Boston, 1983.
- Whitham, G. *Linear and Nonlinear Waves*. John Wiley & Sons, New York, 1974.

Lainelevi modelleerimisest mikrostruktuuriga materjalides

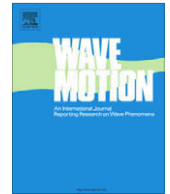
Merle Randrüüt, Andrus Salupere ja Jüri Engelbrecht

On tuletatud mikrostruktuuriga materjali (näiteks komposiidid, metallisulamid, granuleeritud materjalid jne) hierarhilise põhivõrrandi jaoks evolutsioonivõrrand ehk nn ühe laine võrrand, mis kirjeldab mittelineaarsust nii makro- kui mikrotasandil, kusjuures dispersiooniefekt on taandatud Kortewegi-de Vriesi tüüpi dispersioonile. See võimaldab kirjeldada laineleviprotsessi piisava füüsikalise täpsusega, jättes kõrvale algse liikumisvõrrandi. Klassikaline KdV-mudel teist järku mittelineaarsuse ja kuupdispersiooniga viib sümmeetrilise üksiklaine tekkeni makrostruktuuri mittelineaarsuse ja dispersiooni tasakaalu korral. Mikrostruktuuri mittelineaarsus aga häirib seda tasakaalu. Nii põhivõrrandit [8–10] kui sellele vastavat evolutsioonivõrrandit on analüüsitud numbriliselt ja näidatud, et mikrostruktuuri mittelineaarsuse tõttu on üksiklaine ebasümmeetriline.

PUBLICATION III

Merle Randrüüt and Manfred Braun: On one-dimensional solitary waves in microstructured solids. *Wave Motion* **47**(4) (2010) 217–230.[§]

[§]Reprinted with permission from Elsevier.



On one-dimensional solitary waves in microstructured solids

Merle Randrüüt^{a,*}, Manfred Braun^b

^a Centre for Nonlinear Studies, Institute of Cybernetics at Tallinn University of Technology, Akadeemia tee 21, 12618 Tallinn, Estonia

^b University of Duisburg-Essen, Chair of Mechanics and Robotics, Lotharstraße 1, 47057 Duisburg, Germany

ARTICLE INFO

Article history:

Received 17 June 2009

Received in revised form 10 November 2009

Accepted 19 November 2009

Available online 26 November 2009

Keywords:

Microstructure

Hierarchy of waves

Evolution equations

Korteweg–de Vries equation

Solitary waves

ABSTRACT

For describing the longitudinal deformation waves in microstructured solids a Mindlin-type model is used. The embedding of a microstructure in an elastic material is reflected in an inherent length scale causing dispersion of propagating waves. Nonlinear effects, if taken into account, will counteract dispersion. A suitable balance between nonlinearity and dispersion may permit the propagation of solitary waves.

Following previous work by Engelbrecht and others the nonlinear hierarchical model is derived in a one-dimensional setting which corresponds to a two-wave equation. The evolution equation as a simplified model, representing a one-wave equation, is able to grasp the essential effects of microinertia and elasticity of the microstructure. It is shown that the nonlinearity in microscale leads to an asymmetry of the wave profile.

The nonlinear evolution equation as an extended Korteweg–de Vries equation is solved approximately by a series expansion in a small parameter representing the micro-nonlinearity. Already the first approximation indicates the asymmetry of the solitary waves. It is shown that solitary waves will propagate only if the micro-nonlinearity does not exceed some upper bound. For the limiting case, an analytical solution of the extended Korteweg–de Vries equation can be provided and used as a reference for the approximate solutions.

© 2009 Elsevier B.V. All rights reserved.

1. Introduction

In general, macrobehavior of materials depends on properties of the material structure. In contemporary material science and structural mechanics significant attention is devoted to microstructured materials possessing internal scales. This sort of materials like metallic alloys, ceramic composites, polycrystalline solids, functionally graded materials, granular, porous materials, etc., are used for a wide variety of industrial applications since combining the mechanical properties of different constituents, as in composites, yields optimal properties of solids.

In principle, every material has some small-scale structure, since material is never distributed continuously. If we speak of microstructured material we do not mean the molecular or atomic scale. Rather these microstructures are assumed in the range of micrometers, so that they still can be considered as continua. The overall material becomes highly nonhomogeneous due to the embedded microstructures with their different behavior.

Any theory of microstructured material aims to smooth out this inhomogeneity while retaining its influence on the gross behavior of the material. This is done by giving the material more internal degrees of freedom describing the behavior of the embedded microstructures. So the ordinary but highly inhomogeneous material is turned into a homogeneous material which, however, is equipped with more than just a displacement field. Corresponding theories can be traced back to the

* Corresponding author. Tel.: +372 6204173.

E-mail addresses: merler@cens.ioc.ee (M. Randrüüt), manfred.braun@uni-due.de (M. Braun).

meanwhile classical papers by Mindlin [1] and Sun et al. [2]. The connection to Cosserat continua has been established by Herrmann and Achenbach [3].

The application of severe loading conditions, including impact, means generation of deformation waves. The embedding of a microstructure in an elastic material is reflected in an inherent length scale causing dispersion of propagating waves. Nonlinear effects, if taken into account, will counteract dispersion. A suitable balance of nonlinearity and dispersion may permit the propagation of solitary waves.

The theory of solitary waves has originated from the study of surface waves in fluids. Meanwhile, solitary wave propagation in solids as well as in optical systems has gained widespread interest. If one takes shock waves and dispersive waves as two extreme examples of wave motion, the solitary waves share some properties of each of the two classes. They are localized like shock waves and smooth like dispersive waves. Solitary waves may keep their shape over long distances and are, therefore, applicable to signal transmission.

Apart from the possible technical applications, solitary waves are an attractive phenomenon from the mathematical point of view. Especially the solitons, i.e., solitary waves preserving their identity after a collision and satisfying an infinite set of conservation laws, have initiated an extended mathematical research [4].

The underlying physical model equations giving rise to solitary waves must combine two opposing effects, namely dispersivity and nonlinearity. Dispersion requires an inherent length scale, which might represent the scale of a microstructure or simply the cross-sectional scale of a rod. Nonlinearity is always present, at least to a certain degree, since any strictly linear model is just a first approximation of some more general nonlinear theory. Examples of nonlinear and dispersive behavior of solid materials are provided by Samsonov [5] who has verified experimentally and explained theoretically the existence of solitary waves in solids, see also [6,7] and the extensive literature cited therein.

In the absence of both dispersion and nonlinearity the considered model reduces to a simple wave equation with a fixed nonzero propagation velocity. A rather different nonlinear behavior is investigated by Nesterenko [8] and suggested as a model of porous materials. The material is assumed to be composed of micro-bodies which can exchange only compressive contact forces. Due to the typical behavior of Hertz contact the linear response is lost in the natural stress-free state of the material, thus prohibiting the propagation of small-amplitude waves. Despite this “sonic vacuum” there exist solitary waves which, however, “are qualitatively different from the well known weakly nonlinear solitary waves of the Korteweg–de Vries equation” [9]. It should be emphasized that this kind of genuine nonlinearity is not covered by the theory presented here.

Engelbrecht and Pastrone [10] have specialized Mindlin’s model of a microstructured solid to one dimension and augmented it by including nonlinear terms in both macro- and microscale. This model has been studied further in [11–14].

If nonlinearity is restricted to the macroscale the propagation of waves is governed by an equation of Korteweg–de Vries type with the well-known classical solitary waves as possible solution. Taking into account nonlinearity also on the microscale leads to an extended KdV equation with an additional nonlinear term. Closed-form solutions of this extended KdV equation are not available.

The paper is devoted to the case of a one-dimensional microstructured solid with some nonlinearity at the microscale level which is small compared with the combined effect of primary nonlinearity and dispersion. The propagation of waves is governed by the extended KdV equation with a small coefficient at the additional nonlinear term. The cubic equation occurring in the course of the integration process is solved approximately by a series expansion in the small parameter. The integration can then be performed explicitly and eventually yields a solution in form of a series expansion starting with the classical KdV soliton. The first approximation already shows that the solitary waves become asymmetric, as predicted in [11], while the relation between amplitude and propagation speed remains unaffected.

The paper is organized as follows. The basic model following [13,11] is presented in Section 2. In Section 3, the nonlinear evolution equation as an extended KdV equation is derived. Sections 4 and 5 are devoted to the classical KdV soliton and the extended KdV equation, respectively. In Section 6, the cubic first-order differential equation is analyzed, the limiting value of the micro-nonlinearity parameter ε and the phase curves of solitary waves are provided. In Section 7, the approximate solution of the extended KdV equation, and, in Section 8, the analytical solution in the limiting case are presented. A conclusion and final remarks are given in Section 9. The Appendix contains some mathematical details, namely the approximate solution of a cubic equation and the evaluation of an integral needed for the analytical solution.

2. Nonlinear hierarchical model

According to Mindlin’s model of a microstructured solid [1] any material point of the solid represents itself a microcontinuum subject to some deformation. The overall deformation of the microstructured continuum is then described by the macroscopic displacements of its material points, i.e., the centers of the microcontinua, and by the deformation of the microcontinua themselves. The micro-deformations are assumed to be uniform at the microscopic level but may depend on the macroscopic location of the microcontinuum element.

The one-dimensional version of Mindlin’s model, as formulated by Engelbrecht and Pastrone [10,13], is described by two scalar functions, the macro-displacement $u(x, t)$ and the micro-strain $\varphi(x, t)$, both depending on the material coordinate x and the time t . Their relevance is sketched in Fig. 1. In the sequel, subscripts x and t will indicate partial derivatives with respect to the material coordinate x and the time t , respectively.

The kinetic-energy density is composed of its macroscopic and microscopic contributions,

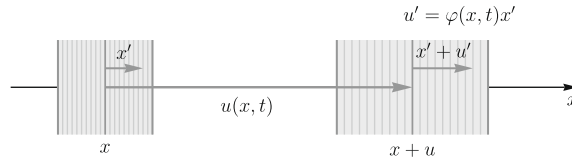


Fig. 1. 1D microstructured material.

$$K = \frac{1}{2} \rho u_t^2 + \frac{1}{2} I \varphi_t^2, \tag{2.1}$$

where ρ and I denote the macroscopic density and the microinertia, respectively. All densities, like ρ , I or the kinetic-energy density K itself, are understood per unit length rather than per unit volume, due to the one-dimensional model. The strain energy or potential energy density, again per unit length, is assumed to depend on the macro-strain u_x , the micro-strain φ and its gradient φ_x ,

$$W = W(u_x, \varphi, \varphi_x). \tag{2.2}$$

By invoking the Euler–Lagrange equations for the Lagrangian density $L = K - W$ one obtains the equations of motion

$$\rho u_{tt} = \sigma_x, \quad I \varphi_{tt} = \eta_x - \tau \tag{2.3}$$

representing the balances of macro- and micromomentum. The stress quantities entering these balances are the derivatives of the strain energy (2.2) with respect to its arguments, namely the macrostress, the microstress, and a quantity called the interactive force,

$$\sigma = \frac{\partial W}{\partial u_x}, \quad \eta = \frac{\partial W}{\partial \varphi_x}, \quad \tau = \frac{\partial W}{\partial \varphi}, \tag{2.4}$$

respectively. It should be noted that, in the one-dimensional setting, the stresses σ and τ have the dimension of force while η has the dimension of a moment.

Up to now the strain energy function has not yet been specified. Following [10–12] we consider the strain energy function

$$W = \frac{1}{2} (\alpha u_x^2 + 2A u_x \varphi + B \varphi^2 + C \varphi_x^2) + \frac{1}{6} (N u_x^3 + M \varphi_x^3) \tag{2.5}$$

involving cubic terms, where α , A , B , C and N , M are material constants. The stresses (2.4) are then

$$\sigma = \alpha u_x + A \varphi + \frac{1}{2} N u_x^2, \quad \tau = A u_x + B \varphi, \quad \eta = C \varphi_x + \frac{1}{2} M \varphi_x^2, \tag{2.6}$$

and the balance Eqs. (2.3) assume the form

$$\begin{aligned} \rho u_{tt} &= \alpha u_{xx} + A \varphi_x + \frac{1}{2} N (u_x^2)_x, \\ I \varphi_{tt} &= C \varphi_{xx} - A u_x - B \varphi + \frac{1}{2} M (\varphi_x^2)_x. \end{aligned} \tag{2.7}$$

The first of these equations governs the macro-displacement $u(x, t)$, which is regarded as the main kinematic variable. The equation, however, is coupled to the second equation which governs the micro-deformation $\varphi(x, t)$.

To study the propagation of waves in the microstructured solid it would be comfortable to have a single partial differential equation for the macroscopic displacement which, however, retains the influence of the microstructure. In principle, the system of Eqs. (2.7) could be contracted to a single equation without neglecting any terms. It would contain time derivatives of fourth-order. The objective of this and related papers is, however, to study waves corresponding to the acoustical branch and how they are influenced by the presence of the microstructure.

To this end, a single partial differential equation is extracted from the system (2.7) which describes a motion in which the macro-displacement prevails while retaining the influence of the microstructure. The procedure to obtain this approximate equation, called the “slaving principle”, is explained in detail in papers by Pastrone and Engelbrecht [10,13]. Here we derive the approximation in a heuristic way which leads to the same result as the rigorous treatment.

Solving the second Eq. (2.7)₂ for the micro-strain one obtains

$$\varphi = -\frac{A}{B} u_x - \frac{1}{B} (I \varphi_{tt} - C \varphi_{xx}) + \frac{M}{2B} (\varphi_x^2)_x. \tag{2.8}$$

This is still a partial differential equation for the micro-strain $\varphi(x, t)$, whose partial derivatives appear on the right-hand side. In a first, rather crude approximation these derivatives are omitted such that the micro-strain is expressed explicitly as $\varphi \approx -(A/B)u_x$ in terms of the macro-strain u_x . This expression is reinserted into the right-hand side of (2.8) to provide the better approximation

$$\varphi = -\frac{A}{B}u_x + \frac{A}{B^2}(Iu_{tt} - Cu_{xx})_x + \frac{A^2M}{2B^3}(u_{xx}^2)_x, \quad (2.9)$$

by which the micro-strain is expressed explicitly in terms of the macro-strain u_x and its derivatives. This expression can be inserted into the first Eq. (2.7)₁ which becomes a nonlinear fourth-order differential equation for the displacement $u(x, t)$,

$$\rho u_{tt} = \left(\alpha - \frac{A^2}{B} \right) u_{xx} + \frac{A^2}{B^2} (Iu_{tt} - Cu_{xx})_{xx} + \frac{1}{2} \left[N(u_x^2)_x + M \frac{A^3}{B^3} (u_{xx}^2)_{xx} \right]. \quad (2.10)$$

This equation can still be condensed by introducing normalized variables and corresponding parameters.

From the original material constants one inherent length and several characteristic velocities can be extracted. The inherent length represents the size of the microstructure. In order to consider this to be small one first has to choose a reference length scale ℓ . The inherent length is then introduced by

$$(\delta\ell)^2 = \frac{IA^2}{\rho B^2}, \quad (2.11)$$

where the small number $\delta \ll 1$ specifies the size of the microstructure to be small compared to the reference length ℓ . Further the characteristic velocities \bar{c}, c_1, c_N and c_M are introduced by

$$\bar{c}^2 = \frac{1}{\rho} \left(\alpha - \frac{A^2}{B} \right), \quad c_1^2 = \frac{C}{I}, \quad c_N^2 = \frac{N}{\rho}, \quad c_M^2 = \frac{MA}{IB\ell}. \quad (2.12)$$

Using these parameters the governing Eq. (2.10) attains the form

$$u_{tt} = \bar{c}^2 u_{xx} + \frac{1}{2} c_N^2 (u_x^2)_x + (\delta\ell)^2 \left(u_{tt} - c_1^2 u_{xx} + \frac{1}{2} \ell c_M^2 u_{xx}^2 \right)_{xx}. \quad (2.13)$$

In a final step the dimensionless variables

$$X = \frac{x}{\ell}, \quad T = \frac{\bar{c}t}{\ell}, \quad \epsilon U = \frac{u}{\ell} \quad (2.14)$$

are introduced. The normalization of the displacement includes another small number $\epsilon \ll 1$, which emphasizes that the displacement u is small compared to the reference length ℓ . The nondimensional form of the governing Eq. (2.10) is now obtained as

$$U_{TT} = U_{XX} + \frac{1}{2} \epsilon \gamma_N^2 (U_X^2)_X + \delta^2 \left(U_{TT} - \gamma_1^2 U_{XX} + \frac{1}{2} \epsilon \gamma_M^2 U_{XX}^2 \right)_{XX}, \quad (2.15)$$

where the velocity ratios

$$\gamma_1 = \frac{c_1}{\bar{c}}, \quad \gamma_N = \frac{c_N}{\bar{c}}, \quad \gamma_M = \frac{c_M}{\bar{c}} \quad (2.16)$$

have been introduced. The macro-nonlinearity is controlled by the small number ϵ , which measures the size of the amplitude, the dispersion is governed by the small number δ^2 emerging from the size of the microstructure, and the micro-nonlinearity is influenced by both numbers.

It should be noted that the normalization of time (2.14)₂ is based on the velocity \bar{c} which seems to be the most natural inherent velocity. Therefore the normalized Eq. (2.15) differs from the one presented in [10], where the normalization is based on the velocity $c_0 = \sqrt{\alpha/\rho}$.

3. Evolution equation

If nonlinear and dispersive terms were absent in the governing Eq. (2.15) a simple wave equation would remain, whose general solution would allow left and right going waves of arbitrary shape traveling undisturbed. Due to the normalization their speed would be unity. To include the cumulative effects of the additional nonlinear and dispersive terms in the governing equation we allow the wave profile to change slowly in time.

Selecting a right going wave the solution is assumed in the form

$$U = f(\xi, \tau), \quad \xi = X - T, \quad \tau = \frac{1}{2} \epsilon T, \quad (3.1)$$

as suggested in [4, p. 6]. Inserting this ansatz into the recent form of the governing Eq. (2.15) and discarding higher-order terms we get the equation

$$-f_{\xi\tau} = \frac{1}{2} \gamma_N^2 (f_\xi^2)_\xi + \frac{\delta^2}{\epsilon} \left(f_{\xi\xi} - \gamma_1^2 f_{\xi\xi} + \frac{1}{2} \epsilon \gamma_M^2 f_{\xi\xi}^2 \right)_{\xi\xi}. \quad (3.2)$$

One can realize that the influences of dispersion and nonlinearity, measured by the two small parameters δ and ϵ , are balanced only if the quotient δ^2/ϵ is of the order of unity. Without loss of generality we may assume that ϵ is equal to δ^2 .

Denoting $f_\xi = \alpha$, the evolution equation assumes the form

$$\alpha_\tau + \frac{1}{2}\gamma_N^2(\alpha^2)_\xi + (1 - \gamma_1^2)\alpha_{\xi\xi\xi} + \frac{1}{2}\epsilon\gamma_M^2(\alpha^2)_{\xi\xi} = 0. \tag{3.3}$$

The same result is obtained via the reductive perturbation method as presented in [15,16].

Keeping track of the transformations of variables (2.14) one finds

$$u_x = \epsilon\alpha, \tag{3.4}$$

i.e., the new dependent variable α represents a magnified strain. The velocity ratios γ_1, γ_N and γ_M defined by (2.16) appear as parameters in the evolution Eq. (3.3) and are responsible for dispersion, macro-nonlinearity and micro-nonlinearity, respectively. If the latter is omitted the evolution equation reduces to the Korteweg–de Vries (KdV) equation.

By suitable transformations of the variables the coefficients of the equation can be standardized. Newell [4] suggests the form

$$q_t + 6qq_x + q_{xxx} = 0 \tag{3.5}$$

which, in our case, has to be supplemented by an additional term representing the micro-nonlinearity. This standardized form is achieved by the transformation

$$\alpha = \frac{6}{\gamma_N^2}(1 - \gamma_1^2)^{1/3}q, \quad \xi = (1 - \gamma_1^2)^{1/3}x, \quad \tau = t, \tag{3.6}$$

where, for convenience, the original space and time variables, x and t , have been reused.

By this transformation, the evolution Eq. (3.3) becomes

$$q_t + 3(q^2)_x + q_{xxx} + 3\epsilon(q_x^2)_{xx} = 0, \tag{3.7}$$

in which only one parameter

$$\epsilon = \frac{\epsilon\gamma_M^2}{(1 - \gamma_1^2)\gamma_N^2} \tag{3.8}$$

remains. It is responsible for the influence of the micro-nonlinearity measured by γ_M as compared to the combined effects of dispersion and macro-nonlinearity.

4. The classical KdV soliton

If the influence of the micro-nonlinearity is omitted the evolution equation is reduced to the Korteweg–de Vries equation which admits solutions in the form of the sech^2 solitons. Although this is well known the integration is briefly reviewed, since it serves as a guideline for treating subsequently the extended Korteweg–de Vries equation.

Solutions of the KdV Eq. (3.5) propagating without any distortion can be found in the form

$$q = q(\theta), \quad \theta = x - ct. \tag{4.1}$$

This ansatz reduces the KdV Eq. (3.5) to the ordinary differential equation

$$-cq' + 3(q^2)' + q''' = 0 \tag{4.2}$$

for the function $q(\theta)$, where primes denote derivatives with respect to the argument θ . Integrating once, the second-order differential equation

$$q'' = A + cq - 3q^2 \tag{4.3}$$

is obtained, where A is a constant of integration.

Using the identity $q'' = q'dq'/dq$ one can write (4.3) in the form of the differential equation of the first-order,

$$q' \frac{dq'}{dq} = A + cq - 3q^2, \tag{4.4}$$

which, by integration, yields

$$\frac{1}{2}q'^2 = B + Aq + \frac{c}{2}q^2 - q^3 \tag{4.5}$$

with an additional constant of integration, B . The final step of integration will lead to an elliptic integral, in general.

The analysis will be restricted here to the special case of solitary waves. It is assumed that, as $\theta \rightarrow \pm\infty$, the function q tends uniformly to zero, i.e., $q \rightarrow 0$, $q' \rightarrow 0$, and $q'' \rightarrow 0$. Therefore, in (4.5) the constants A and B have to vanish. The differential Eq. (4.5) thus attains the simpler form

$$q' = \pm q \sqrt{c - 2q}, \quad (4.6)$$

from which one can see that $q \leq c/2$.

Without loss of generality it may be assumed that q attains its maximum value $a = c/2$ at $\theta = 0$. Then, for growing values of θ , the function $q(\theta)$ must decrease, i.e., $q' < 0$. Separation of variables and definite integration of the differential Eq. (4.6) yields

$$\int_a^q \frac{-dq}{q \sqrt{2(a-q)}} = \theta. \quad (4.7)$$

Carrying out the integration one obtains

$$\sqrt{\frac{2}{a}} \operatorname{arcosh} \sqrt{\frac{a}{q}} = \theta. \quad (4.8)$$

This equation has to be solved for q . Introducing the parameter

$$\eta = \sqrt{\frac{a}{2}} = \frac{\sqrt{c}}{2}, \quad (4.9)$$

the solution of Eq. (3.5) assumes the form

$$q = a \operatorname{sech}^2 \eta \theta. \quad (4.10)$$

Thus, the well-known solitary wave solution is obtained as

$$q = a \operatorname{sech}^2 \eta (x - ct). \quad (4.11)$$

It should be noted that the amplitude a , the wave number η , and the phase speed c are not independent but coupled by (4.9). So the solution contains only one essential parameter.

5. Extended KdV equation

The analysis of the KdV equation as provided in Section 4 is now applied to the extended KdV Eq. (3.7) as far as possible. The ansatz (4.1) can be used unaltered. Inserting it into the extended KdV Eq. (3.7) yields the ordinary differential equation

$$-cq' + 3(q^2)' + q''' + 3\varepsilon(q^2)'' = 0, \quad (5.1)$$

which can be integrated once resulting in

$$q'' + 3\varepsilon(q^2)' = A + cq - 3q^2, \quad (5.2)$$

where A is a constant of integration.

Converting this second-order differential equation for the function $q(\theta)$ into a first-order differential equation for the function $q'(q)$ one obtains

$$q'(1 + 6\varepsilon q') \frac{dq'}{dq} = A + cq - 3q^2. \quad (5.3)$$

One further integration yields

$$\frac{1}{2} q'^2 + 2\varepsilon q'^3 = B + Aq + \frac{c}{2} q^2 - q^3. \quad (5.4)$$

As in the KdV case it is assumed that, for $\theta \rightarrow \pm\infty$, the solution q uniformly tends to zero. Therefore, in (5.4) the constants A and B have to vanish. Thus Eq. (5.4) assumes the form

$$q'^2 + 4\varepsilon q'^3 = q^2(c - 2q). \quad (5.5)$$

In principle, this equation has to be solved for q' and then integrated.

6. Phase curves of solitary waves

Before turning to the last integration step, the cubic first-order differential Eq. (5.5) will be analyzed. Introducing the amplitude $a = c/2$, as in the KdV case, the equation is written as

$$q^2 + 4\epsilon q^3 = 2q^2(a - q). \tag{6.1}$$

It represents a curve in the (q, q') phase plane. A solitary wave $q = q(\theta)$ emerges asymptotically from the negative θ -axis, raises with positive slope until its peak $q(0) = a$, turns to negative slope and approaches asymptotically the θ -axis for $\theta \rightarrow +\infty$. The corresponding phase curve starts in the origin of the (q, q') plane with finite positive slope, follows a loop crossing the q -axis downward at $(a, 0)$, and bends back to the origin at finite slope.

To analyze the principal behavior of the phase curve (6.1) let us define the two functions

$$f(q') = 4\epsilon q^3 + q^2 - g(q) \quad \text{and} \quad g(q) = 2q^2(a - q). \tag{6.2}$$

Their qualitative graphs are shown in Figs. 2 and 3. If $\epsilon > 0$ the function f has a relative maximum

$$f(q'_1) = \frac{1}{108} \frac{1}{\epsilon^2} - g(q) \quad \text{at} \quad q'_1 = -\frac{1}{6\epsilon}. \tag{6.3}$$

If this relative maximum is above the q' -axis there are three zeros, if it is below there is only one.

For any value q attained by the solitary wave there must be a positive and a negative slope q' , which means that the function $f(q')$ must have two zeros, one positive and one negative, for any q in the range $0 < q < a$. In order that there are two zeros, or even three, the relative maximum (6.3)₁ must not be negative. Therefore the parameter ϵ is restricted by the inequality

$$\epsilon \leq \epsilon^* = \frac{1}{6\sqrt{3g(q)}} \tag{6.4}$$

which has to hold for any $q < a$. The inequality must hold even in the worst case, namely, if $g(q)$ attains its biggest value. The function $g(q)$, according to its definition (6.2)₂, has a relative maximum

$$g(q_2) = \left(\frac{2}{3}a\right)^3 \quad \text{at} \quad q_2 = \frac{2}{3}a. \tag{6.5}$$

Thus, for $q \geq 0$, we have

$$g(q) \leq \left(\frac{2}{3}a\right)^3. \tag{6.6}$$

The inequality (6.4) can, therefore, be extended to

$$\epsilon \leq \frac{1}{6\sqrt{3g(q_2)}} = \frac{1}{4a\sqrt{2a}}. \tag{6.7}$$

To get rid of the square root one can express the peak value a in terms of the parameter η by (4.9). Introducing this parameter the inequality (6.7) assumes the form

$$\epsilon \leq \frac{1}{16\eta^3}. \tag{6.8}$$

The extended KdV equation admits solitary waves only up to this limit of the micro-nonlinearity parameter ϵ .

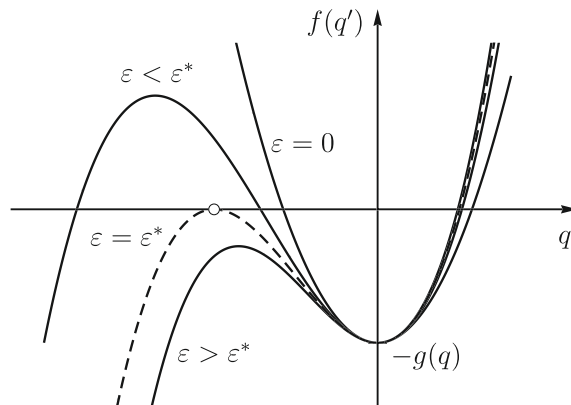


Fig. 2. Graph of the function $f(q')$.

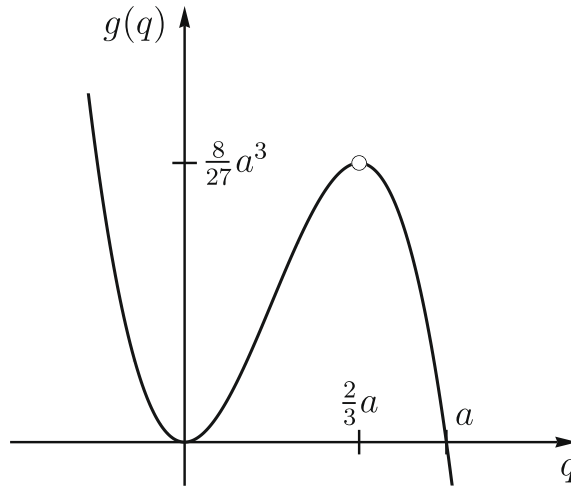


Fig. 3. Graph of the function $g(q)$.

In order to plot the phase curve given by (6.1) without solving a cubic equation one can introduce the parameter

$$p = \frac{q'}{q} \tag{6.9}$$

which represents the slope of the position vector in the phase plane. Eq. (6.1) can then be written in the form

$$p^2(1 + 4\epsilon pq) = 2(a - q). \tag{6.10}$$

Solving this equation for q and recalling (6.9) one obtains a parametric representation of the phase curve in the form

$$q(p) = \frac{a - \frac{1}{2}p^2}{1 + 2\epsilon p^3}, \quad q'(p) = pq(p). \tag{6.11}$$

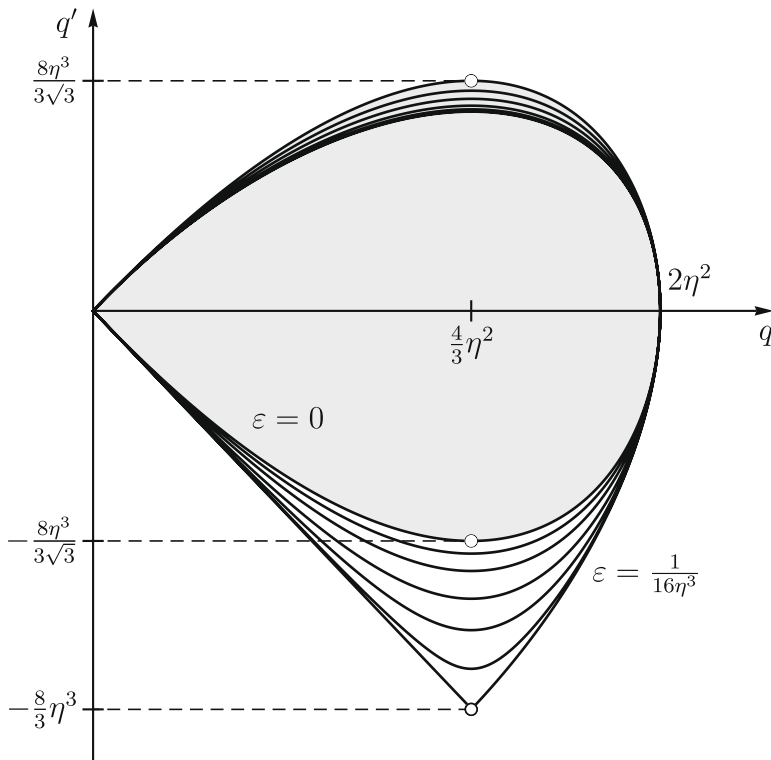


Fig. 4. Phase Curves of the extended KdV equation for different values of ϵ .

The curve parameter p varies in the interval $-\sqrt{2a} \leq p \leq +\sqrt{2a}$. The advantage of this parametric representation is that one does not need to solve the cubic Eq. (6.1) for q' . Using the above parametric representation the phase curves are drawn in Fig. 4 for different values of ε .

For the maximum value

$$\varepsilon = \varepsilon_{\max} = \frac{1}{16\eta^3} \tag{6.12}$$

the parametric representation (6.11) becomes singular at $p = -(2\varepsilon)^{-1/3} = -2\eta$. A detailed analysis shows that the phase curve, in this limiting case, degenerates into a semi-ellipse and a straight line representing a diameter of the ellipse. The final step of integration can be performed explicitly in this case. This will be presented in Section 8.

7. Approximate solution of the extended KdV equation

In order to get the solution $q = q(\theta)$ the first-order differential Eq. (6.1) has to be solved for q' and integrated. Using the abbreviation (6.2)₂ it is written as

$$q'^2 + 4\varepsilon q'3 = g(q). \tag{7.1}$$

Since it is unlikely that one finds an explicit solution after applying Cardano's formula on this cubic equation, an approximate solution by a series expansion in the small parameter ε is used. The corresponding formula is briefly derived in Appendix A. This approach is justified by the fact that solitary wave solutions exist only for small values of the parameter ε satisfying the inequality (6.8).

As in the KdV case it is assumed that the maximum value $a = c/2$ is attained at $\theta = 0$, from where the function $q(\theta)$ decreases as θ increases and vice versa. Applying the formula (A.6)₂ to the cubic Eq. (7.1) one obtains the approximation

$$q' = \mp \sqrt{g(q)} - 2\varepsilon g(q) \mp 10\varepsilon^2 [g(q)]^{3/2} - 64\varepsilon^3 [g(q)]^2 + O(\varepsilon^4), \tag{7.2}$$

where the upper and lower signs are valid for $\theta > 0$ and $\theta < 0$, respectively. For performing the integration also the reciprocal value is needed which, according to (A.8), is obtained as

$$\frac{d\theta}{dq} = \frac{1}{q'} = \frac{\mp 1}{\sqrt{g(q)}} + 2\varepsilon \pm 6\varepsilon^2 \sqrt{g(q)} + 32\varepsilon^3 g(q) + O(\varepsilon^4). \tag{7.3}$$

The definite integration starts with the maximum value $q = a$ attained at $\theta = 0$. Thus one obtains

$$\theta = \int_a^q \left[\frac{\mp 1}{\sqrt{g(q)}} + 2\varepsilon \pm 6\varepsilon^2 \sqrt{g(q)} + 32\varepsilon^3 g(q) + O(\varepsilon^4) \right] dq. \tag{7.4}$$

Inserting the function $g(q)$ from (6.2)₂ and performing the definite integration yields

$$\theta = \pm \sqrt{\frac{2}{a}} \operatorname{arcosh} \sqrt{\frac{a}{q}} - 2\varepsilon(a - q) \mp \frac{2}{5} \varepsilon^2 (2a + 3q)[2(a - q)]^{3/2} - \frac{16}{3} \varepsilon^3 (a^2 + 2aq + 3q^2)(a - q)^2 + O(\varepsilon^4). \tag{7.5}$$

In principle, this equation has to be solved for q to unveil the function $q = q(\theta)$. The inversion cannot be performed in closed form. The graph, however, can also be drawn directly from (7.5).

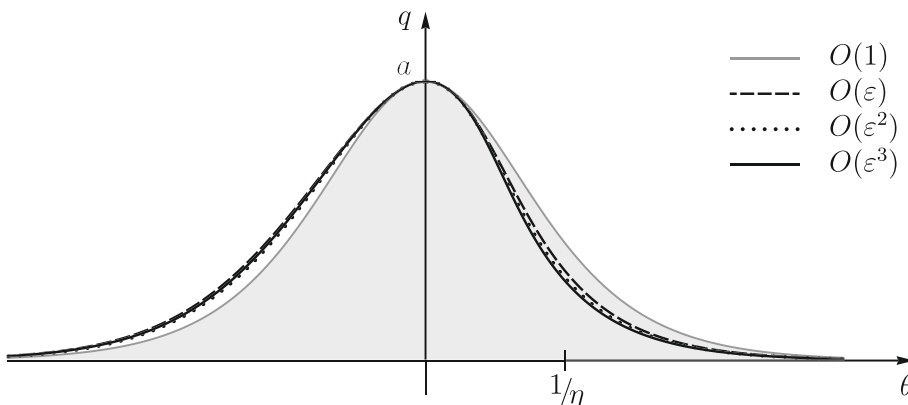


Fig. 5. Solitary wave governed by the extended KdV equation ($\varepsilon = \varepsilon_{\max}$) in different approximations.

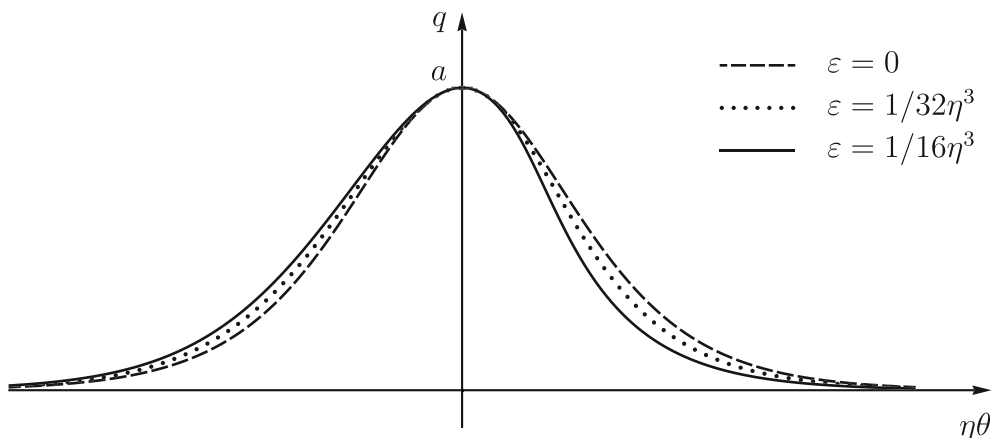


Fig. 6. Approximate $O(\varepsilon^3)$ solutions for different values of the micro-nonlinearity parameter.

Fig. 5 shows subsequent approximations of a solitary wave governed by the extended KdV equation with a fixed value of the micro-nonlinearity parameter ε . Starting from the symmetric KdV soliton even the approximation of order ε exhibits the asymmetric behavior of the solitary wave. The $O(\varepsilon^2)$ and $O(\varepsilon^3)$ approximations come out nearly identical. The convergence behavior is different on the left and on the right side. For $\theta > 0$ the limit is approached from one side while for $\theta < 0$ there is an alternating behavior. A comparison of the approximation with the exact solution is provided in Section 8 for the limiting value of the parameter ε .

The influence of the micro-nonlinearity parameter ε is shown in Fig. 6. Starting from the symmetric KdV soliton ($\varepsilon = 0$) the solitary wave becomes more asymmetric as ε is increased.

To emphasize the relation to the KdV soliton, the arcosh function in (7.5) is inverted, leading to the implicit representation

$$q = a \operatorname{sech}^2 \eta \left[\theta + 2\varepsilon(a - q) \pm \frac{2}{5} \varepsilon^2 (2a + 3q) [2(a - q)]^{3/2} + \frac{16}{3} \varepsilon^3 (a^2 + 2aq + 3q^2)(a - q)^2 + O(\varepsilon^4) \right] \tag{7.6}$$

of the solitary wave. The dependent variable q appears in the argument of the sech function, and the equation cannot be solved explicitly for q .

8. Analytical solution in the limiting case

It has been shown that bounded and closed phase curves $q'(q)$ are possible only if $\varepsilon \eta^3 \leq 1/16$. In addition to the case $\varepsilon = 0$, where one gets the well-known KdV soliton as an analytical representation, it can be shown that an analytical solution in closed form is also possible in the limiting case $\varepsilon \eta^3 = 1/16$.

After inserting the limiting value

$$\varepsilon = \frac{1}{16\eta^3} \tag{8.1}$$

the ordinary differential Eq. (6.1) can be written in the form

$$q'^2 - 4\eta^2 q^2 + \frac{1}{4\eta^3} (q'^3 + 8\eta^3 q^3) = 0. \tag{8.2}$$

The quadratic and cubic parts of this equation allow the factorizations

$$\begin{aligned} q'^2 - 4\eta^2 q^2 &= (q' + 2\eta q)(q' - 2\eta q), \\ q'^3 + 8\eta^3 q^3 &= (q' + 2\eta q)(q'^2 - 2\eta q q' + 4\eta^2 q^2). \end{aligned} \tag{8.3}$$

Thus (8.2) may be written as

$$(q' + 2\eta q) \left[q' - 2\eta q + \frac{1}{4\eta^3} (q'^2 - 2\eta q q' + 4\eta^2 q^2) \right] = 0. \tag{8.4}$$

The phase curve consists of two branches, namely the straight line

$$q' = -2\eta q \tag{8.5}$$

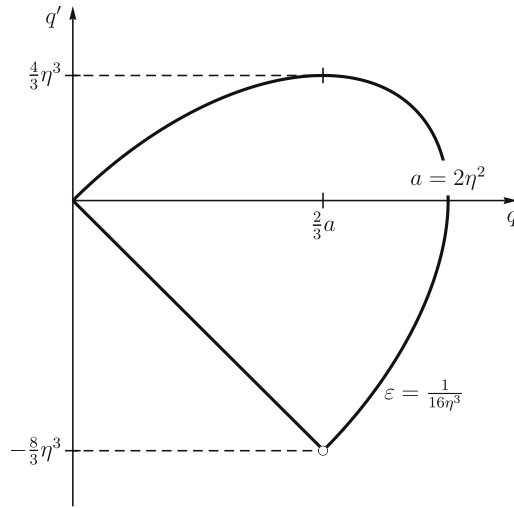


Fig. 7. Phase curve of the extended KdV equation in the limiting case.

and the ellipse

$$q^2 + 2\eta(2\eta^2 - q)q' - 4\eta^2q(2\eta^2 - q) = 0, \tag{8.6}$$

see Fig. 7. Solving the last equation for q' gives the solutions

$$q'_{1,2} = \eta[-(2\eta^2 - q) \pm \sqrt{4\eta^4 + 4\eta^2q - 3q^2}] = \eta[-(a - q) \pm \sqrt{a^2 + 2aq - 3q^2}], \tag{8.7}$$

where, for convenience, the abbreviation $a = 2\eta^2$ has been introduced according to (4.9). Putting together these solutions in the proper order one has to start at the origin which is attained asymptotically for $\theta \rightarrow -\infty$. Then the wave profile will build up with positive slope (8.7), + sign, increasing up to $q'_{\max} = 4\eta^3/3$ at $q = 2a/3$. The peak value of the wave profile $a = 2\eta^2$ is assumed to be attained at $\theta = 0$. For $\theta > 0$ the wave profile will decrease, i.e., it assumes the negative slope (8.7), – sign. At $q = 2a/3$ the steepest decline is reached with the slope $q' = -8\eta^3/3$. At this point the phase curve switches to the linear branch (8.5) until the origin is reached, again asymptotically for $\theta \rightarrow \infty$. Thus the phase curve, as shown in Fig. 7, is represented by

$$\frac{q'}{\eta} = \begin{cases} \sqrt{a^2 + 2aq - 3q^2} - (a - q) & \text{for } \theta \leq 0 \text{ and } 0 \leq q \leq a, \\ -\sqrt{a^2 + 2aq - 3q^2} - (a - q) & \text{for } \theta \geq 0 \text{ and } a \geq q \geq \frac{2}{3}a, \\ -2q & \text{for } \theta \geq 0 \text{ and } \frac{2}{3}a \geq q \geq 0. \end{cases} \tag{8.8}$$

The phase curve is traversed in clockwise sense, as always, since in the upper half-plane ($q' > 0$) the values of q must increase while in the lower half-plane ($q' < 0$) the values of q must decrease. The q -axis is intersected at a right angle except in a point which is reached only asymptotically. Let the right-hand side of (8.8) be abbreviated by $f(q)$. Then the wave profile $q(\theta)$ is the solution of the initial-value problem

$$\frac{dq}{d\theta} = \eta f(q), \quad q(0) = a. \tag{8.9}$$

By separation of variables and subsequent integration the solution is obtained as

$$\int_a^q \frac{dq}{f(q)} = \eta\theta. \tag{8.10}$$

The integral on the left-hand side has still to be evaluated.

For $\theta \leq 0$, the function f is given by (8.8)₁. Using the corresponding definite integral (B.6) with the upper sign, one obtains

$$\ln \frac{a(\sqrt{a^2 + 2aq - 3q^2} + a + q)}{2q^2} + \sqrt{3} \arccos \frac{3q - a}{2a} = -4\eta\theta. \tag{8.11}$$

The maximum slope

$$q'_{\max} = \frac{4}{3}\eta^3 \tag{8.12}$$

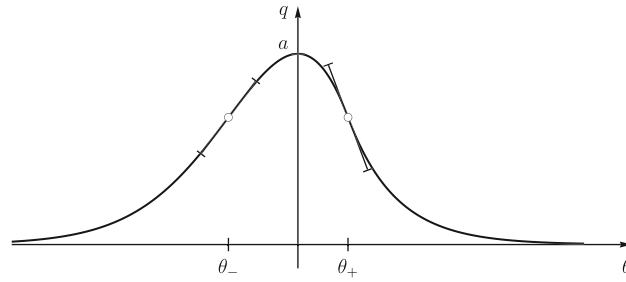


Fig. 8. Profile of the solitary wave in the limiting case.

is attained, according to Fig. 7, when the amplitude is $q = 2a/3$, i.e., at a value of

$$\theta_- = -\frac{1}{4\eta} \left(\ln 3 + \frac{\pi}{\sqrt{3}} \right) \tag{8.13}$$

of the independent variable θ . This branch of the curve ends with the peak value $q = a$ attained at $\theta = 0$, see Fig. 8.

For $\theta \geq 0$ and $a \geq q \geq 2a/3$ the function f is given by (8.8)₂. The definite integral (B.6) with the lower sign yields

$$\ln \frac{\sqrt{a^2 + 2aq - 3q^2} + a + q}{2a} + \sqrt{3} \arccos \frac{3q - a}{2a} = 4\eta\theta. \tag{8.14}$$

The branch ends at

$$\theta_+ = \frac{1}{4\eta} \left(\ln \frac{4}{3} + \frac{\pi}{\sqrt{3}} \right) \tag{8.15}$$

with the minimum (or maximum negative) slope

$$q'_{\min} = -\frac{8}{3}\eta^3 \tag{8.16}$$

at the height $q = 2a/3$. The last branch starts at (8.15), and the function f is given by (8.8)₃. Thus one has to perform the definite integration

$$\int_{2a/3}^q \frac{dq}{q} = -2\eta \int_{\theta_+}^{\theta} d\theta, \tag{8.17}$$

which yields the solution

$$q = \frac{2a}{3} \exp[-2\eta(\theta - \theta_+)]. \tag{8.18}$$

At $\theta = \theta_+$ the branch starts with the slope

$$q'(\theta_+) = -\frac{4}{3}a\eta = -\frac{8}{3}\eta^3. \tag{8.19}$$

This means that the last branch is attached continuously differentiable to the preceding one. The whole wave profile is shown in Fig. 8, where also the tangents at the inflectional points θ_{\mp} are indicated.

A comparison of this exact solution with the approximate solution (7.5) is depicted in Fig. 9. In the left, flat part, the curves coincide excellently while on the steeper flank the approximation is slightly above the exact curve. It should be noted that this good coincidence pertains to the maximum value of the parameter ε allowing a solitary wave solution. For smaller values it should be even better.

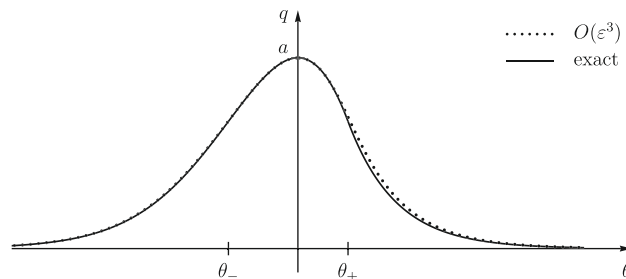


Fig. 9. Exact and approximate solutions in the limiting case $\varepsilon = 1/(16\eta^3)$.

9. Conclusion

From various studies it is known that in a microstructured material solitary waves can propagate if dispersion and non-linearity are balanced appropriately. If the linear dispersion evoked by the microstructure is complemented only by macro-nonlinearity the dynamical behavior is described by the Korteweg–de Vries equation, and the well-known symmetric solitary waves are possible solutions.

If also some nonlinearity in the microscale is included the evolution equation contains an additional nonlinear term which involves higher derivatives. This makes the shape of the solitary waves asymmetric. While this effect has been analyzed before numerically [14], the present paper provides a formula which describes the asymmetric solitary wave analytically, although in some approximation.

It is shown that solitary waves are possible only up to a certain limit of the micro-nonlinearity parameter. For this limit as a special case, the extended KdV equation can be solved explicitly and used as a reference. The approximate solution agrees quite well with the exact one in the limit case, and the coincidence must be even better for smaller values of the micro-nonlinearity parameter.

The results presented in this paper represent, strictly speaking, approximate and—in the special case treated in Section 8—analytical solutions of the extended Korteweg–de Vries equation. This evolution equation describes the slow variations of propagating waves governed by the nondimensional partial differential Eq. (2.15) which, in turn, is obtained using the slaving principle from the original Eq. (2.7) describing the physical model. It is still an open question to what extent the presented solutions, which pertain to the extended KdV Eq. (3.7), are consistent with the original model (2.7). This should be analyzed by numerical studies which, however, are outside of the scope of the present paper.

Appendix A. Approximate solution of a cubic equation

In the analysis of the extended KdV Eq. (3.7) one comes across a cubic equation with a small coefficient at the cubic term. Instead of solving the equation exactly, an approximate solution is used.

The solutions of the cubic equation

$$\varepsilon x^3 + x^2 = a^2, \tag{A.1}$$

with a small coefficient ε , are assumed in the form

$$x = x_0 + \varepsilon x_1 + \varepsilon^2 x_2 + \varepsilon^3 x_3 + O(\varepsilon^4). \tag{A.2}$$

Restricting the expansion to the order ε^3 the square of the series (A.2) is obtained as

$$x^2 = x_0^2 + 2\varepsilon x_0 x_1 + \varepsilon^2 (2x_0 x_2 + x_1^2) + 2\varepsilon^3 (x_0 x_3 + x_1 x_2) + O(\varepsilon^4). \tag{A.3}$$

The third power is needed only up to the order ε^2 , since it will be multiplied by ε . Thus

$$x^3 = x_0^3 + 3\varepsilon x_0^2 x_1 + 3\varepsilon^2 (x_0^2 x_2 + x_0 x_1^2) + O(\varepsilon^3). \tag{A.4}$$

By inserting these series into the cubic Eq. (A.1) and equating coefficients of like powers of ε one obtains a set of equations for the coefficients x_k which finally lead to

$$x_0 = \pm a, \quad x_1 = -\frac{1}{2}a^2, \quad x_2 = \pm \frac{5}{8}a^3, \quad x_3 = -a^4. \tag{A.5}$$

Thus the roots of the cubic Eq. (A.1) are approximated by

$$x_{\pm} = \pm a - \frac{1}{2}\varepsilon a^2 \pm \frac{5}{8}\varepsilon^2 a^3 - \varepsilon^3 a^4 + O(\varepsilon^4) = \pm a \left[1 \mp \frac{1}{2}\varepsilon a + \frac{5}{8}\varepsilon^2 a^2 \mp \varepsilon^3 a^3 + O(\varepsilon^4) \right]. \tag{A.6}$$

The roots (A.6) are those emerging from the two roots of the quadratic equation to which (A.1) reduces for $\varepsilon = 0$. For any $\varepsilon \neq 0$ there must be a third root, which can be expanded into the series

$$x_{\times} = -\frac{1}{\varepsilon} + \varepsilon a^2 + 2\varepsilon^3 a^4 + O(\varepsilon^4). \tag{A.7}$$

This third root, however, is of no relevance in our application.

Within the integration process of Section 7 also the reciprocal roots $1/x_{\pm}$ are needed, which are obtained from (A.6) by the well-known geometric series expansion as

$$\frac{1}{x_{\pm}} = \pm \frac{1}{a} \left[1 \pm \frac{1}{2}\varepsilon a - \frac{3}{8}\varepsilon^2 a^2 \pm \frac{1}{2}\varepsilon^3 a^3 + O(\varepsilon^4) \right] = \pm \frac{1}{a} + \frac{1}{2}\varepsilon \mp \frac{3}{8}\varepsilon^2 a + \frac{1}{2}\varepsilon^3 a^2 + O(\varepsilon^4). \tag{A.8}$$

In principle, the expansions can be extended to higher orders in ε . The level of $O(\varepsilon^3)$ seems to be sufficient for the application here.

Appendix B. Evaluation of some integrals

The integrals needed in Section 8 are not readily available from integral tables but need some transformations. This is indicated here in brief. To evaluate the indefinite integrals

$$I_{\mp} = \int \frac{dx}{\sqrt{a^2 + 2ax - 3x^2} \mp (a - x)} \quad (\text{B.1})$$

the integrand is rewritten as

$$\begin{aligned} \frac{1}{\sqrt{a^2 + 2ax - 3x^2} \mp (a - x)} &= \frac{1}{\sqrt{a-x}(\sqrt{a+3x} \mp \sqrt{a-x})} = \frac{\sqrt{a+3x} \pm \sqrt{a-x}}{4x\sqrt{a-x}} = \frac{1}{4} \left(\frac{a+3x}{x\sqrt{a^2 + 2ax - 3x^2}} \pm \frac{1}{x} \right) \\ &= \frac{1}{4} \left(\frac{a}{x\sqrt{a^2 + 2ax - 3x^2}} + \frac{3}{\sqrt{a^2 + 2ax - 3x^2}} \pm \frac{1}{x} \right). \end{aligned} \quad (\text{B.2})$$

Thus the integration is reduced to the knowledge of the integrals

$$\int \frac{adx}{x\sqrt{a^2 + 2ax - 3x^2}} = -\ln \frac{\sqrt{a^2 + 2ax - 3x^2} + a + x}{x} \quad (\text{B.3})$$

and

$$\int \frac{dx}{\sqrt{a^2 + 2ax - 3x^2}} = -\frac{1}{\sqrt{3}} \arcsin \frac{a-3x}{2a} \quad (\text{B.4})$$

which are found in [17, pp. 759 and 758], for instance. The result is

$$4I_{\mp} = -\ln \frac{\sqrt{a^2 + 2ax - 3x^2} + a + x}{x} + \sqrt{3} \arcsin \frac{3x-a}{2a} \pm \ln \frac{x}{a}. \quad (\text{B.5})$$

Mathematically, the last term could also be written simply as $\ln x$, which differs only by a constant. If x and a have some physical dimension as length, for instance, the logarithm should still be applied to a real number. Therefore the version (B.5) is preferred.

Actually needed in (8.14) are the definite integrals

$$4 \int_a^x \frac{dx}{\sqrt{a^2 + 2ax - 3x^2} \mp (a - x)} = -\ln \frac{\sqrt{a^2 + 2ax - 3x^2} + a + x}{2x} \pm \ln \frac{x}{a} - \sqrt{3} \arccos \frac{3x-a}{2a} \quad (\text{B.6})$$

which are obtained from (B.5) by inserting the bounds.

References

- [1] R.D. Mindlin, Microstructure in linear elasticity, *Arch. Ration. Mech. Anal.* 16 (1964) 51–78.
- [2] C.-T. Sun, J.D. Achenbach, G. Herrmann, Continuum theory for a laminated medium, *J. Appl. Mech. Trans. ASME* 35 (1968) 467–475.
- [3] G. Herrmann, J.D. Achenbach, Application of theories of generalized Cosserat continua to the dynamics of composite materials, in: E. Kröner (Ed.), *Mechanics of Generalized Continua*, Springer, Berlin, Heidelberg, New York, 1968, pp. 69–79.
- [4] A.C. Newell, *Solitons in Mathematics and Physics*, Society for Industrial and Applied Mathematics, Philadelphia, 1985.
- [5] A.M. Samsonov, *Strain Solitons in Solids and How to Construct Them*, Chapman & Hall/CRC, Boca Raton, 2001.
- [6] A.V. Porubov, *Amplification of Nonlinear Strain Waves in Solids*, World Scientific, NJ, 2003.
- [7] A.V. Porubov, *Localization of Nonlinear Deformation Waves*, Fizmatlit, Moscow, 2009 (in Russian).
- [8] V.F. Nesterenko, *Dynamics of Heterogeneous Materials*, Springer, New York, 2001.
- [9] V.F. Nesterenko, C. Daraio, E.B. Herbold, S. Jin, Anomalous wave reflection at the interface of two strongly nonlinear granular media, *Phys. Rev. Lett.* 95 (2005) 158702.
- [10] J. Engelbrecht, F. Pastrone, Waves in microstructured solids with strong nonlinearities in microscale, *Proc. Estonian Acad. Sci. Phys. Math.* 52 (2003) 12–20.
- [11] J. Janno, J. Engelbrecht, Solitary waves in nonlinear microstructured materials, *J. Phys. A: Math. Gen.* 38 (2005) 5159–5172.
- [12] J. Janno, J. Engelbrecht, Waves in microstructured solids: inverse problems, *Wave Mot.* 43 (2005) 1–11.
- [13] J. Engelbrecht, F. Pastrone, M. Braun, A. Berezovski, Hierarchies of waves in nonclassical materials, in: P.-P. Delsanto (Ed.), *The Universality of Nonclassical Nonlinearity: Applications to Non-destructive Evaluations and Ultrasonics*, Springer (2006) 29–48.
- [14] M. Randrüüt, A. Salupere, J. Engelbrecht, On modelling wave motion in microstructured solids, *Proc. Estonian Acad. Sci. Math.* 58 (2009) 241–246.
- [15] J. Engelbrecht, *Nonlinear Wave Processes of Deformation in Solids*, Pitman, Boston, London, Melbourne, 1983.
- [16] A. Jeffrey, J. Engelbrecht, *Nonlinear Waves in Solids*, International Centre for Mechanical Sciences, Courses and Lectures No. 341, Springer, Wien, New York, 1994.
- [17] I.N. Bronstein, K.A. Semendjajew, G. Musiol, H. Mühlig, *Taschenbuch der Mathematik*, Verlag Harri Deutsch, Thun, Frankfurt am Main, 1993.

PUBLICATION IV

Manfred Braun and **Merle Randrüüt**: On periodic waves governed by the extended Korteweg–de Vries equation. *Proceedings of the Estonian Academy of Sciences* **59**(2) (2010) 133–138.



On periodic waves governed by the extended Korteweg–de Vries equation

Manfred Braun^a and Merle Randrüüt^{b*}

^a Chair of Mechanics and Robotics, Institute of Mechatronics and System Dynamics, University of Duisburg-Essen, Lotharstraße 1, 47057 Duisburg, Germany; manfred.braun@uni-due.de

^b Centre for Nonlinear Studies, Institute of Cybernetics at Tallinn University of Technology, Akadeemia tee 21, 12618 Tallinn, Estonia

Received 10 December 2009, accepted 3 February 2010

Abstract. The evolution equation describing the propagation of one-dimensional waves in a microstructured material has the form of an extended Korteweg–de Vries equation, where the additional term reflects the influence of micrononlinearity. As shown by Janno and Engelbrecht (*J. Phys. A: Math. Gen.*, 2005, **38**, 5159–5172), solitary waves in a microstructured material become asymmetric if nonlinearities are taken into account in both macro- and microscale. The present paper generalizes previous results to periodic waves which, in the KdV case, have the form of cnoidal waves. It is shown that, due to the nonlinearity in microscale, these waves become inclined in the same manner as solitary waves, while the relations between the period, amplitude, and velocity are not affected.

Key words: materials with microstructure, cnoidal waves, solitary waves, KdV equation.

1. INTRODUCTION

A linear theory of microstructured solids was proposed by Mindlin [1] in 1964. Engelbrecht and Pastrone [2] specialized this theory to one dimension and, at the same time, generalized it by including nonlinear terms at both macro- and microlevel. To describe the motion of the one-dimensional microstructured solid, they complemented the macroscopic displacement by the microstrain, both of which are considered as functions of the space coordinate and time. The governing equations appear as a system of coupled partial differential equations for the two field variables. Using the so-called slaving principle, Engelbrecht and Pastrone [2] distilled from it a single partial differential equation, which governs mainly the macrodisplacement while retaining, in a first approximation, the influence of the microstructure.

On the basis of this equation the propagation of solitary waves was studied by Janno and Engelbrecht [3]. They showed that the wave profile becomes asymmetric. The evolution equation of these waves assumes the form of an extended Korteweg–de Vries (KdV) equation, where the additional, higher-order term reflects the influence of micrononlinearity. An approximate solution of this equation in analytical form has been provided by Randrüüt and Braun [4].

Besides solitary waves, the KdV equation admits a whole family of periodic solutions, the so-called cnoidal waves, of which the solitary wave is just the limit if the period tends to infinity. The aim of the present paper is to study how these periodic waves are affected if micrononlinearity is taken into account. As can be expected, the waves stay periodic but become inclined in the same manner as solitary waves.

* Corresponding author, merler@cens.ioc.ee

2. EXTENDED KdV EQUATION

As mentioned before, the basic governing equations are not treated directly. Rather, by using the slaving principle, a single partial differential equation is extracted. This, in turn, is analysed via the reductive perturbation method which finally provides an evolution equation describing the perturbation of the wave profile. For the sake of brevity, this whole procedure is not duplicated here. The application of the slaving principle is explained in detail in [2–4], and the evolution equation is derived in [4,5]. It has the form of an extended KdV equation. By scaling the variables appropriately, the evolution equation can be reduced to the standardized form

$$y_t + 3(y^2)_x + y_{xxx} + 3\varepsilon(y_x)_{xx} = 0. \quad (1)$$

The variable y represents a scaled macrostrain. The independent variables are a dimensionless moving space coordinate x and the dimensionless slow time t . The evolution equation describes the slow variation of the wave profile as observed in a frame which is travelling along with the wave at its basic propagation speed. The evolution equation (1) is the starting point of our analysis.

We look for solutions of the form

$$y(x, t) = q(\theta), \quad \theta = x - ct, \quad (2)$$

representing undistorted waves propagating at the velocity c within the moving reference frame. The function $q = q(\theta)$ will then satisfy an ordinary differential equation, which can be integrated twice to result in a first-order differential equation of the form

$$q'^2 + 4\varepsilon q^3 = f(q), \quad f(q) = 2B + 2Aq + cq^2 - 2q^3. \quad (3)$$

The cubic polynomial $f(q)$ on the right-hand side contains three parameters: the velocity c of the wave profile relative to the moving frame and two constants of integration, A and B . Instead of these parameters one can also introduce the three roots of the cubic polynomial and write the polynomial in the form

$$f(q) = 2(q - q_1)(q - q_2)(q_3 - q). \quad (4)$$

We assume the roots $q_1 \leq q_2 \leq q_3$ to be real. It can be easily shown that, if two roots become conjugate complex, there will be no finite solutions of the differential equation (3).

In principle, equation (3) has to be solved for q' and then integrated. However, it is unlikely that this integration can be performed in closed form. Therefore we confine ourselves to an *approximate* solution, assuming the parameter ε to be small. Expanding the roots of the cubic equation (3) in powers of ε , one obtains

$$q' = \pm \sqrt{f(q)} \left\{ 1 \mp 2\varepsilon \sqrt{f(q)} + 10\varepsilon^2 f(q) \mp 64\varepsilon^3 [f(q)]^{3/2} \right\} + O(\varepsilon^4), \quad (5)$$

where $f(q)$ is the cubic polynomial defined by (3)₂. Although, at first glance, this differential equation for $q(\theta)$ seems even more complicated than the original one, it can be integrated in closed form.

3. PHASE PORTRAIT

Before going on with the integration the behaviour of the phase curves $q'(q)$ will be analysed in detail. The polynomial $f(q)$ involves three parameters. In order to get a one-parameter family of curves, two constants should be fixed. Let us suppose that the minimum and the maximum of the polynomial are located at $q = 0$ and $q = a$, respectively, where a is an arbitrary but fixed value. Then the cubic polynomial admits the representation

$$f(q) = b^2 - (2q + a)(q - a)^2, \quad (6)$$

where b is considered as the only free parameter of the function. The phase portrait depicts the family of phase curves $q'(q)$ for different values of the parameter b , while a and ε are kept fixed.

As has been shown in [4], solitary waves are possible solutions of the extended KdV equation only if

$$\varepsilon \leq \varepsilon_{\max} = \frac{1}{2}(3a)^{-3/2}. \tag{7}$$

Figure 1 shows the phase portrait for $\varepsilon = 0.8\varepsilon_{\max}$. There is a pronounced asymmetry which increases with growing values of ε , while for $\varepsilon = 0$ the symmetric phase portrait of the standard KdV equation would be retained. In principle, the whole (q, q') -plane is filled by phase curves. Only those, however, which do not extend to infinity correspond to finite solutions $q = q(\theta)$ of the evolution equation. As can be seen from the figure, it is only the shaded part of the phase plane which contains closed phase curves representing finite waves. Those curves which intersect the q -axis twice at right angles correspond to periodic waves. The limiting curve forms a homoclinic orbit starting and ending at the origin, which means that $q = q' = 0$ is attained asymptotically for $\theta \rightarrow \pm\infty$. This curve corresponds to the limiting solitary wave.

The final integration uses the series expansion (5) rather than the exact phase curves $q'(q)$. In Fig. 2 the exact solution of the cubic equation (3) is contrasted with the approximations (5) allowing for different powers of ε . The $O(1)$ approximation neglects the influence of micrononlinearity and gives the symmetric phase curves of the KdV case. Taking into account the corrections (5) with increasing powers of ε leads to the asymmetric phase curves which are characteristic of the extended KdV equation. The approximations converge to the exact solution. In the upper half-plane the convergence is alternating, in the lower the curves approach the limit from above. Even for $\varepsilon = \varepsilon_{\max}$ the approximation is acceptable for periodic waves. It is still poor at the kink of the phase curve representing the solitary wave. This, however, is the worst case.

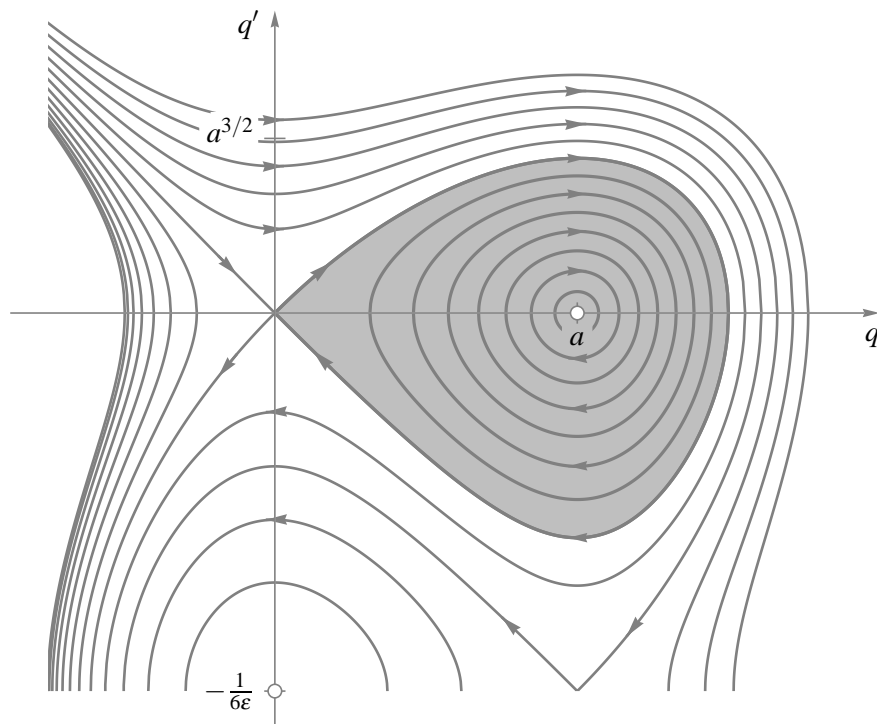


Fig. 1. Phase portrait of the extended KdV equation for $\varepsilon = 0.8\varepsilon_{\max}$.

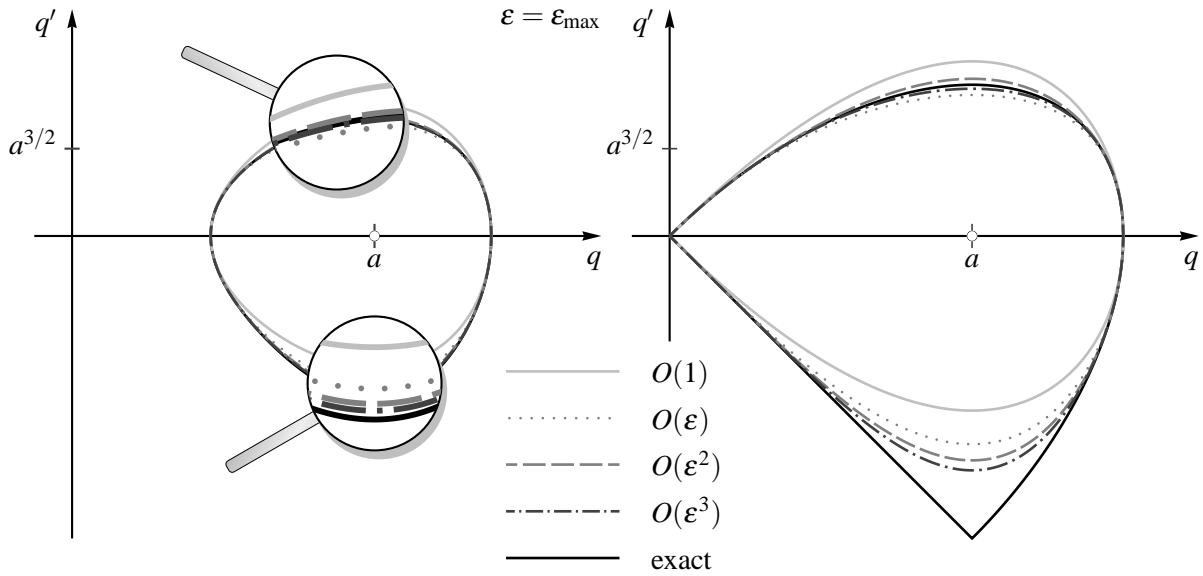


Fig. 2. Approximate phase curves of the extended KdV equation with the maximal micrononlinearity parameter. Left: periodic wave (with magnified areas). Right: limiting solitary wave.

4. ASYMMETRIC PERIODIC WAVES

The final integration will be performed using the approximation of q' by the power series (5). Without loss of generality one may assume that q attains its maximum value q_3 at $\theta = 0$. Using this as the initial condition for the definite integration, the values of q will decrease as θ increases. Therefore the lower signs in (5) are chosen. For performing the integration one needs the reciprocal value $1/q'$ which is obtained as

$$\frac{d\theta}{dq} = \frac{1}{q'} = -\frac{1}{\sqrt{f(q)}} \left[1 - 2\epsilon\sqrt{f(q)} \right] + O(\epsilon^2) = -\frac{1}{\sqrt{f(q)}} + 2\epsilon + O(\epsilon^2). \quad (8)$$

The analysis is restricted here to the $O(\epsilon)$ approximation but can easily be extended to higher orders. With the use of the initial condition $q(0) = q_3$, the integration yields

$$\theta = \int_{q_3}^q \left[\frac{-1}{\sqrt{f(q)}} + 2\epsilon \right] dq. \quad (9)$$

The integral can be evaluated explicitly by using the substitution

$$q = q_2 + (q_3 - q_2) \cos^2 \varphi \quad (10)$$

of the integration variable. Performing the integration gives the result

$$\theta = \frac{1}{\eta} F(\varphi; k) - 2\epsilon(q_3 - q), \quad (11)$$

where F denotes the incomplete elliptic integral of the first kind and the constants

$$\eta = \sqrt{\frac{q_3 - q_1}{2}}, \quad k = \sqrt{\frac{q_3 - q_2}{q_3 - q_1}} \quad (12)$$

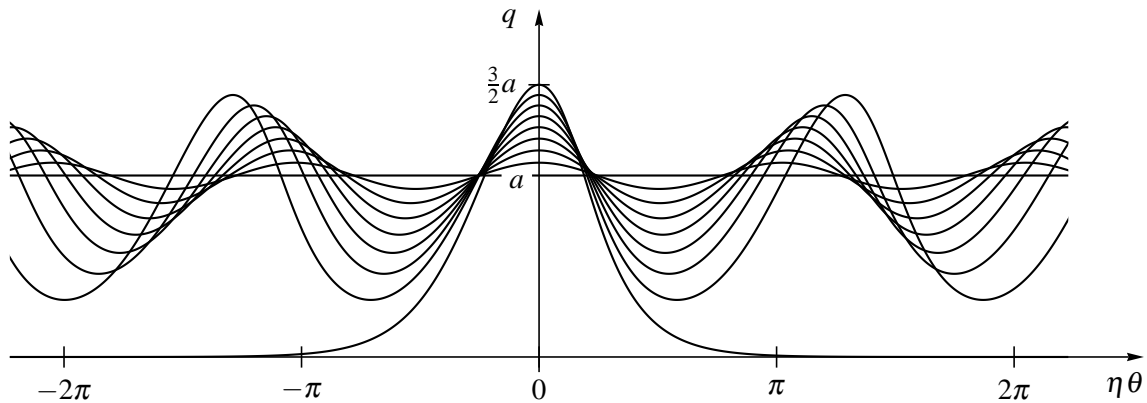


Fig. 3. Periodic waves and solitary wave governed by the extended KdV equation ($\varepsilon = \varepsilon_{\max}$).

have been introduced. Solving (11) for the auxiliary variable φ and resubstituting this into the transformation formula (10) yields

$$q = q_2 + (q_3 - q_2) \operatorname{cn}^2 \eta [\theta + 2\varepsilon(q_3 - q)]. \quad (13)$$

This is an implicit representation of the periodic wave solutions of the extended KdV equation (1), though only in a first approximation. For $\varepsilon = 0$ it passes into the cnoidal wave solution of the KdV equation. Figure 3 shows a family of periodic waves together with their limiting solitary wave, as described by (13). The waves look very much like the corresponding cnoidal waves, but are inclined to the right.

5. CONCLUDING REMARKS

As known from previous studies [4,5], the propagation of one-dimensional deformation waves in a nonlinear microstructured solid leads to an evolution equation which has the form of an extended Korteweg–de Vries equation. Janno and Engelbrecht [3] have demonstrated that, due to the nonlinearity of the microscale, the solitary wave profile becomes asymmetric. The same effect appears in the case of the respective evolution equation which has been solved approximately by Randrüüt and Braun [4]. Although solitary waves constitute the most interesting type of solutions, the same procedure is applied here to a more general case. Solitary waves can be considered as the long-wave limit of periodic solutions which, in the KdV case, have the form of cnoidal waves.

It is shown that, due to the nonlinearity in microscale, cnoidal waves stay periodic but become inclined in the same manner as solitary waves. Compared with the classical cnoidal waves ($\varepsilon = 0$), the periodic waves for $\varepsilon > 0$ have a steeper slope at the leading flank, while the trailing flank falls off gentler. Qualitatively the behaviour is as expected from the solitary-wave limit.

ACKNOWLEDGEMENT

The research was supported by the Estonian Science Foundation (grant No. 7035).

REFERENCES

1. Mindlin, R. D. Microstructure in linear elasticity. *Arch. Rat. Mech. Analysis*, 1964, **16**, 51–78.
2. Engelbrecht, J. and Pastrone, F. Waves in microstructured solids with strong nonlinearities in microscale. *Proc. Estonian Acad. Sci. Phys. Math.*, 2003, **52**, 12–20.
3. Janno, J. and Engelbrecht, J. Solitary waves in nonlinear microstructured materials. *J. Phys. A: Math. Gen.*, 2005, **38**, 5159–5172.

4. Randrüüt, M. and Braun, M. On one-dimensional solitary waves in microstructured solids. *Wave Motion*, 2010, **47**, 217–230.
5. Randrüüt, M., Salupere, A., and Engelbrecht, J. On modelling wave motion in microstructured solids. *Proc. Estonian Acad. Sci. Phys. Math.*, 2009, **58**, 241–246.

Üldistatud Kortewegi-de Vriesi võrrandi perioodilistest lahenditest

Manfred Braun ja Merle Randrüüt

Üksiklainete levi mikrostruktuursetes tahkistes on leidnud põhjalikku käsitlemist Janno ja Engelbrechti [3] poolt. Selle artikli autorid on näidanud, et niisuguste lainete evolutsioonivõrrand on kõrgemat järku lisaliikmega Kortewegi-de Vriesi võrrand (üldistatud KdV-võrrand), kusjuures lisaliige kirjeldab mikrostruktuuri mittelineaarsust. On teada, et mikrostruktuuri mittelineaarsuse tõttu on üksiklaineline ebasümmeetriline.

Üksiklaineid võib vaadelda kui lõpmatuks läheneva lainepikkusega perioodilisi laineid, mida KdV juhtumil nimetatakse knoidaalseteks laineteks. Selles artiklis on uuritud üldistatud KdV-võrrandi perioodilisi lahendeid. Vastavaid faasidiagramme kirjeldab kuupvõrrand, mille lahendite analüütiline integreerimine osutub tõenäoliselt võimatuks. Seetõttu lahendatakse see kuupvõrrand ligikaudselt mikrostruktuuri mittelineaarsuse parameetri väikeste väärtuste korral, mis võimaldab saada perioodilisi lahendeid ilmutamata kujul.

Knoidaalsete lainetega võrreldes on üldistatud KdV-võrrandi perioodilistel lahenditel vastavalt liikumise suunale esikülj järsema kaldega kui tagumine. Mittelineaarne lisaliige ei mõjuta laine amplituudi, perioodi ja levimiskiiruse vahelisi seoseid. Selgub, et lisaliikme mõju perioodilistele lahenditele on samasugune kui üksiklainelisele lahendile, põhjustades laineprofiili ebasümmeetria.

APPENDIX B

CURRICULUM VITAE

CURRICULUM VITAE

1. Personal data

Name Merle Randrüüt
Date and place of birth September 20, 1981, Tallinn, Estonia
Nationality Estonian

2. Contact information

Address Institute of Cybernetics at TUT, Akadeemia tee 21, 12618 Tallinn, Estonia
Phone +372 6204173
E-mail merler@cens.ioc.ee

3. Education

2006 – ... Tallinn University of Technology, Faculty of Science, Engineering Physics, PhD studies
2004 – 2006 Tallinn University of Technology, Faculty of Science, Engineering Physics, MSc
2000 – 2004 Tallinn University of Technology, Faculty of Mechanics, Product Development, BSc

4. Language competence

Estonian native language
English fluent
Russian basic
German basic

5. Professional employment

2009 – ... Tallinn University of Technology, Institute of Cybernetics, Department of Mechanics and Applied Mathematics, Researcher
2007 – ... Tallinn University of Technology, Faculty of Civil Engineering, Department of Mechanics, Chair of Engineering Mechanics, Assistant
2007 – 2007 Estonian Academy of Arts, Faculty of Architecture, Lecturer

- 2006 – 2007 Tallinn University of Technology, Faculty of Civil Engineering, Department of Mechanics, Chair of Engineering Mechanics, Assistant Extraordinarius
- 2005 – 2009 Tallinn University of Technology, Institute of Cybernetics, Department of Mechanics and Applied Mathematics, Technician
- 2005 – 2006 Consolis Engineering Services, Technician
- 2005 – 2005 Tallinn University of Technology, Faculty of Civil Engineering, Department of Mechanics, Chair of Applied Mechanics, Lecturer
- 2003 – 2003 Norma, practical work placement, Constructor

6. Defended theses

- 2006, Modelling of deformation waves in microstructured solids, MSc, supervisor Professor Jüri Engelbrecht, Tallinn University of Technology, Faculty of Science
- 2004, Optimal design of a stepped beam, BSc, supervisor Associate Professor Jüri Kirs, Tallinn University of Technology, Faculty of Mechanics

7. Honours and awards

- 2009, award for the best scientific publication of a young scientist at the Institute of Cybernetics at TUT — Tanel Peets, Merle Randrüüt, and Jüri Engelbrecht: On modelling dispersion in microstructured solids. *Wave Motion* **45**(4) (2008) 471–480
- 2008, TUT Development Fund, Tiina Mõis Scholarship
- 2008, TUT Development Fund, Eesti Raudtee Scholarship
- 2008, special award for the best poster presentation of a young researcher, *11th EUROMECH–MECAMAT conference, Mechanics in microstructured solids: cellular materials, fibre reinforced solids and soft tissues*, Turin, Italy
- 2006, Estonian Academy of Science, 2nd award for a student research (Master’s thesis)
- 2005, TUT Development Fund, Eesti Energia Scholarship
- 2003, TUT Development Fund, Saku Õlletehas Scholarship

8. Field of research

- Deformation waves in microstructured solids

9. Scientific work

Papers

1. Manfred Braun and Merle Randrüüt: On periodic waves governed by the extended Korteweg–de Vries equation. *Proceedings of the Estonian Academy of Sciences* **59**(2) (2010) 133–138.
2. Merle Randrüüt and Manfred Braun: On one-dimensional solitary waves in microstructured solids. *Wave Motion* **47**(4) (2010) 217–230.
3. Merle Randrüüt and Manfred Braun: On solitary waves in one-dimensional microstructured solids. *PAMM. Proceedings in Applied Mathematics and Mechanics*. **9**(1) (2010) 495–496.
4. Merle Randrüüt, Andrus Salupere, and Jüri Engelbrecht: On modelling wave motion in microstructured solids. *Proceedings of the Estonian Academy of Sciences* **58**(4) (2009) 241–246.
5. Andrus Salupere, Merle Randrüüt, and Kert Tamm: Emergence of soliton trains in microstructured materials. In: J. Denier, M. Finn, T. Mattner (editors), *XXII International Congress of Theoretical and Applied Mechanics ICTAM 2008*, CD-ROM Proceedings, August 24–29, Adelaide, Australia 2008.
6. Tanel Peets, Merle Randrüüt, and Jüri Engelbrecht: On modelling dispersion in microstructured solids. *Wave Motion* **45**(4) (2008) 471–480.

Abstracts

1. Manfred Braun and Merle Randrüüt: On periodic waves governed by the extended Korteweg–de Vries equation. In: Arkadi Berezovski and Tarmo Soomere (editors), *International Conference on Complexity of Nonlinear Waves*, October 5–7, 2009, Tallinn University of Technology, Tallinn, Estonia, Book of Abstracts (2009) page 10.
2. Merle Randrüüt and Manfred Braun: On solitary waves in one-dimensional microstructured solids. In: *80th Annual Meeting of the International Association of Applied Mathematics and Mechanics GAMM 2009*, February 9–13, 2009, Gdańsk University of Technology, Gdańsk, Poland, Abstract included at the Conference CD (2009).

3. Jüri Engelbrecht, Merle Randrüüt, and Andrus Salupere: On modelling wave motion in microstructured solids. In: *11th EUROMECH–MECAMAT conference*, Mechanics of microstructured solids: cellular materials, fibre reinforced solids and soft tissues, March 10–14, 2008, Jean-François Ganghoffer and Franco Pastrone (editors), University of Turin, Turin, Italy, Book of Abstracts (2008) 30–31.

Conference and seminar presentations

1. Manfred Braun and Merle Randrüüt. On periodic waves governed by the extended Korteweg–de Vries equation. *International Conference on Complexity of Nonlinear Waves*, Institute of Cybernetics, Tallinn University of Technology, Tallinn, Estonia, October 5–7, 2009.
2. Merle Randrüüt and Manfred Braun. On solitary waves in one-dimensional microstructured solids. *80th Annual Meeting of the International Association of Applied Mathematics and Mechanics GAMM 2009*, Gdańsk University of Technology, Gdańsk, Poland, February 9–13, 2009.
3. Merle Randrüüt. Deformatsioonilained mikrostruktuuriga materjalides: ühedimensioonilised evolutsioonivõrrandid (Deformation waves in microstructured materials: evolution equations). *XIII Estonian Days of Mechanics*, September 15–16, 2008.
4. Andrus Salupere, Merle Randrüüt, and Kert Tamm. Emergence of soliton trains in microstructured materials. *XII International Congress of Theoretical and Applied Mechanics ICTAM 2008*, Adelaide, Australia, August 24–29, 2008.
5. Merle Randrüüt. On deformation waves in microstructured materials: one-dimensional case, evolution equations. *Kolloquium Mechanik*. University of Duisburg-Essen, Duisburg, Germany, July 16, 2008.
6. Jüri Engelbrecht, Merle Randrüüt, and Andrus Salupere. On modelling wave motion in microstructured solids. *11th EUROMECH–MECAMAT conference*, Mechanics in microstructured solids: cellular materials, fibre reinforced solids and soft tissues, Torino, Italy, March 10–14, 2008 (invited lecture).
7. Merle Randrüüt. On modelling deformation waves in microstructured materials: evolution equations. *11th EUROMECH–MECAMAT conference*, Mechanics in microstructured solids: cellular materials, fibre reinforced solids and soft tissues, Torino, Italy, March 10–14, 2008 — special award for the best poster presentation of a young researcher.

ELULOOKIRJELDUS

1. Isikuandmed

Nimi Merle Randrüüt
Sünniaeg ja -koht 20.09.1981, Tallinn, Eesti
Kodakondsus Eesti

2. Kontaktandmed

Aadress TTÜ Küberneetika Instituut, Akadeemia tee 21, 12618 Tallinn
Telefon +372 6204173
E-post merler@cens.ioc.ee

3. Haridus

2006 – ... Tallinna Tehnikaülikool, matemaatika-loodusteaduskond, tehniline füüsika, doktoriõpe
2004 – 2006 Tallinna Tehnikaülikool, matemaatika-loodusteaduskond, tehniline füüsika, MSc
2000 – 2004 Tallinna Tehnikaülikool, mehaanikateaduskond, tootearendus, BSc

4. Keelteoskus

eesti keel emakeel
inglise keel kõrgtase
vene keel põhiteadmised
saksa keel põhiteadmised

5. Teenistuskäik

2009 – ... Tallinna Tehnikaülikool, TTÜ Küberneetika Instituut, mehaanika- ja rakendusmatemaatika osakond, teadur
2007 – ... Tallinna Tehnikaülikool, ehitusteaduskond, mehaanikainstituut, tehnilise mehaanika õppetool, assistent
2007 – 2007 Eesti Kunstiakadeemia, arhitektuuriteaduskond, tunnitavaline õppejõud

- 2006 – 2007 Tallinna Tehnikaülikool, ehitusteaduskond, mehaanikainstituut, tehnilise mehaanika õppetool, erakorraline assistent
- 2005 – 2009 Tallinna Tehnikaülikool, TTÜ Küberneetika Instituut, mehaanika- ja rakendusmatemaatika osakond, tehnik
- 2005 – 2006 Consolis Engineering Services, tehnik
- 2005 – 2005 Tallinna Tehnikaülikool, ehitusteaduskond, mehaanikainstituut, rakendusmehaanika õppetool, tunnitասuline õppejõud
- 2003 – 2003 Norma, inseneripraktika, konstruktor

6. Kaitstud lõputööd

- 2006, Lainelevi modelleerimine mikrostruktuuriga materjalides, MSc, Tallinna Tehnikaülikool, matemaatika-loodusteaduskond, juhendaja professor Jüri Engelbrecht
- 2004, Astmelise varda optimaalne projekteerimine, BSc, Tallinna Tehnikaülikool, mehaanikateaduskond, juhendaja dotsent Jüri Kirs

7. Autasud

- 2009, TTÜ Küberneetika Instituudi aasta parim teaduspublikatsioon noorte kategoorias – Tanel Peets, Merle Randrüüt, and Jüri Engelbrecht: On modelling dispersion in microstructured solids. *Wave Motion* **45**(4) (2008) 471–480 eest
- 2008, TTÜ Arengufond, Tiina Mõisa stipendium
- 2008, TTÜ Arengufond, Eesti Raudtee stipendium
- 2008, eriauhind noorele teadlasele parima postriettekande eest, *11th EU-ROMECH-MECAMAT conference, Mechanics in microstructured solids: cellular materials, fibre reinforced solids and soft tissues*, Torino, Itaalia
- 2006, Eesti Teaduste Akadeemia, üliõpilaste teadustööde konkursi II auhind magistritöö eest
- 2005, TTÜ Arengufond, Eesti Energia stipendium
- 2003, TTÜ Arengufond, Saku Õlletehase stipendium

8. Teadustöö põhisuunad

- Deformatsioonilained mikrostruktuuriga materjalides

9. Teadustegevus

Teadusartiklite, konverentsiteeside ja konverentsi- ning seminariettekannete loetelu on toodud ingliskeelse elulookirjelduse juures.

**DISSERTATIONS DEFENDED AT
TALLINN UNIVERSITY OF TECHNOLOGY ON
NATURAL AND EXACT SCIENCES**

1. **Olav Kongas.** Nonlinear dynamics in modeling cardiac arrhythmias. 1998.
2. **Kalju Vanatalu.** Optimization of processes of microbial biosynthesis of isotopically labeled biomolecules and their complexes. 1999.
3. **Ahto Buldas.** An algebraic approach to the structure of graphs. 1999.
4. **Monika Drews.** A metabolic study of insect cells in batch and continuous culture: application of chemostat and turbidostat to the production of recombinant proteins. 1999.
5. **Eola Valdre.** Endothelial-specific regulation of vessel formation: role of receptor tyrosine kinases. 2000.
6. **Kalju Lott.** Doping and defect thermodynamic equilibrium in ZnS. 2000.
7. **Reet Koljak.** Novel fatty acid dioxygenases from the corals *Plexaura homomalla* and *Gersemia fruticosa*. 2001.
8. **Anne Paju.** Asymmetric oxidation of prochiral and racemic ketones by using sharpless catalyst. 2001.
9. **Marko Vendelin.** Cardiac mechanoenergetics *in silico*. 2001.
10. **Pearu Peterson.** Multi-soliton interactions and the inverse problem of wave crest. 2001.
11. **Anne Menert.** Microcalorimetry of anaerobic digestion. 2001.
12. **Toomas Tiivel.** The role of the mitochondrial outer membrane in in vivo regulation of respiration in normal heart and skeletal muscle cell. 2002.
13. **Olle Hints.** Ordovician scolecodonts of Estonia and neighbouring areas: taxonomy, distribution, palaeoecology, and application. 2002.
14. **Jaak Nõlvak.** Chitinozoan biostratigraphy in the Ordovician of Baltoscandia. 2002.
15. **Liivi Kluge.** On algebraic structure of pre-operad. 2002.
16. **Jaanus Lass.** Biosignal interpretation: Study of cardiac arrhythmias and electromagnetic field effects on human nervous system. 2002.
17. **Janek Peterson.** Synthesis, structural characterization and modification of PAMAM dendrimers. 2002.
18. **Merike Vaher.** Room temperature ionic liquids as background electrolyte additives in capillary electrophoresis. 2002.
19. **Valdek Mikli.** Electron microscopy and image analysis study of powdered hardmetal materials and optoelectronic thin films. 2003.

20. **Mart Viljus.** The microstructure and properties of fine-grained cermets. 2003.
21. **Signe Kask.** Identification and characterization of dairy-related *Lactobacillus*. 2003.
22. **Tiiu-Mai Laht.** Influence of microstructure of the curd on enzymatic and microbiological processes in Swiss-type cheese. 2003.
23. **Anne Kuusksalu.** 2–5A synthetase in the marine sponge *Geodia cydonium*. 2003.
24. **Sergei Bereznev.** Solar cells based on polycrystalline copper-indium chalcogenides and conductive polymers. 2003.
25. **Kadri Kriis.** Asymmetric synthesis of C₂-symmetric bimorpholines and their application as chiral ligands in the transfer hydrogenation of aromatic ketones. 2004.
26. **Jekaterina Reut.** Polypyrrole coatings on conducting and insulating substrates. 2004.
27. **Sven Nõmm.** Realization and identification of discrete-time nonlinear systems. 2004.
28. **Olga Kijatkina.** Deposition of copper indium disulphide films by chemical spray pyrolysis. 2004.
29. **Gert Tamberg.** On sampling operators defined by Rogosinski, Hann and Blackman windows. 2004.
30. **Monika Übner.** Interaction of humic substances with metal cations. 2004.
31. **Kaarel Adamberg.** Growth characteristics of non-starter lactic acid bacteria from cheese. 2004.
32. **Imre Vallikivi.** Lipase-catalysed reactions of prostaglandins. 2004.
33. **Merike Peld.** Substituted apatites as sorbents for heavy metals. 2005.
34. **Vitali Syritski.** Study of synthesis and redox switching of polypyrrole and poly(3,4-ethylenedioxythiophene) by using *in-situ* techniques. 2004.
35. **Lee Põllumaa.** Evaluation of ecotoxicological effects related to oil shale industry. 2004.
36. **Riina Aav.** Synthesis of 9,11-secosterols intermediates. 2005.
37. **Andres Braunbrück.** Wave interaction in weakly inhomogeneous materials. 2005.
38. **Robert Kitt.** Generalised scale-invariance in financial time series. 2005.
39. **Juss Pavelson.** Mesoscale physical processes and the related impact on the summer nutrient fields and phytoplankton blooms in the western Gulf of Finland. 2005.

40. **Olari Ilison.** Solitons and solitary waves in media with higher order dispersive and nonlinear effects. 2005.
41. **Maksim Säkki.** Intermittency and long-range structurization of heart rate. 2005.
42. **Enli Kiipli.** Modelling seawater chemistry of the East Baltic Basin in the late Ordovician–Early Silurian. 2005.
43. **Igor Golovtsov.** Modification of conductive properties and processability of polyparaphenylene, polypyrrole and polyaniline. 2005.
44. **Katrin Laos.** Interaction between furcellaran and the globular proteins (bovine serum albumin β -lactoglobulin). 2005.
45. **Arvo Mere.** Structural and electrical properties of spray deposited copper indium disulphide films for solar cells. 2006.
46. **Sille Ehala.** Development and application of various on- and off-line analytical methods for the analysis of bioactive compounds. 2006.
47. **Maria Kulp.** Capillary electrophoretic monitoring of biochemical reaction kinetics. 2006.
48. **Anu Aaspõllu.** Proteinases from *Vipera lebetina* snake venom affecting hemostasis. 2006.
49. **Lyudmila Chekulayeva.** Photosensitized inactivation of tumor cells by porphyrins and chlorins. 2006.
50. **Merle Uudsemaa.** Quantum-chemical modeling of solvated first row transition metal ions. 2006.
51. **Tagli Pitsi.** Nutrition situation of pre-school children in Estonia from 1995 to 2004. 2006.
52. **Angela Ivask.** Luminescent recombinant sensor bacteria for the analysis of bioavailable heavy metals. 2006.
53. **Tiina Lõugas.** Study on physico-chemical properties and some bioactive compounds of sea buckthorn (*Hippophae rhamnoides* L.). 2006.
54. **Kaja Kasemets.** Effect of changing environmental conditions on the fermentative growth of *Saccharomyces cerevisiae* S288C: auxo-accelerostat study. 2006.
55. **Ildar Nisamedtinov.** Application of ^{13}C and fluorescence labeling in metabolic studies of *Saccharomyces* spp. 2006.
56. **Alar Leibak.** On additive generalisation of Voronoi's theory of perfect forms over algebraic number fields. 2006.
57. **Andri Jagomägi.** Photoluminescence of chalcopyrite tellurides. 2006.
58. **Tõnu Martma.** Application of carbon isotopes to the study of the Ordovician and Silurian of the Baltic. 2006.

59. **Marit Kauk.** Chemical composition of CuInSe₂ monograin powders for solar cell application. 2006.
60. **Julia Kois.** Electrochemical deposition of CuInSe₂ thin films for photovoltaic applications. 2006.
61. **Ilona Oja Aik.** Sol-gel deposition of titanium dioxide films. 2007.
62. **Tiia Anmann.** Integrated and organized cellular bioenergetic systems in heart and brain. 2007.
63. **Katrin Trummal.** Purification, characterization and specificity studies of metalloproteinases from *Vipera lebetina* snake venom. 2007.
64. **Gennadi Lessin.** Biochemical definition of coastal zone using numerical modeling and measurement data. 2007.
65. **Enno Pais.** Inverse problems to determine non-homogeneous degenerate memory kernels in heat flow. 2007.
66. **Maria Borissova.** Capillary electrophoresis on alkylimidazolium salts. 2007.
67. **Karin Valmsen.** Prostaglandin synthesis in the coral *Plexaura homomalla*: control of prostaglandin stereochemistry at carbon 15 by cyclooxygenases. 2007.
68. **Kristjan Piirime.** Long-term changes of nutrient fluxes in the drainage basin of the gulf of Finland — application of the PolFlow model. 2007.
69. **Tatjana Dedova.** Chemical spray pyrolysis deposition of zinc sulfide thin films and zinc oxide nanostructured layers. 2007.
70. **Katrin Tomson.** Production of labelled recombinant proteins in fed-batch systems in *Escherichia coli*. 2007.
71. **Cecilia Sarmiento.** Suppressors of RNA silencing in plants. 2008.
72. **Vilja Mardla.** Inhibition of platelet aggregation with combination of antiplatelet agents. 2008.
73. **Maie Bachmann.** Effect of Modulated microwave radiation on human resting electroencephalographic signal. 2008.
74. **Dan Hivonen.** Terahertz spectroscopy of low-dimensional spin systems. 2008.
75. **Ly Villo.** Stereoselective chemoenzymatic synthesis of deoxy sugar esters involving *Candida antarctica* lipase B. 2008.
76. **Johan Anton.** Technology of integrated photoelasticity for residual stress measurement in glass articles of axisymmetric shape. 2008.
77. **Olga Volobujeva.** SEM study of selenization of different thin metallic films. 2008.

78. **Artur Jõgi.** Synthesis of 4'-substituted 2,3'-dideoxynucleoside analogues. 2008.
79. **Mario Kadastik.** Doubly charged Higgs boson decays and implications on neutrino physics. 2008.
80. **Fernando Pérez-Caballero.** Carbon aerogels from 5-methylresorcinol-formaldehyde gels. 2008.
81. **Sirje Vaask.** The comparability, reproducibility and validity of Estonian food consumption surveys. 2008.
82. **Anna Menaker.** Electrosynthesized conducting polymers, polypyrrole and poly(3,4-ethylenedioxythiophene), for molecular imprinting. 2009.
83. **Lauri Ilison.** Solitons and solitary waves in hierarchical Korteweg-de Vries type systems. 2009.
84. **Kaia Ernits.** Study of In_2S_3 and ZnS thin films deposited by ultrasonic spray pyrolysis and chemical deposition. 2009.
85. **Veljo Sinivee.** Portable spectrometer for ionizing radiation "Gammamapper". 2009.
86. **Jüri Virkepu.** On Lagrange formalism for Lie theory and operadic harmonic oscillator in low dimensions. 2009.
87. **Marko Piirsoo.** Deciphering molecular basis of Schwann cell development. 2009.
88. **Kati Helmja.** Determination of phenolic compounds and their antioxidative capability in plant extracts. 2010.
89. **Merike Sõmera.** Sobemoviruses: genomic organization, potential for recombination and necessity of P1 in systemic infection. 2010.
90. **Kristjan Laes.** Preparation and impedance spectroscopy of hybrid structures based on CuIn_3Se_5 photoabsorber. 2010.
91. **Kristin Lippur.** Asymmetric synthesis of 2,2'-bimorpholine and its 5,5'-substituted derivatives. 2010.
92. **Merike Luman.** Dialysis dose and nutrition assessment by an optical method. 2010.
93. **Mihhail Berezovski.** Numerical simulation of wave propagation in heterogeneous and microstructured materials. 2010.
94. **Tamara Aid-Pavlidis.** Structure and regulation of BDNF gene. 2010.
95. **Olga Bragina.** The role of Sonic Hedgehog pathway in neuro- and tumorigenesis. 2010.